Mathematisches Forschungsinstitut Oberwolfach

Report No. 43/2022

DOI: 10.4171/OWR/2022/43

At the Interface between Semiclassical Analysis and Numerical Analysis of Wave Scattering Problems

Organized by
Simon Chandler-Wilde, Reading
Monique Dauge, Rennes
Euan Spence, Bath
Jared Wunsch, Evanston

25 September – 1 October 2022

Abstract. In this context of wave scattering, both semiclassical analysis and numerical analysis share the same goal – that of understanding the behaviour of the scattered wave – but these two fields operate largely in isolation, mainly because the tools and techniques of the two fields are largely disjoint. In recent years there have been promising examples of successful collaboration at the interface of semiclassical analysis and numerical analysis, to the mutual benefit of both fields. This workshop sought to capitalise on these successes by bringing together members of the semiclassical-analysis and numerical-analysis communities and catalysing activity at this interface.

Mathematics Subject Classification (2020): 35-XX, 65-XX.

Introduction by the Organizers

The scattering and propagation of waves have been studied by mathematicians for many years. This activity has been motivated by a plethora of applications in science and industry, many involving waves in the mathematically-difficult high-frequency limit. Semiclassical analysis (SCA), as a branch of microlocal analysis, rigorously analyses partial differential equations with large (or small) parameters. In the context of high-frequency wave scattering, SCA seeks to describe precisely the extent to which the dynamics of scattered waves is influenced by the scattering of classical Newtonian point particles in the same geometry; this relationship is a version of the correspondence principle of quantum mechanics. On the other hand, the goal of numerical analysis (NA) in this context is to design numerical

methods for computing the scattered wave that are accurate, efficient, and robust, and prove theorems guaranteeing these properties.

This workshop sought to capitalise on recent successful collaborations at the interface of SCA and NA, to the mutual benefit of both fields, by bringing together members of the SCA and NA communities and catalysing activity at this interface.

The first day consisted of three introductory talks on NA (given by Simon Chandler-Wilde, Andrea Moiola, and Martin Gander), aimed primarily at the audience members from the SCA community, and 3 introductory talks on SCA (given by Jeffrey Galkowski, Maxime Ingremeau, and Dean Baskin), aimed primarily at the audience members from the NA community.

A key question in the NA wave problems is: what are appropriate bases in which to represent Helmholtz solutions at high frequency? Correspondingly, a large number of talks touched on aspects of this question. Hongkai Zhao described bounds on the approximate separability of the Helmholtz Green's function in free space, giving lower bounds on the number of degrees of freedom required to approximate Helmholtz solutions. Two complementary talks by David Lafontaine and Markus Melenk showed that the *hp*-finite-element method (*hp*-FEM) (a method based on approximation using piecewise polynomials of increasing degree on meshes with decreasing meshwidth) does not suffer from the pollution effect (i.e., is quasi-optimal with a choice of the number of degrees of freedom $\sim k^d$, where k is the wavenumber and d is the dimension). There were then several talks on the design/use of problem-adapted bases for the Helmholtz equation: the talk by Théophile Chaumont-Frelet described a new method using coherent states in a least-squares framework to solve Helmholtz equation, needing only $\sim k^{d-1/2}$ degrees of freedom. Melissa Tacy discussed, from an SCA point of view, the design of such problem-adapted bases using ideas from harmonic analysis. Fatih Ecevit described the state-of-the-art in hybrid asymptotic methods for scattering by smooth strictly convex obstacles; these methods are based on the Melrose–Taylor parametrix for such scattering problems, and Oana Ivanovici described new results describing the influence of diffraction on dispersive estimates for solutions to the wave equation in the same context.

One established common area of interest between SCA and NA is in the study of resonances, often using complex scaling/perfectly-matched layers to approximate the "outgoing" radiation condition. Anne-Sophie Bonnet-Ben Dhia focused on these questions in the context of wave guides, and, in particular, new questions about reflectionless modes. Monique Dauge and Zoïs Moitier focused on resonances in the classic setting of transmission by a penetrable obstacle, but now also covering the topical case of negative-index materials. Stefan Sauter presented new results on localised Helmholtz solutions created by penetrable obstacles varying on the scale of the wavelength. Laurence Halpern and Jeffrey Rauch described the resolution of long-standing open questions about stability of perfectly-matched layers for Maxwell's equations in the time domain.

Another use of absorbing boundary conditions (such as perfectly-matched layers) is in domain-decomposition methods, and the talk of Thomas Beck described

results on the use of impedance boundary conditions in the context of a hierarchical non-overlapping domain-decomposition method.

A theme running through several talks was that of integral equations: Carolina Urzúa-Torres discussed space-time boundary integral equations for the wave equation, Charles Epstein discussed boundary integral equations for time-harmonic Maxwell's equations in the context of superconductors, Stéphanie Chaillat described simulating underwater explosions via boundary-element methods coupled with finite-element methods, and Martin Costabel presented the first numerical-analysis of the popular Discrete Dipole Approximation method (involving volume integral equations).

Whilst the majority of the talks concerned direct scattering problems (where the task is to find the scattered wave given the obstacle and incident wave), Leonardo Zepeda-Nunez showed that the inverse Liouville scattering problem is asymptotically equivalent to the generalized inverse Helmholtz scattering problem in the high-frequency regime.

Finally, two talks dealt with novel problems related to numerical analysis arising from applications from mathematical physics. Clotilde Fermanian-Kammerer discussed the issues involved with dimension-reduction for complex quantum systems by splitting into weakly interacting subsystems. Alexander Strohmaier and Alden Waters discussed recent work on the analysis of the celebrated Casimir effect, which permits numerical analysis of Casimir energies via the Boundary Element Method.

Acknowledgement: The workshop organizers acknowledge the support of the MFO for D. Obovu and J. Zou under the "Oberwolfach Leibniz Graduate Students" program and the support of the Simons Foundation for B. Engquist under the "Simons Visiting Professors" program.

Workshop: At the Interface between Semiclassical Analysis and Numerical Analysis of Wave Scattering Problems

Table of Contents

Simon Chandler-Wilde (joint with Euan Spence)
Numerical analysis at the semiclassical analysis/numerical analysis interface: issues and case studies 2517

Andrea Moiola
Non-polynomial methods for the Helmholtz equation 2521

Martin J. Gander (joint with Hui Zhang)
Iterative Solvers for Helmholtz Problems by Domain Truncation 2524

Dean Baskin, Jeffrey Galkowski, Maxime Ingremeau
A short introduction to semiclassical analysis 2527

Hongkai Zhao
Why is high frequency Helmholtz equation difficult to solve? 2529

Melissa Tacy
Decompositions that are well adapted to non-constant coefficient PDE . . 2530

Anne-Sophie Bonnet-Ben Dhia (joint with Lucas Chesnel, Vincent Pagneux)
Complex frequency spectra in waveguides: trapped modes, scattering resonances and reflectionless modes 2533

Laurence Halpern, Jeffrey Rauch
Stability and Perfection of PML for Maxwell's Equations on Rectangular Solids 2536

Leonardo Zepeda-Nunez (joint with Qin Li, Shi Chen, and Zhiyan Ding)
High frequency limit for the inverse scattering problem. 2537

Alexander Strohmaier, Alden Waters
Relative traces and numerical computation of spectral functions 2540

Clotilde Fermanian Kammerer (joint with Irene Burghardt, Rémi Carles, Benjamin Lasorne, Caroline Lasser)
Separation of scales: Dynamical approximations for composite quantum systems 2542

Fatih Ecevit
A survey on high-frequency scattering relating to smooth convex scatterers 2545

Théophile Chaumont-Frelet (joint with Victorita Dolean, Maxime Ingremeau)
Efficient approximation of high-frequency Helmholtz solutions by semiclassical Gabor wavelets 2548

David Lafontaine (joint with Jeffrey Galkowski, Euan A. Spence, Jared Wunsch)
Decompositions of high-frequency Helmholtz solutions and application to the finite element method 2550

Jens Markus Melenk (joint with M. Bernkopf, T. Chaumont-Frelet, I. Perugia, A. Rieder)
Regularity by decomposition for the Helmholtz equation in heterogeneous media 2554

Stefan Sauter (joint with Céline Torres)
A Class of Parameter Configurations for Localization of Waves 2557

Thomas Beck (joint with Yaiza Canzani, Jeremy L. Marzuola)
Quantitative bounds on Impedance-to-Impedance operators 2559

Stéphanie Chaillat (joint with Marc Bonnet, Bruno Leblé, Damien Mavaleix-Marchessoux, Alice Nassor)
Fast Boundary Element Methods to simulate underwater explosions and their interactions with submarines (a nice problem to illustrate a lot of modern numerical tools for waves) 2562

Charles Epstein (joint with Leslie Greengard, Manas Rachh)
Static currents in type I superconductors: Numerical methods and the $\lambda_L \to 0$ *limit* 2565

Carolina Urzúa-Torres (joint with Daniël Hoonhout, Olaf Steinbach, Marco Zank)
Space-time Boundary Integral Equations for the Wave Equation 2567

Monique Dauge (joint with Zoïs Moitier)
Imaginary part of resonances in the scattering by transparent or negative obstacles, part I 2570

Zoïs Moitier (joint with Monique Dauge)
Imaginary part of resonances in the scattering by transparent or negative obstacles, part II 2573

Oana Ivanovici
Dispersive estimates for the wave equation outside a general strictly convex obstacle in $\mathbb{R}^3$ 2574

Martin Costabel (joint with Monique Dauge, Khedijeh Nedaiasl)
Stability analysis of the DDA for Dielectric Scattering 2580

Abstracts

Numerical analysis at the semiclassical analysis/numerical analysis interface: issues and case studies

Simon Chandler-Wilde
(joint work with Euan Spence)

1. Introduction

This is the first of three talks that kicked off this programme, introducing issues and problems at the interface between semiclassical analysis (SCA) and numerical analysis (NA) from the NA side, and exhibiting opportunities at the SCA/NA interface through case studies.

1.1. **The model problem.** We focus on a model problem of obstacle scattering in time-harmonic acoustics. Let $\Omega_- \subset \mathbb{R}^d$ ($d \geq 2$) be a bounded Lipschitz open set (the obstacle) such that $\Omega := \mathbb{R}^d \setminus \overline{\Omega_-}$ is a connected Lipschitz domain. The *scattering problem* we consider is: given $k > 0$ (the wavenumber) and an incident plane wave $u^I(x) := \mathrm{e}^{\mathrm{i}kx\cdot d}$, travelling in the direction of the unit vector d, find $u \in C^2(\Omega) \cap H^1_{\mathrm{loc}}(\Omega)$ such that

$$\Delta u + k^2 u = 0 \text{ in } \Omega, \quad u = 0 \text{ on } \Gamma := \partial\Omega, \tag{1}$$

and such that the scattered field $u^S := u - u^I$ satisfies the standard Sommerfeld radiation condition (SRC)

$$\partial_r u^S(x) - \mathrm{i}ku^S(x) = o\big(r^{(1-d)/2}\big) \text{ as } r := |x| \to \infty, \text{ uniformly in } \widehat{x} := x/r.$$

Both SCA and NA seek to understand u, and solution operators, for the above problem. The key NA goal is: *compute u for fixed but arbitrarily large k, to arbitrarily high accuracy, as efficiently as possible.*

1.2. **The Galerkin method.** The standard *Galerkin method (GM)* for solving the above problem starts from a variational formulation: find $v \in \mathcal{H}$ (some complex Hilbert space) such that

$$a(v, w) = F(w) \quad \forall w \in \mathcal{H}, \tag{2}$$

where $a(\cdot,\cdot)$ and $F(\cdot)$ are, respectively, some continuous sesquilinear form and continuous anti-linear functional on $\mathcal{H}$. We choose a sequence $(\mathcal{H}_N)_{N=1}^{\infty}$ of finite dimensional subspaces of $\mathcal{H}$, and, for each $N \in \mathbb{N}$, seek $v_N \in \mathcal{H}_N$ such that

$$a(v_N, w_N) = F(w_N) \quad \forall w_N \in \mathcal{H}_N. \tag{3}$$

To solve our model problem by the GM there are three choices to make:

i) The variational formulation, notably whether to use a *domain-based* formulation or a *boundary-based* formulation; see §2 below.
ii) The choice for $\mathcal{H}_N$. We discuss classical piecewise-polynomial (finite element) subspaces in §3; choices adapted to (1) are discussed in the articles by Ecevit, Chaumont-Frelet, and Moiola in this volume.

iii) How to solve the linear system associated to (3); see the discussion in the article by Gander.

2. Variational formulations

2.1. **Domain-based.** The standard domain-based variational formulation is set in a bounded Lipschitz domain Ω_R with $\overline{\Omega_-} \subset \Omega_R \subset \Omega$ (commonly $\Omega_R := \Omega \cap B_R$, where $B_R := \{x \in \mathbb{R}^d : |x| < R\}$, for some $R > 0$). The unknown is $v := u|_{\Omega_R} \in \mathcal{H} := H^1_0(\Omega_R)$, where $H^1_0(\Omega_R)$ is the closure in $H^1(\Omega_R)$ of $\mathcal{D}_R := \{\phi|_{\Omega_R} : \phi \in C^\infty_0(\Omega)\}$. To obtain (2) multiply the Helmholtz equation (1) by $w \in \mathcal{D}_R$ and integrate by parts. This gives (2) for $w \in \mathcal{D}_R$, so, by density, for all $w \in \mathcal{H}$, where

$$
\begin{aligned}
a(v,w) &:= \int_{\Omega_R} \nabla v \cdot \nabla \bar{w} - k^2 v \bar{w} - \int_{\Gamma_R} \mathrm{DtN}_k(\gamma v)\gamma \bar{w}\, \mathrm{d}s, \\
F(w) &:= \int_{\Gamma_R} \left(\partial_n u^{\mathrm{I}} - \mathrm{DtN}_k(\gamma u^{\mathrm{I}})\right) \gamma \bar{w}\, \mathrm{d}s \quad \forall v, w \in \mathcal{H},
\end{aligned} \tag{4}
$$

$\gamma : H^1(\Omega_R) \to H^{1/2}(\partial\Omega_R)$ is the standard trace operator and $\Gamma_R := \partial\Omega_R \setminus \Gamma$ is the exterior boundary of Ω_R. DtN_k denotes the exact Dirichlet to Neumann (DtN) map for the domain $\Omega^+_R := \mathbb{R}^d \setminus \overline{\Omega_R \cup \Omega_-}$ exterior to Γ_R. Thus, for $g \in H^{1/2}(\Gamma_R)$, $\mathrm{DtN}_k g = \partial_n u$, where $u \in C^2(\Omega^+_R) \cap H^1_{\mathrm{loc}}(\Omega^+_R)$ is the unique solution to the Helmholtz equation (1) in Ω^+_R that satisfies the SRC and $u = g$ on Γ_R. If $\Gamma_R = \partial B_R$ the action of DtN_k can be calculated by separation of variables, but, even when $\Gamma_R = \partial B_R$, it can be attractive, for efficiency, to approximate DtN_k by a local absorbing boundary condition approximating the SRC, the simplest of which is the impedance boundary condition[1]

$$
\partial_n u - \mathrm{i}ku = 0 \quad \text{on } \Gamma_R, \tag{5}
$$

or to approximate DtN_k using PML (complex scaling in a layer around Ω_R with $u = 0$ on the outer boundary); see [7] and the references therein.

2.2. **Boundary-based.** Alternatively one can derive a variational formulation (2) via a boundary integral equation (BIE) formulation. The so-called *direct* route to a BIE is Green's representation theorem [2, Thm. 2.21], that, for $x \in \Omega$,

$$
\begin{aligned}
u^{\mathrm{S}}(x) &= -\int_\Gamma \left(\Phi(x,y)\partial_n u^{\mathrm{S}}(y) - \partial_{n(y)}\Phi(x,y)\gamma u^{\mathrm{S}}(x)\right)\, \mathrm{d}s(y) \\
&= -\int_\Gamma \left(\Phi(x,y)\partial_n u^{\mathrm{S}}(y) + \partial_{n(y)}\Phi(x,y) u^{\mathrm{I}}(x)\right)\, \mathrm{d}s(y),
\end{aligned}
$$

where we've used the boundary condition (1) to obtain the 2nd expression, and $\Phi(x,y)$ is the Helmholtz fundamental solution, $\Phi(x,y) = \exp(\mathrm{i}k|x-y|)/(4\pi|x-y|)$ for $d = 3$. Taking Dirichlet, Neumann, or impedance traces in the above equation gives a BIE (see, e.g., [2, §2.5, 2.6]), in operator form

$$
A\, \partial_n u^{\mathrm{S}} = f, \tag{6}
$$

[1]Note that (1) with the SRC replaced by (5) is a classic NA model problem.

where A is a linear combination of boundary integral operators (BIOs) and the identity that is a bounded linear operator on some Hilbert space $\mathcal{H}$ ($\mathcal{H} = H^{-1/2}(\Gamma)$ and $L^2(\Gamma)$ are common choices). This leads to (2) with $v = \partial_n u^{\mathrm{S}}$ and $a(v,w) := (Av,w)_{\mathcal{H}}$, $F(w) := (f,w)_{\mathcal{H}}$, where $(\cdot,\cdot)_{\mathcal{H}}$ is the inner product on $\mathcal{H}$.

3. Piecewise polynomial spaces $\mathcal{H}_N$ for FEM/BEM

The standard NA choice for $\mathcal{H}_N$ is a space of piecewise polynomials. We construct on the bounded domain G ($G = \Omega_R$ or Γ) a *mesh* $\mathcal{M}$, a finite collection of relatively open disjoint *elements* $\tau \subset G$, such that $G = \cup_{\tau\in\mathcal{M}}\overline{\tau}$. The standard setup is that each τ is the image of a fixed *reference element* $\mathcal{R}$ under a diffeomorphism $\chi_\tau : \mathcal{R} \to \tau$ (standard choices for $\mathcal{R}$ are a unit cube or a unit simplex, e.g., [9]). We choose $p \in \mathbb{N}\cup\{0\}$, denote by $\mathbb{P}_p$ the set of polynomials of (total or coordinate) degree $\le p$ on $\mathcal{R}$ (e.g., [9]), and define $\mathcal{H}_N$ to be the set of $w_N : G \to \mathbb{C}$ such that, for each $\tau \in \mathcal{M}$, $w_N|_\tau = P \circ \chi_\tau^{-1}$, with $P \in \mathbb{P}_p$. Without further constraint the functions in this space $\mathcal{H}_N$ are, generically, discontinuous at the boundary of each τ. If needed to ensure $\mathcal{H}_N \subset \mathcal{H}$ (e.g., if $\mathcal{H} = H^1_0(\Omega_R)$) we also require that each $w_N \in C(\overline{G})$. We term the GM (3) with this $\mathcal{H}_N$ the *finite element method (FEM)* when $G = \Omega_R$, the *boundary element method (BEM)* when $G = \Gamma$.

This construction is made for each $N \in \mathbb{N}$. With the hope of achieving that the GM solution $v_N \to v$ it is standard to require that i) $h := \max \mathrm{diam}(\tau) \to 0$ as $N \to \infty$ (this termed the h-FEM/BEM); or ii) $p \to \infty$ (p-FEM/BEM); or iii) $h \to 0$ and $p \to \infty$ simultaneously (hp-FEM/BEM). Crucial (and this is very much an endeavour at the SCA/NA interface) are sharp bounds for the *best approximation error* $\min_{w_N\in\mathcal{H}_N} \|v - w_N\|_{\mathcal{H}}$ as a function of Ω, k, h and p. By the Whittaker-Nyquist-Shannon criterion we expect that $\dim(\mathcal{H}_N) \sim k^m$, where m is the dimension of G ($m = d$ if $G = \Omega_R$, $= d-1$ if $G = \Gamma$) should be necessary and sufficient to ensure $\min_{w_N\in\mathcal{H}_N} \|v - w_N\|_{\mathcal{H}}$ remains small as $k \to \infty$. That G is lower dimensional is a significant advantage for the boundary-based formulation, but the linear system associated to (3) is dense rather than sparse as in the domain-based formulation.

4. NA of the Galerkin method

The major goal in the NA of a particular Galerkin method is to prove *quasi-optimality*, that, for some constant $C_{\mathrm{qo}} > 0$ independent of N,

$$\|v - v_N\|_{\mathcal{H}} \le C_{\mathrm{qo}} \min_{w_N\in\mathcal{H}_N} \|v - w_N\|_{\mathcal{H}}, \tag{7}$$

at least for all sufficiently large N, where v and v_N are the solutions of (2) and (3), respectively. The standard framework where this holds is where $a(\cdot,\cdot)$ is both *continuous* and *coercive*, i.e., for constants C_{cont}, $C_{\mathrm{coer}} > 0$,

$$|a(u,w)| \le C_{\mathrm{cont}}\|u\|_{\mathcal{H}}\|w\|_{\mathcal{H}} \quad \text{and} \quad |a(w,w)| \ge C_{\mathrm{coer}}\|w\|^2_{\mathcal{H}} \quad \forall u,w \in \mathcal{H}. \tag{8}$$

By *Céa's lemma* (an extension of Lax-Milgram), it follows from (8) that (3) has exactly one solution $v_N \in \mathcal{H}_N$ for all $N \in \mathbb{N}$ and (7) holds with $C_{\mathrm{qo}} = C_{\mathrm{cont}}/C_{\mathrm{coer}}$. One reason why the FEM for Helmholtz is "hard" from an NA perspective is

that $a(\cdot,\cdot)$, given by (4), is not coercive; if w vanishes on Γ_R then $a(w,w) = \|\nabla w\|^2_{L^2(\Omega_R)} - k^2\|w\|^2_{L^2(\Omega_R)}$ whereas $\|w\|^2_{\mathcal{H}} = \|\nabla w\|^2_{L^2(\Omega_R)} + \|w\|^2_{L^2(\Omega_R)}$.

5. Case studies at the SCA/NA interface

We finish with three examples of work at this interface.

5.1. **Hybrid NA-asymptotic methods.** Consider our model problem when Ω_- is C^∞ and strictly convex. Melrose and Taylor [11] through SCA methods studied the $k \to \infty$ asymptotics of $\eta^{\text{slow}}(x) := k^{-1}\partial_n u(x)/\mathrm{e}^{\mathrm{i}kx\cdot d}$, for $x \in \Gamma$, especially near shadow boundaries. Combining these results with NA, Dominguez, Graham and Smyshlyaev [5] showed, in 2D, that a k-dependent mesh and $\dim(\mathcal{H}_N) \sim k^{1/9}$ keeps $\|\eta^{\text{slow}} - v_N\|_{L_2(\Gamma)}$ small as $k \to \infty$, where v_N is a GM solution to a BIE formulation; this is improved to k^ε, $\forall \varepsilon > 0$, in [6], and see the article by Ecevit.

5.2. **"Pollution" in FEM/BEM.** If $a(\cdot,\cdot)$ is only *compactly perturbed coercive* (see, e.g., [3, §2.2]), then, provided (2) is uniquely solvable, (7) holds for $N \geq N_0$, for some sufficiently large N_0, but how do C_{qo} and N_0 depend on k? To control $\min_{w_N \in \mathcal{H}_N} \|v - w_N\|_{\mathcal{H}}$, $\dim(\mathcal{H}_N) \sim k^d$ is sufficient for h-FEM, but $\dim(\mathcal{H}_N) \gg k^d$ is needed for (7) with C_{qo} independent of k, the so-called "pollution effect" [1]. For h-BEM there is no pollution if Ω is C^∞ and non-trapping [8]. Similarly, (7) holds for hp-FEM/BEM with C_{qo} independent of k provided $p \sim \log k$; see [10, 7] and the references therein, and the articles by Lafontaine and Melenk.

5.3. **k-dependence of BIOs.** A great SCA/NA question is how do the condition numbers $\text{cond}(A) := \|A\|\|A^{-1}\|$ of the BIOs A arising in (6) depend on k (and Ω), and how does this translate to discretisations of A? A recent review is [4, §6.5].

References

[1] I. M. Babuška, S. A. Sauter, *Is the pollution effect of the FEM avoidable for the Helmholtz equation considering high wavenumbers?* SIAM J. Numer. Anal. **34** (1997), 2392–2423.

[2] S. N. Chandler-Wilde, I. G. Graham, S. Langdon, E. A. Spence, *Numerical-asymptotic boundary integral methods in high-frequency acoustic scattering*, Acta Numerica **21** (2012), 89–305.

[3] S. N. Chandler-Wilde, D. P. Hewett, A. Moiola, J. Besson, *Boundary element methods for acoustic scattering by fractal screens*, Numer. Math. **147** (2021), 785–837.

[4] S. N. Chandler-Wilde, E. A. Spence, A. Gibbs, V. P. Smyshlyaev, *High-frequency bounds for the Helmholtz equation under parabolic trapping and applications in numerical analysis*, SIAM J. Math. Anal. **52** (2020), 845–893.

[5] V. Dominguez, I. G. Graham, V. P. Smyshlyaev, *A hybrid numerical-asymptotic boundary integral method for high-frequency acoustic scattering*, Numer. Math. **106** (2007), 471–510.

[6] F. Ecevit, H. C. Özen, *Frequency-adapted Galerkin boundary element methods for convex scattering problems*, Numer. Math. **135** (2017), 27–71.

[7] J. Galkowski, D. Lafontaine, E. A. Spence, J. Wunsch, *The hp-FEM applied to the Helmholtz equation with PML truncation does not suffer from the pollution effect* (2022), preprint at arXiv:2207.05542

[8] J. Galkowski, E. A. Spence, *Does the Helmholtz boundary element method suffer from the pollution effect?* SIAM Review, to appear, preprint at arXiv:2201.09721

[9] I. G. Graham, W. McLean, *Anisotropic mesh refinement: the conditioning of Galerkin boundary element matrices and simple preconditioners*, SIAM J. Numer. Anal. **44** (2006), 1487–1513.

[10] M. Bernkopf, T. Chaumont-Frelet, J. M. Melenk, *Wavenumber-explicit stability and convergence analysis of hp finite element discretizations of Helmholtz problems in piecewise smooth media* (2022), preprint at arXiv:2209.03601

[11] R. B. Melrose and M. E. Taylor, *Near peak scattering and the corrected Kirchhoff approximation for a convex obstacle*, Adv. Math. **55** (1985), 242–315.

Non-polynomial methods for the Helmholtz equation

Andrea Moiola

Classical numerical schemes such as the finite and the boundary element methods (FEM and BEM) approximate the solutions of boundary value problems (BVPs) with piecewise-polynomial functions. On the other hand, several schemes that use non-polynomial basis functions have been developed. This talk surveys some of these methods in the case of the homogeneous Helmholtz equation (HHE) $\Delta u + k^2 u = 0$ with $k > 0$. (Many of the methods and the results are available also for vector problems, i.e. for linear time-harmonic electromagnetic and elastic waves.)

Motivation. The use of polynomial approximating functions is appealing because polynomials (i) are easy and cheap to manipulate and evaluate, both analytically and on a computer, (ii) can approximate any target function u, with rates that only depend on the regularity of u and that are very well understood. On the other hand, piecewise-polynomial spaces are typically not adapted to the special PDE under consideration: e.g. the same discrete spaces are used for approximating both Helmholtz and Laplace BVPs. Non-polynomial approximating functions allow to construct discrete spaces that are better adapted to the PDE, with the final goal of achieving better accuracy with fewer degrees of freedom (DOFs). This is particularly relevant for high-frequency problems, where classical methods often fail to deliver acceptable accuracy at affordable cost.

Trefftz methods. Trefftz methods are numerical methods that use basis functions that, in each element of a mesh, are particular solutions of the PDE to be approximated. They can be of Galerkin or collocation type. Since the HHE does not admit non-trivial polynomial solutions, Trefftz methods for this equation necessarily use non-polynomial basis functions. A survey of Trefftz methods for the HHE is in [4]. Typical Trefftz basis functions (in 2D, for simplicity) [4, §3] are:

- plane waves (PWs) $\mathrm{e}^{\mathrm{i}k\mathbf{d}\cdot\mathbf{x}}$, where $\mathbf{d} \in \mathbb{R}^2$ is a unit vector;
- circular waves, or Fourier–Bessel functions, $J_\ell(kr)\mathrm{e}^{\mathrm{i}\ell\theta}$, with (r, θ) the polar coordinates in the plane, J_ℓ the first-kind Bessel function, $\ell \in \mathbb{Z}$;
- angular waves, with the same expression of circular waves but $\ell \notin \mathbb{Z}$;
- fundamental solutions and multipoles $H_\ell^{(1)}(kr)\mathrm{e}^{\mathrm{i}\ell\theta}$;

- evanescent plane waves (EPWs) $\mathrm{e}^{\mathrm{i}k\mathbf{d}\cdot\mathbf{x}}$, where $\mathbf{d}\in\mathbb{C}^2$ is a complex vector with $\mathbf{d}\cdot\mathbf{d}=1$ (they propagate in direction $\Re\mathbf{d}$ and their amplitudes decay exponentially in the orthogonal direction);
- "waveband" Herglotz functions $\int_{\varphi_1}^{\varphi_2}\mathrm{e}^{\mathrm{i}k\mathbf{x}\cdot\binom{\cos\varphi}{\sin\varphi}}\mathrm{d}\varphi$.

Analogue bases exist for 3D problems. PWs are usually preferred because of their simplicity and the low evaluation cost (they are just complex exponentials). Moreover, it is possible to compute integrals of (products of derivatives of) PWs over polytopes analytically [4, §4.1], greatly reducing the need for quadrature rules, which are very expensive for high-frequency problems.

Trefftz-DG. Differently from polynomials, Trefftz basis functions cannot be easily matched on interfaces between mesh element. Thus Trefftz methods typically employ discrete functions that are discontinuous across elements: continuity and boundary conditions are imposed weakly by the variational formulation in a discontinuous Galerkin (DG) setting. Numerous variations of this approach have been developed, see [4, §2]. Some of these Trefftz-DG methods are provably well-posed and quasi-optimal for any choice of Trefftz discrete space, as a consequence of coercivity in a skeleton norm. The ultra-weak variational formulation (UWVF) of [2] is a Trefftz-DG method originally written as a domain-decomposition scheme.

Approximation. A key ingredient in the design and the analysis of a Trefftz method is the ability of the discrete space to approximate general Helmholtz solutions. An explicit integral operator (Vekua operator) maps Helmholtz solutions to harmonic functions on the same domain and circular/spherical waves to harmonic polynomials. This allows to deduce error bounds for the approximation of Helmholtz solutions by circular/spherical waves from similar results for the approximation of harmonic functions by harmonic polynomials. Together with the Jacobi–Anger expansion, this implies error bounds for the approximation by PWs, with convergence rates in the element size and in the number of PWs (h and p convergence). The decay of the error in the number of DOFs is faster than the analogous one for polynomial spaces. This is because PWs are a more specialised tool: they are able to approximate only Helmholtz solutions and very good at this.

Instability. All Trefftz methods for the HHE, in particular those based on PWs, suffer from a strong instability: when the discrete space is enriched, numerical cancellation in machine arithmetic prevents from obtaining the theoretical convergence rates. This is the main obstacle that so far prevented the widespread use of Trefftz schemes and is usually blamed on the ill-conditioning of the linear system to be solved. Several recipes have been devised to tackle this instability, [4, §4.3]. In [6] it is shown that it is impossible to approximate general Helmholtz solutions in the unit disc with small-coefficient representations $\sum_{m=1}^{M} v_m \mathrm{e}^{\mathrm{i}k\mathbf{d}_m\cdot\mathbf{x}}$ in any PW basis, thus cancellation in computer arithmetic computations is unavoidable.

Evanescent PWs. A possible solution to the instability of Trefftz schemes is the use of judiciously chosen evanescent plane waves as basis functions. In [6], it

is proved that all Helmholtz solutions on the unit disc are continuous superpositions of EPWs $u(\mathbf{x}) = \int_{\{\mathbf{d}\in\mathbb{C}^2, \mathbf{d}\cdot\mathbf{d}=1\}} v(\mathbf{d})\mathrm{e}^{\mathrm{i}k\mathbf{d}\cdot\mathbf{x}}\mathrm{d}\mathbf{d}$ and the coefficient function v in this representation is bounded in a weighted L^2 norm. Finite-dimensional EPW spaces are constructed according to a rule coming from sampling theory and it is shown numerically that this allows to overcome the instability barrier and obtain arbitrarily accurate and robust approximations in machine arithmetic.

Partition of unity method (PUM). A way (different from DG) to enforce inter-element continuity is to use as basis functions products between PWs (or other Helmholtz solution with good approximation properties) and partition of unity functions, such as linear or bilinear FEM bases. This provides non-Trefftz H^1-conforming methods and allows to use standard variational formulations, [5].

MFS. Trefftz schemes have been often used as "meshless methods", i.e. using basis elements that are solution of the given PDE over the whole computational domain Ω, [4, §2.4]. A special case is the "method of fundamental solutions" (MFS), where $u(\mathbf{x})$ is approximated by $\sum_{j=1}^{\#DOFs} a_j H_0^{(1)}(k|\mathbf{x}-\mathbf{y}_j|)$, with nodes $\mathbf{y}_j$ in the complement of Ω. The MFS is simple and can be highly accurate, but the choice of the nodes $\mathbf{y}_j$ is delicate and strongly affects stability and accuracy, [1].

Quasi-Trefftz. For problems with smooth variable coefficients, Trefftz discrete spaces cannot be constructed in practice. Quasi-Trefftz schemes have been devised: the basis functions are approximate solution of the PDE, i.e. they are solution "up to some order" in Taylor-polynomial sense. Different types of quasi-Trefftz methods for Helmholtz have been designed, involving polynomials, modulated plane waves and "generalised plane waves" (exponentials of polynomials).

HNA-BEM. BEMs rephrase Helmholtz BVPs as boundary integral equations (BIEs) and approximate some traces of the BVP solution on the domain boundary. Non-polynomial BEMs approximate scattering problems by exploiting geometric optics (GO) and the geometric theory of diffraction (GTD), which give information on the solution in the high-frequency limit $k \to \infty$. These methods are thus called "hybrid numerical-asymptotics" (HNA). GO and GTD allow to write scattering problem solutions as sum of waves with different amplitudes and phases: $u(\mathbf{x}) \sim \sum_{j=1}^{J} v_j(\mathbf{x})\mathrm{e}^{\mathrm{i}k\phi_j(\mathbf{x})}$. HNA methods use the phases $\mathrm{e}^{\mathrm{i}k\phi_j(\mathbf{x})}$ provided by GO/GTD and approximate the amplitudes $v_j(\mathbf{x})$ with piecewise polynomials.

For instance, let Ω_- be a sound-soft convex polygonal scatterer and choose a BIE whose solution (to be approximated) is the normal derivative $\partial_{\mathbf{n}}u$ of the acoustic field. On a side of Ω_- of length L, $\partial_{\mathbf{n}}u(\mathbf{x}(s)) = \Psi(s) + v^+(s)\mathrm{e}^{\mathrm{i}ks} + v^-(L-s)\mathrm{e}^{-\mathrm{i}ks}$, where Ψ is a known GO term and $\mathbf{x}(s)$ is the arclength parametrisation of the side. The functions $v^\pm$ are singular only at $s = 0$. Piecewise-polynomial spaces on meshes graded towards the polygon corners give exponential-in-DOF convergence and a cost that, in practice, is independent of the wavenumber.

HNA-BEMs deliver excellent accuracy and efficiency, backed by a rigorous theory, but their scope of application is still quite limited. An excellent survey of HNA-BEM for Helmholtz scattering problems in two dimensions is [3].

References

[1] A.H. Barnett, T. Betcke, *Stability and convergence of the method of fundamental solutions for Helmholtz problems on analytic domains*, J. Comput. Phys. **227** (2008), 7003–7026.

[2] O. Cessenat, B. Despres, *Application of an ultra weak variational formulation of elliptic PDEs to the 2-dimensional Helmholtz problem*, SIAM J. Numer. Anal. **35** (1998), 255–299.

[3] S.N. Chandler-Wilde, I.G. Graham, S. Langdon, E.A. Spence, *Numerical-asymptotic boundary integral methods in high-frequency acoustic scattering*, Acta Numer. **21** (2012), 89–305.

[4] R. Hiptmair, A. Moiola, I. Perugia, *A survey of Trefftz methods for the Helmholtz equation*, Lect. Notes Comput. Sci. Eng. **114** (2016), 237–278.

[5] J.M. Melenk, I. Babuška, *The partition of unity finite element method: basic theory and applications*, Comput. Methods Appl. Mech. Engrg. **139** (1996), 289–314.

[6] E. Parolin, D. Huybrechs, A Moiola, *Stable approximation of Helmholtz solutions by evanescent plane waves*, arXiv:2202.05658 (2022).

Iterative Solvers for Helmholtz Problems by Domain Truncation

Martin J. Gander

(joint work with Hui Zhang)

My presentation introduced the participants from semi-classical analysis to the numerical analysis of iterative solvers for time harmonic wave propagation. I started with two problems related to a given matrix $A \in \mathbb{R}^{n\times n}$: solving linear systems, and computing eigenvalues and eigenvectors,

$$A\boldsymbol{u} = \boldsymbol{f}, \quad A\boldsymbol{\phi}_j = \lambda_j \boldsymbol{\phi}_j, \quad j = 1, 2, \ldots, n.$$

The first problem is mathematically trivial, one can use Gaussian Elimination (1798), which leads to a factored form $LU\boldsymbol{u} = \boldsymbol{f}$, L and U lower and upper triangular, and one then solves the linear system in two steps: $L\boldsymbol{v} = \boldsymbol{f}$, and $U\boldsymbol{u} = \boldsymbol{v}$. The computational cost is $O(n^3)$ for the LU-factorization, and $O(n^2)$ for the triangular solves, and the computation finishes in a finite number of steps. There is no such method to compute in a finite number of steps the eigenvalues and eigenvectors when $n > 4$ (Galois theory for polynomials of degree> 4). Nevertheless we can obtain the result also in $O(n^3)$, like for solving the linear system of equations, because there is a very efficient iterative method, the QR algorithm, for solving the eigenvalue problem approximately!

When solving the prototype problem for time harmonic wave propagation, namely the Helmholtz equation

$$\Delta u + \omega^2 u = \frac{\partial^2 u}{\partial x^2} + \frac{\partial^2 u}{\partial y^2} + \omega^2 u = f, \tag{1}$$

a finite difference discretization (based on Taylor expansions with step size h to approximate the derivatives) leads to a linear system with the equations for $u_{ij} \approx u(x_i, y_j)$ at each grid point (x_i, y_j), $x_i = ih$, $y_j = jh$, given by

$$-(u_{i,j-1} + u_{i-1,j} - 4u_{i,j} + u_{i+1,j} + u_{i,j+1}) + \omega^2 h^2 u_{ij} = h^2 f_{ij}, \; f_{ij} := f(x_i, y_j). \tag{2}$$

The complexity of direct solvers based on Gaussian elimination for such problems is shown in Fig. 1, theoretically and also running Matlab on my Laptop.

LU cost	$d=1$	$d=2$	$d=3$
using banded	$O(n)$	$O(n^2)$	$O(n^{7/3})$
using sparsity	$O(n)$	$O(n^{3/2})$	$O(n^2)$
dense matrix	$O(n^3)$	$O(n^3)$	$O(n^3)$

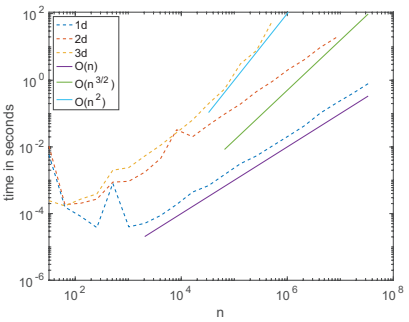

FIGURE 1. Theoretical and measured complexities of sparse direct LU-factorizations for Helmholtz finite difference matrices.

Since iterations made the hard eigenvalue problem as easy as the linear system, one can wonder if one can solve the discretized Helmholtz problem (2) faster by iteration than by Gaussian elimination. Basic iterative methods for linear systems split the matrix A into two other matrices, $A = M - N$, M invertible, and starting with $\boldsymbol{u}_0 \in \mathbb{R}^n$ iterate for $k = 0, 1, 2, \ldots$

$$M\boldsymbol{u}_{k+1} = N\boldsymbol{u}_k + \boldsymbol{f}. \tag{3}$$

Jacobi's Method (1845) uses $M := D = \mathrm{diag}(A)$, $N = D - A$, which leads to

$$\boldsymbol{u}_{k+1} = D^{-1}(D-A)\boldsymbol{u}_k + D^{-1}\boldsymbol{f} = \boldsymbol{u}_k + D^{-1}(\boldsymbol{f} - A\boldsymbol{u}_k), \tag{4}$$

and thus the error $\boldsymbol{e}_k := \boldsymbol{u} - \boldsymbol{u}_k$ satisfies

$$\boldsymbol{e}_{k+1} = \boldsymbol{e}_k - D^{-1}A\boldsymbol{e}_k = (I - D^{-1}A)^{k+1}\boldsymbol{e}_0. \tag{5}$$

The cost is $O(n)$ per iteration for Laplace/Helmholtz problems, and one can show for Laplace problems one needs $O(n^2)$ iterations for convergence and thus $O(n^3)$ overall cost for such sparse problems, worse than the direct solvers in Fig. 1.

To improve this, a Krylov method finds a better residual polynomial p_{k+1},

$$\boldsymbol{e}_{k+1} = p_{k+1}(D^{-1}A)\boldsymbol{e}_0 \tag{6}$$

with $p_{k+1}(D^{-1}A)$ much smaller than $(I - D^{-1}A)^{k+1}$ in (5). For example Conjugate Gradients (CG) finds a p_k that minimizes the energy norm $||\boldsymbol{e}_k||_{D^{-1/2}AD^{-1/2}}$, and GMRES minimizes $||D^{-1}(\boldsymbol{f} - A\boldsymbol{u}_k)||_2$. For Laplace type problems, CG reduces the number of iterations to $O(n)$, so we still have $O(n^2)$ overall cost, and for Helmholtz problems convergence is much worse, see [1].

Another improvement is multigrid, which uses a damped Jacobi iteration

$$\boldsymbol{u}_{k+1} = \boldsymbol{u}_k + \gamma D^{-1}(\boldsymbol{f} - A\boldsymbol{u}_k), \quad \gamma \in (0, 2) \tag{7}$$

to remove high frequency error components very efficiently for Laplace problems and $\gamma = \frac{2}{3}$. One then performs a few damped Jacobi steps on the fine grid, and once the error is smooth corrects it on a coarser, cheaper grid which now can well represent the smooth error. Doing this recursively, the number of iterations

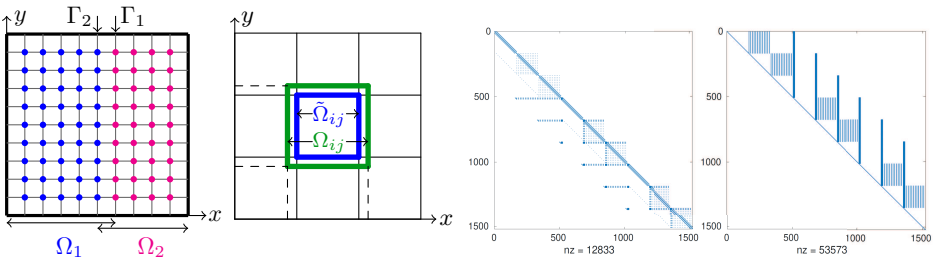

FIGURE 2. From left to right: Block Jacobi unknowns on the grid; general domain decomposition of the square into 9 subdomains; block L and U factors giving an optimal Schwarz method.

needed becomes $O(1)$ for Laplace problems, and thus the overall solution cost is now $O(n)$, much better than the direct solvers in Fig. 1, but again for Helmholtz problems multigrid does not work at all [1].

One can finally use a better preconditioner M in the splitting $A = M - N$, instead of $M = D$. For example Gauss-Seidel uses $M = \text{tril}(A)$, the lower triangular part, but this also requires $O(n^2)$ iterations for Laplace problems already. Using $M = LU$ from Gaussian elimination gives $\boldsymbol{e}_1 = (I - (LU)^{-1}A)\boldsymbol{e}_0 = 0$, optimal convergence in one step! Thus approximate LU-factorizations $A \approx \tilde{L}\tilde{U}$ are interesting, but also fail for Helmholtz [1]. One can also use preconditioning with a Block Jacobi method,

$$\text{(8)} \qquad \begin{bmatrix} A_{11} & \\ & A_{22} \end{bmatrix} \begin{bmatrix} \boldsymbol{u}_1{}^{k+1} \\ \boldsymbol{u}_2{}^{k+1} \end{bmatrix} = - \begin{bmatrix} & A_{12} \\ A_{21} & \end{bmatrix} \begin{bmatrix} \boldsymbol{u}_1{}^{k} \\ \boldsymbol{u}_2{}^{k} \end{bmatrix} + \begin{bmatrix} \boldsymbol{f}_1 \\ \boldsymbol{f}_2 \end{bmatrix},$$

which gives the parallel Schwarz method of Lions (1988), see Fig. 2 (left),

$$\text{(9)} \qquad \begin{array}{rcll} (\Delta + \omega^2) u_1{}^{k+1} &=& f_1 & \text{in } \Omega_1, \\ u_1{}^{k+1} &=& u_2{}^{k} & \text{on } \Gamma_1, \end{array} \qquad \begin{array}{rcll} (\Delta + \omega^2) u_2{}^{k+1} &=& f_2 & \text{in } \Omega_2, \\ u_2{}^{k+1} &=& u_1{}^{k} & \text{on } \Gamma_2, \end{array}$$

that needs also $O(1)$ iterations for Laplace problems if the overlap does not depend on the mesh parameter h, like multigrid. Block Gauss-Seidel would just be alternating Schwarz, using in the last line of (9) $u_1{}^{k+1}$.

Schwarz Methods by Domain Truncation use better transmission conditions than the Dirichlet values in (9). For a 3×3 decomposition as for example in Figure 2 (second from the left), with $\tilde{\Omega}_{ij}$ non-overlapping, and Ω_{ij} enlarged overlapping subdomains, the method, also called optimized Schwarz method, is

$$\text{(10)} \qquad \begin{array}{rcll} (\Delta + \omega^2) u_{ij}^{k+1} &=& f & \text{in } \Omega_{ij}, \qquad i,j = 1,2,3, \\ \mathcal{B}_{ij} u_{ij}^{k+1} &=& \mathcal{B}_{ij} u_{lm}^{k} & \text{on } \Omega_{ij} \cap \tilde{\Omega}_{lm} \qquad l,m = 1,2,3,\ l,m \neq i,j. \end{array}$$

The transmission operators $\mathcal{B}_{ij}$ are optimized based on the intuition that the subdomain solution is like a truncated solution part of the global solution, and one thus either uses absorbing boundary conditions (ABCs, going back to the seminal work by Engquist and Majda (1977)), or Perfectly Matched Layers (PML) going back to Beranger (1994). The best possible choice of $\mathcal{B}_{ij}$ comes from an exact

block-LU decomposition, and the sparsity pattern for the 3×3 decomposition is shown in Figure 2 (right). The method then converges in one iteration, like for the LU-decomposition we saw earlier, but we do not yet understand what these operators are. If the decomposition was just into strips, the operators would be the transparent ones involving the Dirichlet to Neumann (DtN) operators, see [2].

References

[1] O. Ernst, M.J. Gander, *Why it is difficult to solve Helmholtz problems with classical iterative methods*, Numerical Analysis of Multiscale problems (2012), 325–363.

[2] M.J. Gander, H. Zhang, *Factorizations, Sweeping Preconditioners, Source Transfer, Single Layer Potentials, Polarized Traces, and Optimized Schwarz Methods*, SIAM Review **61(1)** (2019), 3–76.

[3] M.J. Gander, H. Zhang, *Schwarz method by domain truncation*, Acta Numerica **31** (2022), 1–134.

A short introduction to semiclassical analysis

Dean Baskin, Jeffrey Galkowski, Maxime Ingremeau

Semiclassical analysis is a set of techniques designed to study the asymptotic behaviour of some partial differential equations with a small parameter $\hbar > 0$. Most of the time, these equations are linear, and the semiclassical parameter $\hbar$ is related to the typical wavelength of the solutions of the equation. A standard example of an equation to which semiclassical techniques can be applied is the Helmholtz equation

$$-\hbar^2 \Delta u - u = f,$$

possibly with variable coefficients. In particular, the limit $\hbar \to 0$, corresponding to rapidly oscillating solutions, is very singular.

The aim of this mini-lecture is not to replace a proper course on semiclassical analysis (which would require much more time), but rather to present the kind of tools semiclassical analysis can offer (and highlight their interest to the applied mathematician), as well as to give a flavour of semiclassical proofs. In particular, the theorems were never presented in their most general version, and the proofs were rather sketchy. For more precise statements and their proofs, there are many good references, including [1], [3], [4] and [2, Appendix E].

In the first part of the lecture, J. Galkowski describes the kind of equations which can be studied using semiclassical analysis, and the kind of results it could give. He explains the importance of thinking in *phase-space* $\mathbb{R}^{2d}$, by describing at the same time a function in position and Fourier space. To do this, it is convenient to use *pseudodifferential operators*, which are operators $\mathrm{Op}_\hbar(a)$ which

- depend on a symbol $a(x, \xi)$ which is a (smooth) function on $\mathbb{R}^{2d}$;
- act on functions on $\mathbb{R}$.

When the symbol a depends only on the x variable, then $\mathrm{Op}_\hbar(a)$ is just the multiplication by a. When a is a polynomial in ξ with coefficients independent of x, then $\mathrm{Op}_\hbar(a)$ is a differential operator with constant coefficients, obtained by

replacing each ξ_j by $\frac{h}{i}\partial_{x_j}$; more generally, when a depends only on ξ, $\mathrm{Op}_\hbar(a)$ is a Fourier multiplier.

For instance, the Helmholtz operator $u \mapsto -\hbar^2\Delta u - u$ can be seen as a pseudo-differential operator with symbol $|\xi|^2 - 1$.

The main properties of pseudodifferential operators are recalled, concerning their boundedness properties, and how they can be composed, and the properties of their commutators.

In the second part of the lecture, M. Ingremeau explains how one can tell that an operator is globally invertible, and find an approximate expression for its inverse, if its symbol is non-vanishing: this applies for instance to operators like

$$-\hbar^2\Delta u + u,$$

possibly with variable coefficients.

When trying to solve a partial differential equation like

$$P_\hbar u = f, \tag{1}$$

it is often the case that the symbol of $P_\hbar$ vanishes, so that $P_\hbar$ can only be inverted in some region of phase-space where the symbol is non-zero: this is the content of microlocal ellipticity. To solve an equation like (1), we must thus ensure that f is localized in the region of phase-space where $P_\hbar$ is invertible. The correct notion of localization in phase-space is that of *wavefront set*, which measures, around every point x, the set of directions ξ in which the function f can oscillate at scales $\approx h$.

In the last part of the lecture, D. Baskin presents theorems about the wavefront set of a solution of a partial differential equation.

If u is a solution of

$$P_\hbar u = 0,$$

where $P_\hbar$ is a pseudodifferential operator with symbol p, then the wavefront set of u must be included in $\{(x,\xi) \in \mathbb{R}^{2d}; p(x,\xi) = 0\}$.

A more precise result is the *propagation of singularities*, saying that the wavefront set is invariant by the Hamiltonian flow induced by the symbol p.

In other words, imagine that the solution u has some oscillations (at scale $\hbar$) near x_0 in the direction ξ_0. Suppose you take (x_0, ξ_0) as initial datas for Newton's equation with an energy p, and obtain a trajectory $(x_t, \xi_t)_{t\in\mathbb{R}}$. Then for each $t \in \mathbb{R}$, u has oscillations near x_t in the direction ξ_t.

A precise statement of this result, as well as a sketch of proof, is given in the case where $p = |\xi|^2 - 1$, so that $P_\hbar = -\hbar^2\Delta - 1$.

References

[1] M. Dimassi, J. Sjostrand, *Spectral asymptotics in the semi-classical limit* (2019) Cambridge university press.

[2] S. Dyatlov, M. Zworski, *Mathematical theory of scattering resonances* (2019). American Mathematical Soc.

[3] A. Martinez, *An introduction to semiclassical and microlocal analysis*, (2002), New York : Springer.

[4] M. Zworski *Semiclassical analysis*, American Mathematical Society (2012)

Why is high frequency Helmholtz equation difficult to solve?

Hongkai Zhao

The minimum number of terms needed in a separable approximation for a Green's function reveals the intrinsic complexity of the solution space of the underlying differential equation. It also has implications for whether low rank structures exist in the linear system after numerical discretization. The Green's function for a coercive elliptic differential operator in divergence form was shown to be highly separable [1] and efficient numerical algorithms exploiting low rank structures of the discretized systems were developed. In this presentation we study the approximate separability of the Green's function of the Helmholtz equation in the high frequency limit. We show (1) lower bounds based on an explicit characterization of the correlation between two Green's functions and a tight dimension estimate for the best linear subspace to approximate a set of decorrelated Green's functions, (2) upper bounds based on constructing specific separable approximations, (3) sharpness of these bounds for a few case studies of practical interest.

Define the Green's function of the Helmholtz equation

$$\Delta_{\mathbf{x}} G(\mathbf{x},\mathbf{y}) + k^2 n^2(\mathbf{x}) G(\mathbf{x},\mathbf{y}) = \delta(\mathbf{x}-\mathbf{y}), \quad \mathbf{x},\mathbf{y} \in \mathbb{R}^d. \tag{1}$$

The approximate separability of $G(\mathbf{x},\mathbf{y})$ is defined as the following: given two sets $X, Y \subseteq \Omega \subseteq \mathbb{R}^d$ and $\epsilon > 0$, there is a smallest N^ϵ such that there are $f_l(\mathbf{x}), g_l(\mathbf{y}), \mathbf{x} \in X, \mathbf{y} \in Y, l = 1, 2, \ldots, N^\epsilon$

$$\left\| G(\mathbf{x},\mathbf{y}) - \sum_{l=1}^{N^\epsilon} f_l(\mathbf{x}) g_l(\mathbf{y}) \right\|_{X\times Y} \leq \epsilon, \quad \mathbf{x} \in X, \mathbf{y} \in Y, \tag{2}$$

where $\|\cdot\|_{X\times Y}$ is the norm of some function space to which G, f_l, g_l belong.

If one views $G(\mathbf{x},\mathbf{y})$ as a family of functions in some function space defined on X with norm $\|\cdot\|_X$ and parameterized by $\mathbf{y} \in Y$ (the role of $\mathbf{x}$ and $\mathbf{y}$ can be reversed), this is related to the Kolmogorov n-width [1] for this family of functions in the function space. Any linear subspace of the function space that approximates this family of functions to the tolerance ϵ has a dimension of at least N^ϵ and the space spanned by $f_l(\mathbf{x}), l = 1, 2, \ldots, N^\epsilon$ is an optimal one.

Our main results [2] are:

- A characterization of the correlation (or angle) between two Green's functions of the Helmholtz equation in the high frequency limit: there is some $\alpha \geq 0$,

$$(\|G_0(\cdot,\mathbf{y}_1)\|_2 \|G_0(\cdot,\mathbf{y}_2)\|_2)^{-1} \left| \int_X G_0(\mathbf{x},\mathbf{y}_1)\overline{G}_0(\mathbf{x},\mathbf{y}_2) d\mathbf{x} \right| \lesssim (k|\mathbf{y}_1 - \mathbf{y}_2|)^{-\alpha}$$

[1] Kolmogorov n-width of a set S in a normed space W is its worst-case distance to the best n dimensional linear subspace L_n:

$$d_n(S,W) := \inf_{L_n} \sup_{f\in S} \inf_{g\in L_n} \|f-g\|_W,$$

as $k|\mathbf{y}_1-\mathbf{y}_2| \to \infty$, where α depends on $\dim(X)$ and the locations of $\mathbf{y}_1, \mathbf{y}_2$ with respect to X.

- Lower and upper bound estimates for the approximate separability for the Green's functions of the Helmholtz equation in the high frequency limit: for two fixed compact manifolds X, Y with $\dim(X) \geq \dim(Y) = s$ and α being the smallest number (least decorrelation rate) for any pair $\mathbf{y}_1, \mathbf{y}_2 \in Y$ as defined above, one has

$$N_k^\epsilon \gtrsim \begin{cases} k^{2\alpha}, & \alpha < \frac{s}{2}, \\ \\ k^{s-\delta}, & \alpha \geq \frac{s}{2}, \end{cases}$$

and

$$N_k^\epsilon \lesssim k^{s+\delta},$$

as $k \to \infty$ for any $\delta > 0$. Both estimates are sharp if $\alpha \geq \frac{s}{2}$, which occurs in many practical situations, e.g., X, Y are boundaries ($\dim(X) = \dim(Y) = s = 2$) of scatterers in three dimensions.
- Explicit estimates for the approximate separability of the Green's functions of the Helmholtz equation and their sharpness for situations that are commonly used in practice. These include cases with fixed X, Y, which are not highly separable, and highly separable cases with k dependent X, Y, e.g., the setting for the butterfly algorithm.

References

[1] M. Bebendorf and W. Hackbusch, *Existence of $\mathcal{H}$-matrix approximants to the inverse FE-matrix of elliptic operator with L^∞-coefficients*, Numer. Math. 95 (2003), no. 1, 1–28.

[2] B. Engquist and H. Zhao *Approximate Separability of the Green's Functions of the Helmholtz Equation in the High Frequency Limit*, Communications on Pure and Applied Mathematics, Vol. 71 (11), 2220-2274, 2018.

Decompositions that are well adapted to non-constant coefficient PDE

Melissa Tacy

In both numerical and harmonic analysis it is frequently advantageous to express solutions to PDEs as sum a (or integral) of "simple" component/analysis functions. For example the Fourier transform

$$\mathcal{F}[u] = \int e^{-i\langle x,\xi\rangle} u(x) dx$$

decomposes u into plane wave components. For a decomposition to be useful the component functions should be well adapted to the PDE, ideally the component functions should solve, or approximately solve, the PDE. This has the effect of producing sparse decompositions useful in both analysis and numerical reconstruction.

When working with constant coefficient PDE the Fourier transform has a number of natural advantages. For example consider

$$P(D)u = 0 \quad \text{or} \quad P(D)u = \text{small} \tag{1}$$

where P is a differential operator with symbol

$$p(\xi) = \sum_{|\alpha| \leq N} c_\alpha \xi^\alpha.$$

Approximate solutions, u, to (1) have the property that their Fourier transform must be supported near the set $\{\xi \mid p(\xi) = 0\}$. Therefore we can choose a set of component functions that incorporate this geometry. For example if $P(D) = -\Delta - \lambda^2$ a well-adapted set of component functions defined via their Fourier transform might be allowed to be quite coarse away from $|\xi| = \lambda$ (as solutions to the PDE should not include a large contribution from these terms) but should be more refined near $|\xi| = \lambda$. What about non-constant coefficient PDE?

Here we cannot simply use the Fourier transform however we can use some ideas from microlocal analysis to build well adapted component functions for general PDE from those adapted to simple constant coefficient equations. One of the early successes of microlocal analysis was developing a technique turning complicated PDE into simple ones via an application of a Fourier integral operator FIO. In [1] Fefferman describes this as "the algorithm of the 70s". Here we describe it within the semiclassical context. Suppose u is an approximate solution to a semiclassical pseudodifferential equation

$$p(x, hD)u = \text{small} \quad p(x, hD)u = \frac{1}{(2\pi h)^n} \int e^{\frac{i}{h}\langle x,\xi\rangle} p(x, \xi)u(y)dyd\xi.$$

The pseudodifferential calculus tells us that if $p(x, \xi)$ is bounded away from zero, $p(x, hD)$ is invertible. Therefore good solutions to $p(x, hD)u = 0$ must be semiclassically microlocalised near the set $\{(x, \xi) \mid p(x, \xi) = 0\}$. Now suppose that this set is locally a graph (as is often the case). In the phase space setting we can define maps that straighten out $\{(x, \xi) \mid p(x, \xi) = 0\}$ to become $\{\xi_1 = 0\}$. The set $\{\xi_1 = 0\}$ is associated with the very simple PDE, $hD_{x_1}v = 0$. Can we then quantise any of the phase space maps to work on the level of operators? The theory of semiclassical FIOs tells that in this case we can. That is we can produce an operator W so that

$$hD_{x_1}W = Wp(x, hD)$$

and that (in this case) W is unitary. We now have an algorithm for solving the non-constant coefficient equation.

(1) First microlocalise to regions where $\{(x, \xi) \mid p(x, \xi) = 0\}$ is locally a graph. It may be necessary to solve on a number of different pieces and later glue the solutions together.
(2) Produce a semiclassical FIO, W, satisfying $hD_{x_1}W = Wp(x, hD)$.
(3) Let $v = Wu$, then v is a approximate solution to $hD_{x_1}v = 0$.
(4) Solve for v, then invert to find u.

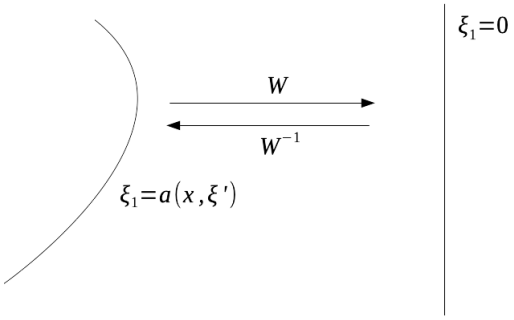

FIGURE 1. The FIO converts a general pseudodifferential equation $p(x, hD)u = 0$ into the simple differential equation $hD_{x_1}v = 0$.

Let's see what happens when we combine FIOs with an analysis/synthesis system. That is let Λ be a parameter space and ϕ_λ an analysing function with analysis operator

$$T_\lambda[v] = \langle v, \phi_\lambda \rangle.$$

Suppose further that we have a synthesis procedure

$$v(x) = \int T_\lambda[v]\phi_\lambda d\mu(\lambda)$$

for some suitable measure μ on Λ. Now if we apply W^{-1} we have (at least formally)

$$u = \int T_\lambda[v][W^{-1}\phi_\lambda](x)d\mu(\lambda).$$

So we can think of this as a synthesis for u in terms of the functions $W^{-1}\phi_\lambda$. If the ϕ_λ functions are well-adapted to hD_{x_1} the resultant functions $W^{-1}\phi_\lambda$ will be well-adapted to $p(x, hD)$. This way of thinking about developing component functions is very flexible. There are many systems of functions that are well adapted to hD_{x_1}. For example either the Fourier transform or the wavelet transform. Any combination of these can generate component functions well-adapted to $p(x, hD)$ via an application of a semiclassical FIO. The choice of decomposition will then depend very much on the features of the system under study. For example the wavelet type transforms have an advantage (over the Fourier transform) of locality which can be useful when we need to treat inherently local features, such as boundaries or corners.

REFERENCES

[1] C. Fefferman, *The uncertainty principle*, Bull. Amer. Math. Soc. **9:2** (1983), 129–206.

Complex frequency spectra in waveguides: trapped modes, scattering resonances and reflectionless modes

Anne-Sophie Bonnet-Ben Dhia
(joint work with Lucas Chesnel, Vincent Pagneux)

1. Definition of trapped modes and reflectionless modes

We consider for simplicity the case of a 2D acoustic waveguide occupying the strip $\mathbb{R} \times (0,1)$, with a compactly supported perturbation of velocity. In time-harmonic regime ($e^{-i\omega t}$), the acoustic pressure u satisfies the equations

$$\Delta u + k^2(1+\rho)u = 0 \ \text{ in } \Omega \ \text{ and } \ \frac{\partial u}{\partial \nu} = 0 \ \text{ on } \partial\Omega, \tag{1}$$

where $k = \omega/c$ (c being the sound velocity) and $\rho \in L^\infty(\Omega)$ is a compactly supported function. To fix ideas, we suppose that $\rho(x,y) = 0$ if $|x| > 1$.

Problem (1) can be considered as an eigenvalue problem where k^2 is the eigenvalue and u the eigenfunction. More precisely, one can define several eigenvalue problems by adding to equations (1) conditions on u at infinity. Let us define two physically relevant possibilities.

Trapped modes. Trapped modes correspond to solutions of (1) such that $u \in L^2(\Omega)$, $u \neq 0$. From a spectral point of view, trapped modes correspond to eigenvalues that are embedded in the essential spectrum of the self-adjoint operator $A = -(1+\rho)^{-1}\Delta u$ on $L^2(\Omega)$ with Neumann boundary conditions. As embedded eigenvalues, they are both difficult to study and to compute numerically, which gave rise to a huge literature (see for instance [1]). We denote by $\mathcal{T}$ the set of (real) values of k for which trapped modes exist.

Reflectionless modes. A less usual point of view [2, 3] is to consider a second family of modes which correspond to real values of k such that (1) has a solution $u \neq 0$ which is *ingoing* on the left-hand side of the perturbation and *outgoing* on its right-hand side. This can be formulated as follows:

$$u(x,y) = \sum_{n^2\pi^2 < k^2} A_n^{\pm} \cos(n\pi y) e^{i\beta_n x} + \sum_{n^2\pi^2 > k^2} B_n^{\pm} \cos(n\pi y) e^{-\beta_n |x|} \ \text{ for } |x| > 1$$

where $\beta_n = \sqrt{k^2 - n^2\pi^2}$ for $n^2\pi^2 < k^2$ and $\beta_n = \sqrt{n^2\pi^2 - k^2}$ for $n^2\pi^2 > k^2$.

If the coefficients $A_n^{\pm}$ are not all zero, such modes correspond to configurations where an incident wave (superposition of propagating modes) coming from the left interacts with the perturbation without producing any reflection. As a consequence, all the energy is transmitted from the left to the right, and the perturbation is non detectable, with this experiment, by an observer located far on its left-hand side. We denote by $\mathcal{N}$ the set of (real) values of k for which reflectionless modes exist.

By definition, if the coefficients $A_n^{\pm}$ vanish, the above solution is a trapped mode, so that $\mathcal{T} \subset \mathcal{N}$.

An important remark is that, due to energy conservation, trapped modes frequencies can be characterized as real values of k such that (1) has a solution $u \neq 0$ which is *outgoing* on both sides of the perturbation. This definition is very similar to that of reflectionless modes. The only difference is the behavior of u on the left-hand side of the perturbation: outgoing for trapped modes, ingoing for reflectionless modes.

2. Complex-scaling

Classical complex-scaling. A classical method to compute trapped modes is to introduce a complex scaling [4]. To do that, we consider the following complex-scaled operator

$$A_\alpha u = -(1+\rho)^{-1}\left(\alpha(x)\frac{\partial}{\partial x}\left(\alpha(x)\frac{\partial u}{\partial x}\right)+\frac{\partial^2 u}{\partial y^2}\right)$$

where the complex-scaling function α is defined as follows, for some $\theta \in (0, \pi/2)$:

$$\alpha(x) = 1 \text{ if } |x| < 1 \text{ and } \alpha(x) = e^{-i\theta} \text{ if } |x| > 1.$$

One can show that the spectrum of A_α (still with Neumann boundary conditions) as a non-selfadjoint unbounded operator of $L^2(\Omega)$, is the (disjoint) union of a discrete spectrum $\sigma_{disc}(A_\alpha)$ and an essential spectrum $\sigma_{ess}(A_\alpha)$, this latter, characterized by Weyl sequences, being as follows:

$$\sigma_{ess}(A_\alpha) = \cup_{n\geq 0}\{n^2\pi^2 + e^{-2i\theta}t^2; t \in \mathbb{R}\}.$$

The interest is that now, trapped modes correspond to real isolated eigenvalues of A_α that can be computed easily:

$$\mathcal{T} = \{k | k^2 \in \sigma_{disc}(A_\alpha)\} \cap \mathbb{R}.$$

In addition, we find some complex discrete eigenvalues that correspond to the so-called complex scattering frequencies [5].

Conjugate complex-scaling. We use a similar idea to compute reflectionless modes. But since the behavior of u is different between trapped modes and reflectionless modes on the left-hand side of the perturbation, we modify the complex-scaling there. More precisely we use two conjugated complex-scaling parameters on both sides of the perturbation. This leads to define the following operator (still with Neumann boundary conditions)

$$A_{\tilde{\alpha}} u = -(1+\rho)^{-1}\left(\tilde{\alpha}(x)\frac{\partial}{\partial x}\left(\tilde{\alpha}(x)\frac{\partial u}{\partial x}\right)+\frac{\partial^2 u}{\partial y^2}\right)$$

where the complex-scaling function $\tilde{\alpha}$ is defined as follows:

$$\tilde{\alpha}(x) = \alpha(x) \text{ if } x > -1 \text{ and } \alpha(x) = e^{i\theta} \text{ if } x < -1.$$

Now the essential spectrum is symmetric with respect to the real axis:

$$\sigma_{ess}(A_{\tilde{\alpha}}) = \bigcup_{n\geq 0}\{n^2\pi^2 + e^{2i\theta}t^2; t \in \mathbb{R}\} \cup \{n^2\pi^2 + e^{-2i\theta}t^2; t \in \mathbb{R}\}.$$

In general (see [2] for pathological counter-examples), the remaining part of the spectrum is discrete, and reflectionless modes coincide with discrete real eigenvalues of $A_{\tilde{\alpha}}$:

$$\mathcal{N} = \{k | k^2 \in \sigma_{disc}(A_{\tilde{\alpha}})\} \cap \mathbb{R}.$$

In addition, we find some complex discrete eigenvalues, which are, for reflectionless modes, analogous to scattering resonances for trapped modes.

3. Numerical illustrations

For computations, the waveguide is truncated, and a Neumann condition is imposed on the artificial boundaries. The effect of the truncation is a discretization of the essential spectrum. Below are the k-spectra obtained with both classical and conjugated complex scaling, for $\theta = \pi/4$, in the case of a rectangular non penetrable obstacle located in the middle of the waveguide.

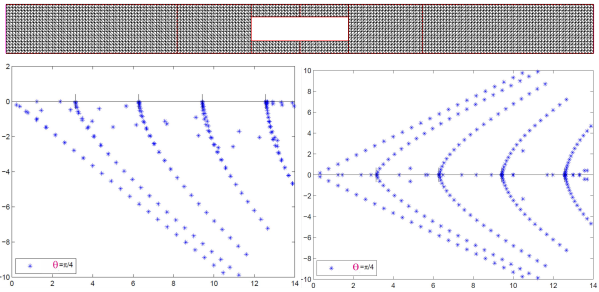

The results are as expected from the theory. The branches of essential spectrum are clearly identifiable. With classical complex-scaling, there are two real eigenvalues with $k \in (0, \pi)$ corresponding to trapped modes, that also appear with conjugated complex-scaling. But for this latter case, there are many other real eigenvalues, corresponding to reflectionless modes. Note that the existence of trapped modes is due to the symmetry of the geometry with respect to the horizontal mid-axis of the waveguide. Thanks to the other symmetry, with respect to the vertical axis, and to the choice of complex conjugated complex-scaling parameters, the problem with conjugated complex-scaling is $\mathcal{PT}$-symmetric. This is the reason of the symmetry of the second spectrum with respect the real axis.

References

[1] D.V. Evans, M. Levitin, and D. Vassiliev, *Existence theorems for trapped modes J. Fluid. Mech.* **261** (1994), 21–31.

[2] A.-S. Bonnet-BenDhia, L. Chesnel and V. Pagneux, *Trapped modes and reflectionless modes as eigenfunctions of the same spectral problem*, Proc. R. Soc. A. **474** (2018).

[3] W.R. Sweeney, C.W. Hsu and A.D. Douglas, *Theory of reflectionless scattering modes*, Phys. Rev. A **102** (2020).

[4] J. Aguilar and J.-M. Combes, *A class of analytic perturbations for one-body schrödinger hamiltonians*, *Comm. Math. Phys.* **22** (1971), 269–279.

[5] A. Aslanyan, L. Parnovski, and D. Vassiliev, *Complex resonances in acoustic waveguides*, *Quart. J. Mech. Appl. Math.* **53** (2000), 429–447.

Stability and Perfection of PML for Maxwell's Equations on Rectangular Solids

Laurence Halpern, Jeffrey Rauch

This talk, shared by the two authors, presents some results from our analysis of Perfectly Matched Layers and Initial Boundary Value Problems in a rectangular solid $\mathcal{Q}$. The critically important case is Maxwell's equations with a smaller rectangular domain of interest $\mathcal{Q}_I$ containing the supports of the currents and charges, and smooth absorptions $\sigma_j(x_j)$ supported in $\mathcal{Q} \setminus \mathcal{Q}_I$. We presented the following results.

1. *The proof of perfection from* [2] *in the case that* $\mathcal{Q} = \mathbb{R}^3$ *and the coefficients of the underlying operator are constant on the complement of* $\mathcal{Q}_I$. Though perfection for such time domain problems is much stated, to our knowledge this is the only proof of perfection. We show that if the Bérenger layers define a problem that is at least weakly well posed, then the layer is perfectly matched. The proof uses three key elements that recur in other contexts. The proof proceeds by Laplace transform with Laplace transform variable τ. When τ is real, perfection is a consequence of a conjugation by a change of variable that is real for $\tau \in \mathbb{R}_+$. The identity of perfection follows for general τ by analytic continuation.

It is notable that perfection follows by an analyticity argument. It is analyticity in τ that is a consequence of causality. It is not analyticity in x, that is not available in these hyperbolic problems.

2. *An example from* [4] *is presented showing that the standard Bérenger Layers have non trivial reflections when the underlying operator has coefficients with non vanishing derivative in the normal direction at* $\partial\mathcal{Q}_I$. This is done for discontinuous absorptions by constructing an infinitely accurate geometric optics solution with a high frequency wave approaching the interface at $\partial\mathcal{Q}_I$. The geometric optics solution reveals a non vanishing reflection coefficient one order smaller in $1/k$ than the principal reflection of standard absorbing boundary conditions. This proves that one can not simply apply Bérenger's plane wave argument to problems with frozen coefficients. In keeping with the topic of the meeting the two scale expansions of geometric optics are examples of semiclassical analysis. Qualitatively similar results hold if it is a j^{th} normal derivative that is discontinuous.

3. *In this meeting we announced for the first time our stability theorem for PML for Maxwell's equations in the time domain truncated at a rectangular box on which standard absorbing boundary conditions (ABC) are imposed.*

The analysis proceeds by Laplace transform. The key existence step is made for a carefully constructed boundary value problems for a system of complex Hemholtz equations. The problem is difficult for several reasons.

First, it inherits difficults of the real Helmholtz equations. For example, the boundary conditions on the different faces of $\partial\mathcal{Q}$ are different. For a second example, a weak formulation of (div,curl) type is used because it is adapted to the ABC. The (div,curl) Dirichlet integral is less positive than the classical Dirichet form.

• When τ is complex the Helmholtz problem lacks positivity and symmetry properties present when τ is real. The estimates involve a subtle dance involving the real and imaginary parts of an associated quadratic form.

• The quadratic form yields boundary terms that cannot be simply absorbed by terms of favorable sign. They require a generalizations of trace estimates of the sort introduced by Jerison and Kenig [5] for harmonic functions in Lipschitz domains and by Mitrea [6] for Maxwell. Real coordinate stretching and analytic continuation from the reals is used again.

• Uniqueness was the hardest part of our analytis of symmetric hyperbolic problems with trihedral corners in [3]. Uniqueness for the Maxwell PML with ABC is reduced by an analytic continuation argument to a uniqueness of the Laplace transform for τ large real. That can be proved by the strategy in [3] using the $H^{1/2}$ estimate of [1]. Shorter still is to use the recent H^1 estimate of [7].

References

[1] M. Costabel. *A remark on the regularity of solutions of Maxwell's equations on Lipschitz domains*, Mathematical Methods in the Applied Sciences, **12**(4) (1990),365–368.

[2] L. Halpern, S. Petit-Bergez, and J. Rauch. *The analysis of matched layers*, Confluentes Math., **3**(2) (2011),159–236.

[3] L. Halpern and J. Rauch. *Hyperbolic boundary value problems with trihedral corners*, Discrete Contin. Dyn. Syst., **36**(8) (2016),4403–4450.

[4] L. Halpern, L. Métivier, J. Rauch and J. Ryan. *Nobody's Perfect; Matched Layers for Heterogeneous Media*, SIAM Journal on Scientific Computing, **41**(1) (2019), A1–A25.

[5] D. S. Jerison and C. E. Kenig. *The Neumann problem on Lipschitz domains*, Bulletin (New Series) of the American Mathematical Society, **4**(2) (1981), 203–207.

[6] M. Mitrea. *The method of layer potentials in electromagnetic scattering theory on non-smooth domains*, Duke Mathematical Journal, **77**(1) (1995), 111–133, .

[7] S. Nicaise and J. Tomezyk. *The time-harmonic Maxwell equations with impedance boundary conditions in polyhedral domains*, Maxwell's Equations: Analysis and Numerics, Radon Series on Computational and Applied Mathematics,**24** (2019), 285–340.

High frequency limit for the inverse scattering problem.

Leonardo Zepeda-Nunez

(joint work with Qin Li, Shi Chen, and Zhiyan Ding)

The wave-particle duality of light has been one of the greatest enigmas in the natural sciences since antiquity: one of the earlier works can be traced back dating back to Euclid's treatise in light, *Catoptrics* (280 B.C.). In a nutshell, light can be either described as an electromagnetic (EM) wave governed by the Maxwell's equations, or as a stream of particles, called photons, governed by the radiative transport equation (RTE).

Although the advent of quantum mechanics at the onset of the last century partially solved the riddle, due to computational considerations, light continues to be modeled either as a particle or as a wave depending on the target application. One of such applications are inverse problems, which can be roughly described as

reconstructing unknown parameters within a domain of interest by data comprised of observations on its boundary.

Unfortunately, the properties of the inverse problems are highly dependent on the specific modeling of the underlying physical phenomena, even though, in principle, they share the same microscopic description. In particular, the stability of the inverse problem, i.e., how sensitive is the reconstruction of the unknown parameter to perturbations in the data, is surprisingly disparate [6, 3], thus creating an important gap between the wave and particle descriptions, which we seek to bridge in this talk.

We consider a time-harmonic wave-like description governed by the Helmholtz equation given by

$$\left(\Delta + k^2 n\right) u(x) = 0\,, \tag{1}$$

where u is the wave field, and $n(x)$ is the refractive index of the medium.

We also consider a particle-like description governed by the Liouville equation, which is a simplified RTE, given by:

$$v \cdot \nabla_x f - \nabla_x n \cdot \nabla_v f = 0\,, \tag{2}$$

where $f(x, v)$ is the distribution of photon particles, and n is still the refractive index. The Liouville equation describes the trajectories of photons via its characteristics: $\dot{x} = v$ and $\dot{v} = -\nabla_x n$.

Following the wave and photon descriptions, we define the forward problem as calculating either the wave-field, or the photon distribution from the refractive index by solving either the Helmholtz or the Liouville equations. The wave-particle duality, when translated to mathematical language, corresponds to the fact that the solutions obtained by the Helmholtz and Liouville equations are asymptotically close when $k \to \infty$, see [1].

We consider a modified full aperture inverse scattering problem: we seek to reconstruct an unknown environment within a domain of interest by probing it with tightly concentrated monochromatic beams originated from the boundary of the domain, in which the response of the unknown medium to the impinging beam is measured at its boundary. This measurement is performed by a measurement operator that is model-specific and plays an important role in the stability. When the beam is modeled as a wave, i.e., using the Helmholtz equation as a forward model, we call this process *generalized Helmholtz scattering problem*, and when the beam is modeled as a flux of photons, i.e., using the Liouville equation as a forward model, we refer to this process as the *Liouville scattering problem* (often called as the *optical tomography problem*).

Although the two different formulations seek to solve the same underlying physical problem, our understanding of the two inverse problems seems to suggest different stability properties. The traditional inverse scattering problem, using either near-field or far-field data is ill-posed: small perturbations in the measurements usually lead to large deviations in the reconstructions [4, 5], whereas, the inverse Liouville equation is well-conditioned: a small perturbation is reflected by a small error in the reconstruction [7].

Thus the observation that the stability for both problems is different seems to be at odds with the fact that the Liouville equation and the Helmholtz equation are asymptotically close in the high-frequency regime. We show that this can be fixed by modifying the sampling operator. The new formulation dubbed the generalized inverse scattering problem, converges to the Liouville inverse problem in the high-frequency limit. The convergence from the Helmholtz equation to the Liouville equation is conducted through the Wigner transform [8], and the convergence of the measuring operators is achieved through the Husimi transform [2]. Both convergences are obtained asymptotically in the $k \to \infty$ limit. This convergence allows us to conclude the following:

The inverse Liouville scattering problem is asymptotically equivalent to the generalized inverse Helmholtz scattering problem in the high-frequency regime.

In this talk we will formulate the statement above in a mathematically precise manner, and we provide extensive numerical evidence supporting it. We connect the two seemingly distinct inverse problems, and suggests that in the high-frequency regime, probing an unknown object with a single frequency is already enough for its reconstruction, with properly prepared data in the generalized inverse scattering setting. This partially answers the stability question regarding the inverse scattering. This can be viewed as the counterpart of the asymptotic multiscale study conducted in the forward setting. In particular, semi-classical limit is a theory that connects quantum mechanical and the classical mechanical description: the proposed formulation for the inverse scattering problem can be regarded as taking the (semi-)classical limit in the inverse setting.

The new inverse wave scattering formulation coupled with PDE-constrained optimization seems to be empirically less prone to cycle-skipping, i.e., convergence to spurious local minima [10], than its standard counterparts [9]. We finally show several experiments showcasing this property of the formulation in different set ups.

References

[1] Guillaume Bal, George Papanicolaou, and Leonid Ryzhik. Radiative transport limit for the random Schrödinger equation. *Nonlinearity*, 15(2):513, 2002.

[2] Jean-David Benamou, François Castella, Theodoros Katsaounis, and Benoit Perthame. High frequency limit of the Helmholtz equations. *Rev. Mat. Iberoam.*, 18(1):187–209, 2002.

[3] Shi Chen and Qin Li. Semiclassical limit of an inverse problem for the Schrödinger equation. *Res. Math. Sci.*, 8(3):1–18, 2021.

[4] David L Colton and Rainer Kress. *Inverse Acoustic and Electromagnetic Scattering Theory*, volume 93. Springer, 2019.

[5] Peter Hähner and Thorsten Hohage. New stability estimates for the inverse acoustic inhomogeneous medium problem and applications. *SIAM J. Math. Anal.*, 33(3):670–685, 2001.

[6] Sei Nagayasu, Gunther Uhlmann, and Jenn-Nan Wang. Increasing stability in an inverse problem for the acoustic equation. *Inverse Problems*, 29(2):025012, 2013.

[7] Roman G Novikov. Small angle scattering and X-ray transform in classical mechanics. *Ark. Mat.*, 37(1):141–169, 1999.

[8] Leonid Ryzhik, George Papanicolaou, and Joseph B Keller. Transport equations for elastic and other waves in random media. *Wave motion*, 24(4):327–370, 1996.

[9] Jean Virieux, Amit Asnaashari, Romain Brossier, Ludovic Métivier, Alessandra Ribodetti, and Wei Zhou. *6. An introduction to full waveform inversion*, pages R1–1–R1–40. Society of Exploration Geophysicists, 2017.
[10] Jean Virieux and Stéphane Operto. An overview of full-waveform inversion in exploration geophysics. *Geophysics*, 74:WCC1–WCC26, 2009.

Relative traces and numerical computation of spectral functions

Alexander Strohmaier, Alden Waters

The relative trace for the Laplace operator

We consider a (non-empty open) bounded smooth domain $\Omega \subset \mathbb{R}^d, d \geq 2$ with connected exterior which is the union of two connected components Ω_1 and Ω_2. To this scenario one can associate four unbounded self-adjoint operators in $L^2(\mathbb{R}^d)$. These operators are as follows:

(1) the operator Δ defined by the Dirichlet quadratic form on $H^1_0(\mathbb{R}^d \setminus \partial\Omega)$
(2) the operator Δ_1 defined by the Dirichlet quadratic form on $H^1_0(\mathbb{R}^d \setminus \partial\Omega_1)$
(3) the operator Δ_2 defined by the Dirichlet quadratic form on $H^1_0(\mathbb{R}^d \setminus \partial\Omega_2)$
(4) free Laplacian Δ_0 with form domain $H^1(\mathbb{R}^d)$ and domain $H^2(\mathbb{R}^d)$.

Throughout we fix $m \geq 0$. For $s \in \mathbb{R}$ define

$$(\Delta + m^2)^s, \quad (\Delta_1 + m^2)^s, \quad (\Delta_2 + m^2)^s, \quad (\Delta_0 + m^2)^s$$

by the functional calculus for unbounded self-adjoint operators. Assuming $s > 0$ or $m > 0$ these are densely defined operators whose domain contains the dense subset $C_0^\infty(\mathbb{R}^d \setminus \partial\Omega)$. In particular, the operator

$$D_s = (\Delta + m^2)^s - (\Delta_1 + m^2)^s - (\Delta_2 + m^2)^s + (\Delta_0 + m^2)^s$$

is densely defined and contains $C_0^\infty(\mathbb{R}^d \setminus \partial\Omega)$ in its domain. It is known that

$$(\Delta + m^2)^s - (\Delta_0 + m^2)^s$$

is a trace-class operator if $m > 0, s < -\frac{d}{2}$. We have shown in [1] that the operator D_s is much better behaved and is trace-class for any $s > 0$. We call $\mathrm{tr}(D_s)$ the *relative trace* of the operator $(\Delta + m^2)^s$. In particular it has a unique bounded extension to all of $L^2(\mathbb{R}^d)$. Moreover, its trace can be computed in terms of Fredholm determinants of single layer operators, as follows:

$$\mathrm{tr}(D_s) = \frac{2s}{\pi} \sin(\pi s) \int_m^\infty \lambda^{2s-1} \frac{\lambda}{\sqrt{\lambda^2 - m^2}} \Xi(\mathrm{i}\lambda) \mathrm{d}\lambda.$$

Here $\Xi(\lambda)$ is a holomorphic function in the upper half plane that decays exponentially fast along the positive imaginary axis. The function $\Xi(\lambda)$ continuously extends to a neighborhood of 0 in $\mathbb{R}$. Hence, the integral is absolutely convergent. This function $\Xi(\lambda)$ can be expressed in terms of layer potentials. To this end, let $S_\lambda : L^2(\partial\Omega) \to L^2(\partial\Omega)$ be the single layer operator, i.e. the integral operator on $\partial\Omega$ whose integral kernel is the free Green's function at frequency λ. Similarly, we have the single layer operators of the individual objects $S_{j,\lambda} : L^2(\partial\Omega_j) \to L^2(\partial\Omega_j)$.

The function Ξ is defined as the Fredholm logarithmic determinant of the operator $S_\lambda \circ (S_{1,\lambda} \oplus S_{2,\lambda})^{-1}$, i.e.

$$\Xi(\lambda) = \log \det(S_\lambda \circ (S_{1,\lambda} \oplus S_{2,\lambda})^{-1}).$$

Application in quantum field theory: One reason why this formula is significant is that for $s = \frac{1}{2}$ the trace $\frac{1}{2}\mathrm{tr}(D_{\frac{1}{2}})$ has a physical interpretation. It is the Casimir energy, or vacuum energy, of the scalar field of mass m with Dirichlet boundary conditions. Its variation when one of the objects is moved rigidly was shown to be the Casimir force as computed from the stress energy tensor in quantum field theory of the free scalar field, as proved in [3]. The above relative trace $\mathrm{tr}(D_s)$ is therefore a way to rigorously define a finite Casimir energy and allow for numerical computations of it. Indeed, such formulae were used in the physics literature to compute the Casimir forces between objects, starting from a different microscopic description of the effect in terms of fluctuating surface current. The theory also relates these quantities to the Duistermaat-Guillemin trace formula in a rigorous manner, and we refer to [4] for a detailed analysis of the connection.

The relative trace in the Maxwell setting: The situation for Maxwell's equations is more complicated, but of course actual Casimir forces are due to interactions of the photon field with the material and hence are described by Maxwell's equations. We are now reporting on the results obtained in [5] where we specialise to dimension three but allow for domains with reduced regularity. In this section therefore $\Omega \subset \mathbb{R}^3$ is a bounded strongly Lipschitz domain, again with connected exterior, and consisting of two connected components Ω_1 and Ω_2. Now Δ denotes the Laplace operator with *relative boundary conditions* acting on vector fields. These boundary conditions roughly require the tangential component of the vector-field to vanish, and the divergence to satisfy Dirichlet boundary conditions. These boundary conditions correspond to Maxwell's equations in a domain where $\partial\Omega$ is a perfect conductor. As before one can then define $\Delta, \Delta_1, \Delta_2$, and Δ_0. We also have the second order differential operator $\delta\mathrm{d} = \mathrm{curl}\,\mathrm{curl}$. Here d is the differential, and δ the codifferential and we have identified 1-forms and vector-fields. If Ω is smooth, let

$$H^{-\frac{1}{2}}(\mathrm{Div}, \partial\Omega) = \{f \in H^{-\frac{1}{2}}(\partial\Omega, T\partial\Omega) |\ \mathrm{Div} \in H^{-\frac{1}{2}}(\partial\Omega)\}. \tag{1}$$

This space can also be defined by local coordinate charts in the Lipschitz case. Recall that $H^s(\mathbb{R}^d)$ is invariant under Lipschitz mappings if $|s| \leq 1$. Let γ_t be the continuous extension of the map $f \mapsto (\nu \times f)|_{\partial\Omega}$ and $G_\lambda(x, y)$ the standard Green's function in $\mathbb{R}^3$ for the Helmholtz equation. We now let $\mathcal{L}_\lambda$ denote the standard electric field boundary layer operator for the Maxwell equations acting on the trace space $H^{-\frac{1}{2}}(\mathrm{Div}, \partial\Omega)$. This operator is defined as

$$\mathcal{L}_\lambda = \gamma_t \tilde{\mathcal{L}}_\lambda \quad \text{where} \quad \tilde{\mathcal{L}}_\lambda a = \langle \mathrm{curlcurl} G_\lambda(x, \cdot), a \rangle_{L^2(\partial\Omega)} \tag{2}$$

and $a \in H^{-\frac{1}{2}}(\mathrm{Div}, \partial\Omega)$.

The main result of [5] is that the relative operator

$$D_s = \Delta^s \delta \mathrm{d} - \Delta_1^s \delta \mathrm{d} - \Delta_2^s \delta \mathrm{d} + \Delta_0^s \delta \mathrm{d}$$

is trace-class in $L^2(\mathbb{R}^3, \mathbb{C}^3)$ for any $s > -1$ and its trace is computed as

$$\mathrm{tr}(D_s) = \frac{2(s+1)}{\pi} \sin(\pi(s+1)) \int_0^\infty \lambda^{2s+1} \Xi(\mathrm{i}\lambda) \mathrm{d}\lambda,$$

where Ξ is a function holomorphic in the upper half plane and near zero given by

$$\Xi(\lambda) = \log\det\left(\mathcal{L}_\lambda \circ (\mathcal{L}_{1,\lambda} \oplus \mathcal{L}_{2,\lambda}^{-1})^{-1}\right), \quad \text{on } H^{-\frac{1}{2}}(\mathrm{Div}, \partial\Omega).$$

The well defined quantity $\frac{1}{2}\mathrm{tr}(D_{-\frac{1}{2}})$ is expressed in terms of the Maxwell layer potential operators. The careful analysis of these operators at $\lambda = 0$ shows that for the relative trace the pole cancellation occurs which makes the object well defined. The quantity $\frac{1}{2}\mathrm{tr}(D_{-\frac{1}{2}})$ is important because it corresponds to the physical Casimir energy of the quantum photon field between perfect conductors. Forthcoming numerical experiments using BEM++ method can compute this object quickly and efficiently.

References

[1] F. Hanisch, A. Strohmaier and A. Waters. A relative trace formula for obstacle scattering. Duke Math. J. 171 (2022), no. 11, 2233–2274.

[2] A. Strohmaier and A. Waters. The Birman-Krein formula for differential forms and electromagnetic scattering. *Bull. Sci. Math. 179 (2022), Paper No. 103166, 27 pp.*

[3] Y.L. Fang and A. Strohmaier A mathematical analysis of Casimir interactions I. *Ann. Henri Poincaré 23 (2022), no. 4, 1399–1449.*.

[4] Y.L. Fang and A. Strohmaier Trace singularities in obstacle scattering and the Poisson relation for the relative trace, *Ann. Math. Qué. 46 (2022), no. 1, 55–75.* .

[5] A. Strohmaier and A. Waters. The relative trace formula in electromagnetic scattering and boundary layer operators. *arXiv:2111.15331.*

Separation of scales: Dynamical approximations for composite quantum systems

Clotilde Fermanian Kammerer

(joint work with Irene Burghardt, Rémi Carles, Benjamin Lasorne, Caroline Lasser)

We present different results obtained in collaboration with chemists [1] and [2].

Composite quantum-dynamical systems. We consider systems that can be partitioned into weakly interacting subsystems, similar to system-bath type situations, according to

$$i\partial_t \psi = H\psi, \quad \psi_{|t=0} = \psi_0$$

with

$$H = H_x + H_y + W(x,y), \quad (t,x,y) \in \mathbb{R} \times \mathbb{R}^n \times \mathbb{R}^d,$$
$$H_x = -\frac{1}{2}\Delta_x + V_1(x), \quad H_y = -\frac{1}{2}\Delta_y + V_2(y)$$

We assume that the initial data has some tensor structure

$$\psi_0(x,y) = \varphi_0^x(x)\varphi_0^y(y)$$

and we investigate a coupling regime that is partially flat, i.e., slowly varying with respect to one set of variables:

$$\|\nabla_y W(x,y)\|_{L^\infty} \ll 1 \ \text{ or } \ \|\nabla_x \nabla_y W(x,y)\|_{L^\infty} \ll 1.$$

It corresponds for example to reactive molecular fragments embedded in a large molecular bath (a protein, or a solvent).

The ansatz. We use a factorized wave function ansatz

$$\psi_{\text{app}}(t,x,y) = \mathrm{e}^{iS(t)}\, \varphi^x(t,x)\varphi^y(t,y)$$

which corresponds to replacing the interaction term W by an adequate potential.

We consider two schemes of dimension reduction: one based on Taylor expansion (collocation)

$$W_{\text{bf}}\,(x,y) = W(x,0) + W(0,y) - W(0,0)$$

and the other one based on partial averaging (mean-field)

$$W_{\text{mf}}\,(t,x,y) = \langle W\rangle_y(t,x) + \langle W\rangle_x(t,y) - \langle W\rangle(t)$$

with

$$\langle W\rangle = \frac{\int_{\mathbb{R}^{n+d}} W(x,y)\,|\varphi^x(t,x)\varphi^y(t,y)|^2\,dxdy}{\int_{\mathbb{R}^{n+d}} |\varphi^x(t,x)\varphi^y(t,y)|^2\,dxdy},$$

$$\langle W\rangle_x = \frac{\int_{\mathbb{R}^d} W(x,y)\,|\varphi^x(t,x)|^2\,dx}{\int_{\mathbb{R}^d} |\varphi^x(t,x)|^2\,dx},$$

$$\langle W\rangle_y = \frac{\int_{\mathbb{R}^n} W(x,y)\,|\varphi^y(t,y)|^2\,dy}{\int_{\mathbb{R}^d} |\varphi^y(t,y)|^2\,dy}.$$

In the collocation case, the action is taken as $S(t) = tW(0,0)$ and in the mean-field cas as

$$S(t) = \int_0^t \langle W\rangle(s)\,ds.$$

Dirac-Frenkel variational principle. The mean-field approximation stems from a Dirac Frenkel variational principle using the manifold

$$\mathcal{M} = \left\{u = \varphi^x \otimes \varphi^y \mid \varphi^x \in L^2_x,\ \varphi^y \in L^2_y\right\}.$$

One projects the solution on the manifold $\mathcal{M}$ with the constraints $\partial_t u(t) \in \mathcal{T}_{u(t)}\mathcal{M}$ and

$$\langle v, i\partial_t u(t) - Hu(t)\rangle = 0, \ \ \forall v \in \mathcal{T}_{u(t)}\mathcal{M}.$$

The observation that the tangent to $\mathcal{M}$ in u is

$$\mathcal{T}_u\mathcal{M} = \left\{v^x \otimes \varphi^y + \varphi^x \otimes v^y \mid v^x \in L^2_x,\ v^y \in L^2_y\right\}, \ \ u = \varphi^x \otimes \varphi^y$$

leads to the formula for H_{mf} (see [3, 4]).

The approximation. We analyzed in [1] the error for the wave function and for the action of observables, obtaining comparable estimates for both approaches:

$$\|\psi(t)-\psi_{\rm app}(t)\|_{L^2} \le \begin{cases} \text{const.}\, \|\nabla_y W\|_{L^\infty} \|\varphi_0^x\|_{L^2_x} \int_0^t \|y\varphi^y(s)\|_{L^2_y}\, ds \\ \text{const.}\, \|\nabla_x \nabla_y W\|_{L^\infty} \int_0^t \|x\varphi^x(s)\|_{L^2_x} \|y\varphi^y(s)\|_{L^2_y}\, ds \end{cases}$$

These estimates hold under very general assumptions that can be easily relaxed:

- Assumptions on the potential:

$$V_1 \in C^\infty(\mathbb{R}^n;\mathbb{R}),\ V_2 \in C^\infty(\mathbb{R}^d;\mathbb{R}),\ W \in C^\infty(\mathbb{R}^{n+d};\mathbb{R}).$$

- Assumptions on the data:

$$\varphi_0^x \in \mathcal{S}(\mathbb{R}^n;\mathbb{C}), \quad \varphi_0^y \in \mathcal{S}(\mathbb{R}^d;\mathbb{C}) \quad (\text{hence } \psi_0 \in \mathcal{S}(\mathbb{R}^{n+d};\mathbb{C})).$$

One can also obtain estimates in Sobolev weighted spaces.

Numerical realizations. Numerical studies are presented in [2] to assess error estimates for a separable (Hartree) approximation for dynamically evolving composite quantum systems which exhibit distinct scales defined by their mass and frequency ratios. Specifically, we consider a representative two-dimensional tunneling system where a double well and a harmonic coordinate are cubically coupled.

$$V_1(x) = \frac{x^2}{2}\left(\frac{x}{2\ell}-1\right)^2, \quad V_2(y) = \frac{\omega}{2}y^2, \quad W(x,y) = \frac{\varepsilon^2}{2}xy^2.$$

The initial data is taken as a Gaussian

$$\psi_0(x,y) = (2\pi)^{-1/2}\omega^{-1/4}\mathrm{e}^{-\frac{x^2}{2}-\frac{y^2}{2\omega}}.$$

In the formula above ω is the frequency ratio, ε the mass ratio and ℓ the distance between the wells.

The time-dependent Hartree approximation is compared with a fully correlated solution, for different parameter regimes

$$\varepsilon = \omega\sqrt{\frac{\alpha-1}{2\ell}}, \ \ \alpha \in \left\{\frac{1}{4},\frac{1}{3},\frac{1}{2},\frac{3}{4},\frac{2}{3},1\right\}.$$

The impact of the coupling and the resulting correlations are quantitatively assessed in terms of a time-dependent reaction probability along the tunneling coordinate. We will show that the numerical error is correctly predicted on moderate time scales by a theoretically derived error estimate.

Quantum-classical systems. Further, we also study in [1] the situation where one of the sets of variables is semiclassically scaled in the variable y:

$$H_y = -\frac{\varepsilon^2}{2}\Delta_y + V_2(y).$$

We derive a quantum-classical formulation for initial data that have a semi-classical component in the y variable

$$\psi_0(x,y) = \varphi_0^x(x)\, g^\varepsilon(y), \ \ g^\varepsilon(y) = (2\pi)^{-d/2}\varepsilon^{-d/4}\,\mathrm{Exp}\left(-\frac{|y-q_0|^2}{\varepsilon} + \frac{i}{\varepsilon}p_0\cdot(y-q_0)\right)$$

We use an ansatz of the form

$$\psi(t,x,y) = \psi_1^\varepsilon(t,x)\,\mathrm{e}^{\frac{i}{\varepsilon}S(t)+\frac{i}{\varepsilon}p(t)\cdot(y-q(t))}\; u_2\left(t, \frac{y-q(t)}{\sqrt{\varepsilon}}\right)$$

with action $S(t)$ and trajectories $q(t), p(t)$ that are either classical trajectories or variational ones.

Conclusion. The present study is the first step towards a general analysis of scale separation in the context of tensorized wavefunction representations as considered in MCTDH and G-MCTDH schemes (see [5])

$$\psi_{\mathrm{app}}(t,x,y) = \sum_{j,\ell} a_{j\ell}(t)\,\varphi_j^{(x)}(t,x)\,\varphi_\ell^{(y)}(t,y)$$

where the families $(\varphi_j^{(x)}(t))_{j\geq 1}$ and $(\varphi_\ell^{(y)}(t))_{\ell\geq 1}$ satisfy orthonormality or rank conditions and the complex coefficients $a_{k\ell}(t)$ gauge constraints.

References

[1] I. Burghardt, R. Carles, C. Fermanian Kammerer, B. Lasorne and C. Lasser, *Separation of scales: a quantum-classical approach for complex systems and a system-bath ansatz*, J. Phys. A: Math. Theor. **54** (2021) 414002.

[2] I. Burghardt, R. Carles, C. Fermanian Kammerer, B. Lasorne, C. Lasser, *Dynamical approximations for composite quantum systems: Assessment of error estimates for a separable ansatz*, J. Phys. A: Math. Theor. **55** (2022) 224010.

[3] C. Lasser and C. Lubich, *Computing quantum dynamics in the semiclassical regime*, Acta Numer. **29** (2020), 229–401.

[4] C. Lubich, *From quantum to classical molecular dynamics: reduced models and numerical analysis,* Zürich Lectures in Advanced Mathematics (EMS, Zürich), 2008.

[5] S. Römer and I. Burghardt *Towards a variational formulation of mixed quantum-classical molecular dynamics*, Molecular Physics, **111** (2013), 3618–362.

A survey on high-frequency scattering relating to smooth convex scatterers

Fatih Ecevit

1. Single scattering

The two-dimensional single scattering problem for a plane wave $u^{\mathrm{inc}}(x,k) = e^{ik\,\alpha\cdot x}$ impinging on a smooth compact convex obstacle K has been the content of extensive research in the last twenty years.

High-frequency integral equation methodologies aimed at frequency independent simulations, in this connection, are almost entirely related to the Dirichlet boundary condition [4, 12, 5, 10, 9]. These methods rely on the Melrose-Taylor

asymptotic expansion [13, 11]

$$\eta(x,k) = e^{ik\,\alpha\cdot x}\eta^{\text{slow}}(x,k) \sim e^{ik\,\alpha\cdot x}\sum_{p,q\geq 0} a_{p,q}(x,k) \tag{1}$$
$$= e^{ik\,\alpha\cdot x}\sum_{p,q\geq 0} k^{\frac{2-2p-3q}{3}}\, b_{p,q}(x)\,\Psi^{(p)}(k^{\frac{1}{3}}Z(x))$$

where η is the unknown normal derivative of the total field on ∂K. Here $b_{p,q}$ and Ψ are complex-valued smooth functions; $\Psi(\tau) \sim \sum_{j=0}^{\infty} a_j \tau^{1-3j}$ as $\tau \to \infty$, and it rapidly decreases in the sense of Schwartz as $\tau \to -\infty$; and Z is a real-valued smooth function reflecting the geometry of the scattering problem. More precisely, it is positive on $\partial K^{\text{IL}} = \{x \in \partial K : \alpha \cdot \nu(x) < 0\}$ (ν is the exterior unit normal), negative on $\partial K^{SR} = \{x \in \partial K : \alpha \cdot \nu(x) > 0\}$, and vanishes to first order on $\partial K^{SB} = \{x \in \partial K : \alpha \cdot \nu(x) = 0\}$. Recently developed Galerkin boundary element methods [10, 9] based on a detailed study of the asymptotic expansion (1) demand an $\mathcal{O}(k^{\epsilon})$ increase, for any $\epsilon > 0$, in the number of degrees of freedom to maintain accuracy with increasing frequency. Moreover, these methods are frequency independent when a sufficient number of terms in the asymptotic expansion (1) is incorporated into integral equation formulations [6].

The Neumann boundary condition has been considered only recently [8]. The Melrose-Taylor asymptotic expansion in this case [13, 8] takes on the form of a fourfold asymptotic series

$$\eta(x,k) = e^{ik\,\alpha\cdot x}\eta^{\text{slow}}(x,k) \tag{2}$$
$$\sim e^{ik\,\alpha\cdot x}\sum_{\substack{p,q,r\geq 0\\ \ell\leq -1}} k^{-\frac{1+2p+3q+r+\ell}{3}+(\ell+1)_-}\, b_{p,q,r,\ell}(x)\,(\Psi^{r,\ell})^{(p)}(k^{\frac{1}{3}}Z(x))$$

where η is the unknown total field on the boundary ∂K, $t_- = \min\{t, 0\}$, $b_{p,q,r,\ell}$ are complex-valued smooth functions, Z is the same function as in the Dirichlet case, and $\Psi^{r,\ell}$ are complex-valued smooth functions with an asymptotic expansion $\Psi^{r,\ell}(\tau) \sim \sum_{j=0}^{\infty} a_{r,\ell,j}\tau^{1+\ell-2r-3j}$ as $\tau \to \infty$, and they rapidly decrease in the sense of Schwartz as $\tau \to -\infty$. The Galerkin boundary element methods developed in [8] display the same characteristics as in their Dirichlet counterparts [10, 6, 9].

As stated above, in (1) and (2), the behavior of the functions Ψ and $\Psi^{r,\ell}$ is characterized as a decay in the sense of Schwarz as $\tau \to -\infty$. A rigorous precise description, in connection therewith, remains as an important open problem as this would allow for not only the construction of better approximations on ∂K^{SR} but also the derivation of asymptotic expansions for occluded multiple scattering problems.

2. Multiple scattering

High-frequency scattering problems in the exterior of a disjoint union $K = \bigcup_{j=1}^{N} K_j$ of smooth compact convex obstacles K_j gives rise to a variety of non-trivial sub-problems. In this case, the multiple scattering formulation can be based either on a Neumann series decomposition applied to integral equations [11, 1, 7], or directly

on partial differential equation formulations [2]. In both cases, an important subproblem is the derivation of asymptotic expansions of multiple scattering iterations $\{\eta_m\}_{m\geq 0}$ relating to an arbitrary sequence of obstacles $\{K_m\}_{m\geq 0} \subset \{K_1, \ldots, K_N\}$ with $K_{m+1} \neq K_m$; η_m is the unknown normal derivative of the m-th total field on ∂K_m for the Dirichlet boundary condition, and it is the m-th total field on ∂K_m for the Neumann case. As shown in [11, 1, 2], for each of these conditions the unknown η_m admits a phase extraction in the form

$$\eta_m(x,k) = e^{ik\,\phi_m(x)}\eta_m^{\text{slow}}(x,k)$$

where the phase ϕ_m is the optical ray distance as a result of m-reflections,

$$\eta_m^{\text{slow}}(x,k) \sim \sum_{p,q\geq 0} a_{p,q,m}(x,k) = \sum_{p,q\geq 0} k^{\frac{2-2p-3q}{3}}\, b_{p,q,m}(x)\, \Psi^{(p)}(k^{\frac{1}{3}} Z_m(x))$$

for the Dirichlet boundary condition, and

$$\begin{aligned}\eta_m^{\text{slow}}(x,k) &\sim \sum_{\substack{p,q,r\geq 0\\ \ell\leq -1}} a_{p,q,r,\ell,m}(x,k)\\ &= \sum_{\substack{p,q,r\geq 0\\ \ell\leq -1}} k^{-\frac{1+2p+3q+r+\ell}{3}+(\ell+1)_-}\, b_{p,q,r,\ell,m}(x)\, (\Psi^{r,\ell})^{(p)}(k^{\frac{1}{3}} Z_m(x))\end{aligned}$$

for the Neumann case; the function Z_m is the same in both cases and has the same geometric structure as the function Z appearing in (1) and (2).

For the Dirichlet case, rate of convergence formulas for multiple scattering iterations η_m confined to periodic orbits were derived based on explicit representations of the leading order terms $a_{0,0,m}$ in the form of iterated continued fractions on illuminated regions [11, 1]. In two dimensions [11] these rate of convergence formulas imply, for instance, for a two periodic orbit

$$\frac{\eta_{m+2}}{\eta_m} \approx \frac{1}{\sqrt{(1+d\,\kappa_1)\,(1+d\,\kappa_2)\left(1+\sqrt{1-\dfrac{1}{(1+d\,\kappa_1)\,(1+d\,\kappa_2)}}\right)}}$$

where d is the distance between the scatterers, and κ_j are the curvatures at the distance minimizing points. In three dimensions [1], the asymptotic rate of convergence depends on the distance, the principal curvatures at the distance minimizing points, and the relative rotational angle between the principal directions. These rate of convergence formulas, as justified by numerical tests, are accurate within errors of $\mathcal{O}(k^{-1})$ with increasing frequency. Yet, a completely rigorous proof relating to the actual densities η_m remains as an open problem.

Acceleration of convergence of the multiple scattering series has also been considered [3]. The approach in [3] was based on a novel modification of a Krylov subspace method coupled with a preconditioning technique relying on Kirchhoff approximations. In configurations consisting of more than two scatterers, the problem of collectively computing the exponentially increasing number of single scattering returns entering in the Neumann series iterations remains as an open

problem. While, perhaps, this issue can be resolved using the stabilization of multiple scattering ray paths, computation of the remaining infinite tail in the multiple series scattering poses an additional difficulty since the series may actually diverge.

References

[1] A. Anand, Y. Boubendir, F. Ecevit, F. Reitich, *Analysis of multiple scattering iterations for high-frequency scattering problems. II. The three-dimensional scalar case*, Numer. Math. **114**(3) (2010), 373–427.

[2] Y. Boubendir, F. Ecevit, *Asymptotic expansions of high-frequency multiple scattering iterations for sound hard scattering problems*, submitted.

[3] Y. Boubendir, F. Ecevit, F. Reitich, *Acceleration of an iterative method for the evaluation of high-frequency multiple scattering effects*, SIAM J. Sci. Comput. **39**(6) (2017), B1130–B1155.

[4] O.P. Bruno, C.A. Geuzaine, J.A. Monroe, F. Reitich, *Prescribed error tolerances within fixed computational times for scattering problems of arbitrarily high frequency: the convex case*, Phil. Trans. R. Soc. London **362** (2004), 629–645.

[5] V. Domínguez, I.G. Graham, V.P. Smyshlyaev, *A hybrid numerical-asymptotic boundary integral method for high-frequency acoustic scattering*, Numer. Math. **106**(3) (2007), 471–510.

[6] F. Ecevit, *Frequency independent solvability of surface scattering problems*, Turkish J. Math. **42**(2) (2018), 407–422.

[7] F. Ecevit, A. Anand, Y. Boubendir, *Galerkin boundary element methods for high-frequency multiple-scattering problems*, J. Sci. Comput. **83**(1) (2020), Paper No. 1, 21p.

[8] F. Ecevit, Y. Boubendir, A. Anand, S. Lazergui, *Spectral Galerkin boundary element methods for high-frequency sound-hard scattering problems*, Numer. Math. **150**(3) (2022), 803–847.

[9] F. Ecevit, H.H. Eruslu, *A Galerkin BEM for high-frequency scattering problems based on frequency-dependent changes of variables*, IMA J. Numer. Anal. **39**(2) (2019), 893–923.

[10] F. Ecevit, H.Ç. Özen, *Frequency-adapted Galerkin boundary element methods for convex scattering problems*, Numer. Math. **135**(1) (2017), 27–71.

[11] F. Ecevit, F. Reitich, *Analysis of multiple scattering iterations for high-frequency scattering problems. I. The two-dimensional case*, Numer. Math. **114**(2) (2009), 271–354.

[12] D. Huybrechs, S. Vandewalle, *A sparse discretization for integral equation formulations of high frequency scattering problems*, SIAM J. Sci. Comput. **29**(6) (2007), 2305–2328.

[13] R.B. Melrose, M.E. Taylor, *Near peak scattering and the corrected Kirchhoff approximation for a convex obstacle*, Adv. Math. **55** (1985), 242–315.

Efficient approximation of high-frequency Helmholtz solutions by semiclassical Gabor wavelets

Théophile Chaumont-Frelet

(joint work with Victorita Dolean, Maxime Ingremeau)

The numerical solution of high-frequency scattering problems, although being central in a large number of applications, remains to this day a computational challenge. This is largely due to the fact that standard numerical tools based on piecewise polynomial approximations require (at least) a constant number of degrees of freedom (DOFs) per wavelength. Thus, considering a wavenumber k, and a domain in $\mathbb{R}^d$ with diameter ℓ, polynomial-based methods require about $k\ell$ DOFs in each space dimensions.

More concretely, finite element methods require about $(k\ell)^d$ DOFs to represent with a uniform accuracy as the frequency increased [2]. Despite the large number of required DOFs, the advantages of finite element methods is that they lead to a sparse matrix and readily apply in heterogeneous media.

When the Green's function is available, the Helmholtz problem can be reformulated as a boundary integral equation. Then [3], boundary element methods may be employed to accurately represent the solution with only $(k\ell)^{d-1}$ DOFs. However, the resulting discretization matrix is dense, and it is in general not possible to account for heterogeneous media.

The purpose of the present work is to introduce a new family of basis functions that (i) easily operate in heterogeneous media, (ii) lead to essentially sparse Galerkin matrices and (iii) correctly represent high-frequency solutions to scattering problem with $(k\ell)^{d-1/2}$ DOFs.

The proposed method relies on semi-classical Gabor wavelets, namely, functions of the form

$$\Psi_{k,\boldsymbol{m},\boldsymbol{n}}(\boldsymbol{x}) := \left(\frac{k}{\pi}\right)^{d/4} e^{-\frac{k}{2}|\boldsymbol{x}-\sqrt{\pi/k}\boldsymbol{m}|^2} e^{ik\sqrt{\pi/k}\boldsymbol{n}\cdot\boldsymbol{x}}, \qquad \boldsymbol{m},\boldsymbol{n}\in\mathbb{Z}^d$$

as basis functions. Crucially, each of these shape functions is micro-localized around a single point in phase space. Specifically, $\Psi_{k,\boldsymbol{m},\boldsymbol{n}}$ is concentrated around the point $\sqrt{\pi/k}\boldsymbol{m}$ whereas its semi-classical Fourier transform is localized around $\sqrt{\pi/k}\boldsymbol{n}$. We may thus think about this family of basis functions as a Cartesian grid of $\mathbb{R}^{2d}$ with lattice points spaced by about $k^{-1/2}$.

The key idea of the proposed method is that the micro-localization properties of the shape functions may be combined with micro-localization properties of high-frequency solutions, which are explicitly known from semi-classical analysis. Specifically, it is known that the solution of a high-frequency scattering problem is concentrated around the characteristic set

$$\Sigma := \{(\boldsymbol{x},\boldsymbol{\xi})\in\mathbb{R}^{2d};\ p(\boldsymbol{x},\boldsymbol{\xi})=0\}$$

of the symbol p associated with the Helmholtz problem. The symbol itself is explicitly known from the coefficients describing the propagation medium, so that the hypersurface Σ is explicitly available. We can thus define a discretization space by selecting the shape functions micro-localized close to Σ.

Our main result is that, given an arbitrarily small $\varepsilon > 0$, the discretization space

$$W := \mathrm{Vect}\left\{\Psi_{k,\boldsymbol{m},\boldsymbol{n}};\ \left|p\left(\sqrt{\frac{\pi}{k}}\boldsymbol{m},\sqrt{\frac{\pi}{k}}\boldsymbol{n},\right)\right| \le k^{-1/2+\varepsilon}\right\}$$

contains $(k\ell)^{d-1/2+\varepsilon}$ DOFs while ensuring that

$$\min_{w\in W}\|\boldsymbol{\nabla}(u-w)\|_{L^2} \le C_\varepsilon,$$

uniformly in k, where u is the solution to the scattering problem [1].

References

[1] T. Chaumont-Frelet, V. Dolean and M. Ingremeau, *Efficient approximation of high-frequency Helmholtz solutions by Gaussian coherent states*, arXiv preprint 2208.04851 (2022).

[2] M.J. Melenk and S.A. Sauter, *Wavenumber explicit convergence analysis for Galerkin discretizations of the Helmholtz equation*, SIAM J. Numer. Anal. **49** (2011), 1210–1243.

[3] J. Galkowski and E.A. Spence *Does the Helmholtz boundary element method suffer from the pollution effect?*, arXiv preprint 2201.09721 (2022).

Decompositions of high-frequency Helmholtz solutions and application to the finite element method

David Lafontaine

(joint work with Jeffrey Galkowski, Euan A. Spence, Jared Wunsch)

Motivation and informal statement of our results. We are interested in the Helmholtz equation in the exterior of an obstacle $\mathcal{O}$, with Dirichlet boundary condition and Sommerfeld radiation condition at infinity (corresponding to the fact that we are looking for an *outgoing* wave)

$$\begin{cases} \Delta u + k^2 u = f & \text{in } \mathbb{R}^d \backslash \mathcal{O}, \\ u = 0 & \text{on } \partial\mathcal{O}, \\ \partial_r u - iku = o(r^{-(d-1)/2}) & \text{as } r \to \infty. \end{cases}$$

A popular choice to solve numerically such an equation is the *hp*-finite element method (*hp*-FEM), where one decreases the meshsize h and increases the polynomial degree p of the approximation, both depending on the frequency k of the solution, to obtain accuracy. A natural question in this framework is the following: *what is a condition on h, p, and k for these methods to converge?* As the solution oscillates at scale k^{-1}, we should need at least a number of degrees of freedom $\#\text{DOF} \gtrsim k^d$. Is it enough ?

Melenk and Sauter [MS10, MS11] gave a positive answer to this question when the obstacle is *analytic* (see also [MPS13] and [EM12] for the interior impedance problem). They have shown that, under the conditions

$$\frac{hk}{p} \leq C_1, \qquad p \geq C_2 \log k,$$

the solution to the discrete problem exists, is unique, and is quasi-optimal (that is, it is the best possible approximation of the solution by a piecewise polynomial, up to a multiplicative constant). In particular, under these conditions, one can construct h and p so that the number of degrees of freedom of the problem verifies

$$\#\text{DOF} \simeq \left(\frac{p}{h}\right)^d \lesssim k^d.$$

In other words, *hp*-FEM applied to this setting does not suffer from the *pollution effect* that plagues the h-FEM (where p is left constant), for which one needs strictly more degrees of freedom than k^d to maintain accuracy [BS00].

The proof of Melenk and Sauter [MS10, MS11] is based on a decomposition of the Helmholtz solutions

$$(\star) \qquad u = u_{H^2} + u_{\mathcal{A}},$$

where u_{H^2} verifies *better* estimates in the frequency k than u, and $u_{\mathcal{A}}$ verifies the same estimates in k as u but is *analytic*. The idea is that u_{H^2} contains the high frequencies ($\gtrsim k$) of the solution, and $u_{\mathcal{A}}$ the low frequencies ($\lesssim k$). Their proof of the decomposition ($\star$) is based on explicit computations that cannot be generalised in a straightforward way to more general problems, such as the Helmholtz equation with variables coefficients, despite the large interest for such a problem.

In the works [LSW22, GLSW21, GLSW22], we tackled the question of *understanding the frequency-decomposition ($\star$) in the most general possible situation.* We obtained the following results.

(1) In [LSW22], we obtained the decomposition ($\star$) for the variable C^∞ coefficients equation in $\mathbb{R}^d$.
(2) Then, in [GLSW21], we have shown such a decomposition in the very general *black-box scattering* framework of Sjöstrand-Zworski.
(3) Finally, in [GLSW22], we extended this result to the problem truncated with a Perfectly Matched Layer (PML).

In particular, one can apply our results to show that *hp*-FEM applied to the equation

(a) without obstacle and with variable C^∞ coefficients,
(b) posed in the exterior of an analytic obstacle and with variable C^∞ coefficients which are analytic near the obstacle,

does not suffer from the pollution effect, both for the outgoing problem and PML.

Some ideas behind the proofs of the results [LSW22, GLSW21, GLSW22]**.** The decomposition in $\mathbb{R}^d$ for the C^∞ variable-coefficients equation [LSW22] is obtained by projecting the solution u, spatially truncated in the ball $B(0,R)$ where we seek to obtain the decomposition, on its high ($\gtrsim k$) and low ($\lesssim k$) Fourier modes. In other words, we define

$$u_{H^2} := \Pi_{\mathrm{High}}(\varphi u), \quad u_{\mathcal{A}} := \Pi_{\mathrm{Low}}(\varphi u),$$

where $\varphi \in C_c^\infty$ is equal to one in $B(0,R)$, Π_{Low} is defined as a Fourier multiplier truncating in Fourier variables $\leq \mu k$ for some $\mu \gg 1$, and $\Pi_{\mathrm{High}} := I - \Pi_{\mathrm{Low}}$. Thanks to its Fourier localisation, it is immediate to see that $u_{\mathcal{A}}$ is analytic, and even entire, using Parseval identity. On the other hand, the bound on u_{H^2} is obtained using *semiclassical ellipticity*: for μ large enough, u_{H^2} lives in phase-space where the equation is invertible modulo negligible terms.

Attempting to generalize this method [LSW22] to setups including boundaries, we run into technical issues involving the extension of solutions to the whole space when trying to use frequency projections defined from Fourier multipliers. Instead, we have another idea: rather use frequency projections defined *through the functional calculus*. In other words, we define

$$\Pi_{\mathrm{High}} = (1-\psi)(P), \quad \Pi_{\mathrm{Low}} := \psi(P),$$

where P is the operator associated with our Helmholtz equation $Pu + k^2 u = f$ and $\psi \in C_c^\infty(\mathbb{R})$, and u_{H^2} and $u_{\mathcal{A}}$ will be defined as previously. This idea has two immediate advantages: these projections commute with the equation, and we can now try to work with an operator P as general as possible. Taking advantage of the later, we will work in the very general *black-box scattering* framework of Sjöstrand and Zworski [SZ91], where in addition to some suitable compatibility conditions, P is only assumed to be a self-adjoint operator coinciding with the Laplacian outside "the black-box" $B(0, R_0)$, where it is left unspecified. Following this idea, we were able to show a very general, albeit abstract decomposition result, reading in an informal way:

Theorem 1 (Main abstract decomposition from [GLSW21], informal version)**.** *Let P be a black-box scattering operator of Sjöstrand-Zworski. We make the following assumptions.*

- (H1) *The solution operator associated with the Helmholtz equation is polynomially bounded in the frequency k.*
- (H2) *One has an estimate quantifying the regularity of P "inside the black-box" $B(0, R_0)$.*

Then, any solution u of the Helmholtz equation $(P+k^2)u = k^2 f$ can be decomposed as

$$u = u_{H^2} + u_{\mathcal{A}}.$$

Where

- *u_{H^2} verifies a black-box version of the estimate*
$$\|u\|_{L^2} + k^{-m}\|u\|_{\dot{H}^m} \lesssim \|f\|_{L^2}.$$
- *$u_{\mathcal{A}}$ verifies the same estimates in k as u but is* regular*. This regularity is dictated by the regularity of the underlying problem as measured by (H2).*

The bound on u_{H^2} relies once again on ellipticity : near the black-box, we are able to show an abstract ellipticity result from functional-calculus abstract manipulations; whereas away from the black-box, the functional calculus coincides with the semiclassical pseudo-differential calculus up to negligible terms as observed by Sjöstrand [Sj97], and we are able to use genuine semiclassical ellipticity as in [GLSW21]. On the other hand, the regularity bounds on $u_{\mathcal{A}}$ follow from the morphism property of the functional calculus together with the estimate (H2).

As the assumption (H1) (arising similarly in [LSW22]) always holds outside a set of frequencies of arbitrarily small measure [LSW21], the key to apply such a result to concrete Helmholtz problems is to find a suitable estimate of type (H2). For example, outside an analytic Dirichlet obstacle for the equation with C^∞ variable-coefficients which are analytic near the obstacle, we are able to use as (H2) an heat-flow estimate (more precisely, we combine a folklore estimate tracing back to [Fri69] with the more recent [EMZ17]) to obtain a decomposition in this set-up, allowing us to show the sharp convergence result for *hp*-FEM.

Whereas we first obtained these results for the outgoing Helmholtz solutions, the corresponding PML problems have the substantial additional difficulty that

the scaled Laplacian is a non self-adjoint operator. In [GLSW22], building on the outgoing case and the recent progress [GLS21] on PML accuracy, we were able to obtain strictly analogous results in such a setup, using frequency cut-offs defined via the *non-scaled* calculus as in [GLSW21] together with the (semiclassical) ellipticity of PML in the scaling region.

References

[BS00] I. M. Babuška and S. A. Sauter, *Is the pollution effect of the FEM avoidable for the Helmholtz equation considering high wave numbers?*, SIAM Review (2000), 451–484.

[EM12] S. Esterhazy and J. M. Melenk, *On stability of discretizations of the Helmholtz equation*, Numerical Analysis of Multiscale Problems (I. G. Graham, T. Y. Hou, O. Lakkis, and R. Scheichl, eds.), Springer, 2012, pp. 285–324.

[EMZ17] L. Escauriaza, S. Montaner, and C. Zhang, *Analyticity of solutions to parabolic evolutions and applications*, SIAM J. Math. Anal. **49** (2017), no. 5, 4064–4092. MR 3713902

[Fri69] A. Friedman, *Partial differential equations*, Holt, Rinehart and Winston, Inc., New York-Montreal, Que.-London, 1969. MR 0445088

[GLS21] J. Galkowski, D. Lafontaine, and E. A. Spence, *Perfectly-matched-layer truncation is exponentially accurate at high frequency*, arXiv preprint arXiv:2105.07737 (2021).

[GLSW21] J. Galkowski, D. Lafontaine, E. A. Spence, and J. Wunsch, *Decompositions of high-frequency Helmholtz solutions via functional calculus, and application to the finite element method*, arXiv preprint arXiv:2102.13081 (2021).

[GLSW22] ———, *The hp-FEM applied to the Helmholtz equation with PML truncation does not suffer from the pollution effect*, arXiv preprint arXiv:2207.05542 (2022).

[LSW21] D. Lafontaine, E. A. Spence, and J. Wunsch, *For most frequencies, strong trapping has a weak effect in frequency-domain scattering*, Communications on Pure and Applied Mathematics **74** (2021), no. 10, 2025–2063.

[LSW22] ———, *Wavenumber-explicit convergence of the hp-FEM for the full-space heterogeneous Helmholtz equation with smooth coefficients*, Comp. Math. Appl. **113** (2022), 59–69.

[MPS13] J. M. Melenk, A. Parsania, and S. Sauter, *General DG-methods for highly indefinite Helmholtz problems*, Journal of Scientific Computing **57** (2013), no. 3, 536–581.

[MS10] J. M. Melenk and S. Sauter, *Convergence analysis for finite element discretizations of the Helmholtz equation with Dirichlet-to-Neumann boundary conditions*, Math. Comp **79** (2010), no. 272, 1871–1914.

[MS11] ———, *Wavenumber explicit convergence analysis for Galerkin discretizations of the Helmholtz equation*, SIAM J. Numer. Anal. **49** (2011), 1210–1243.

[Sj97] J. Sjöstrand, *A trace formula and review of some estimates for resonances*, 377–437. MR 1451399

[SZ91] J. Sjöstrand and M. Zworski, *Complex scaling and the distribution of scattering poles*, J. Amer. Math. Soc. **4** (1991), no. 4, 729–769. MR 1115789

Regularity by decomposition for the Helmholtz equation in heterogeneous media

Jens Markus Melenk
(joint work with M. Bernkopf, T. Chaumont-Frelet, I. Perugia, A. Rieder)

On a bounded domain $\Omega \subset \mathbb{R}^d$, $d \in \{2,3\}$, we consider the Helmholtz equation

$$-\nabla \cdot (A(x)\nabla u) - k^2 n^2(x) u = f \quad \text{in } \Omega. \tag{1}$$

Here, Ω has an analytic boundary $\Gamma := \partial\Omega$, $A \in L^\infty(\Omega, \mathbb{R}^{d\times d})$ is pointwise symmetric positive definite with $0 < a_{\min}\,\mathrm{I} \le A(x)$ for $x \in \Omega$ and $n \in L^\infty(\Omega)$ with $0 < n_{\min} \le n(x)$ for $x \in \Omega$. Furthermore, A and n are piecewise analytic, i.e., Ω can be decomposed as $\overline{\Omega} = \cup_{j=1}^J \overline{P_j}$ where each open P_j has an analytic boundary, and A, n are analytic on $\overline{P_j}$ for each $j \in \{1,\dots,J\}$. We set $\Gamma_{\mathrm{int}} := \left(\cup_{j=1}^J \partial P_j\right) \setminus \Gamma$. We assume that $k \ge k_0 > 0$. Our regularity results will involve classes of piecewise analytic functions so that for open sets $\omega \subset \mathbb{R}^d$ we denote

$$\mathcal{A}(M,\gamma,\omega) := \{u \in C^\infty(\omega) \,|\, \|D^\alpha u\|_{L^2(\omega)} \le M\gamma^{|\alpha|} \max\{k,|\alpha|+1\}^{|\alpha|} \quad \forall \alpha \in \mathbb{N}_0^d\}.$$

Analyticity classes of functions on Γ can be defined as traces of functions from an analyticity class in a neighborhood of Γ.

1. Bounded domains

The simplest setting is to equip (1) with the impedance boundary condition

$$\mathbf{n} \cdot A\nabla u - \mathbf{i}ku = g \quad \text{on } \Gamma \tag{2}$$

for some $g \in L^2(\Gamma)$. Here, $\mathbf{n}$ stands for the outer normal vector. Problem (1), (2) is understood in the weak sense, i.e., to seek $u \in H^1(\Omega)$ such that

$$B(u,v) := \int_\Omega (A(x)\nabla u)\cdot\nabla\overline{v} - k^2\int_\Omega n^2(x) u\overline{v} + \mathbf{i}k\int_\Gamma u\overline{v} = \ell(v) := \int_\Omega f\overline{v} + \int_\Gamma g\overline{v} \tag{3}$$

for all $v \in H^1(\Omega)$. We assume *polynomial well-posedness* of the problem (1), (2), i.e., there are $C > 0$, $\theta \ge 0$ independent of k such that the solution u satisfies

$$\|u\|_{1,k} := \|\nabla u\|_{L^2(\Omega)} + k\|u\|_{L^2(\Omega)} \le Ck^\theta \left[\|f\|_{L^2(\Omega)} + k^{1/2}\|g\|_{L^2(\Gamma)}\right]. \tag{4}$$

Given a closed $V_N \subset H^1(\Omega)$, the Galerkin approximation $u_N \in V_N$ to u is given by the condition

$$\forall v \in V_N: \quad B(u_N, v) = \ell(v). \tag{5}$$

Introducing the adjoint solution operator S_k^* by the condition

$$\forall v \in H^1(\Omega): \quad B(v, S_k^* f) = \int_\Omega v\overline{f}$$

and the adjoint approximation property

$$\eta := \sup_{f\in L^2(\Omega)} \inf_{v\in V_N} \frac{\|S_k^* f - v\|_{1,k}}{\|f\|_{L^2(\Omega)}}$$

one can show (see, e.g., [6, 7]) quasioptimality of the Galerkin error $\|u - u_N\|_{1,k}$ provided that $k\eta$ is sufficiently small. To quantify η, k-explicit regularity assertions for the solution of Helmholtz problems (note: $S_k^* f$ solves again a Helmholtz problem akin to (1), (2)) are necessary. We have, generalizing [6, 7]:

Theorem 1. *There are constants C, $\gamma > 0$ independent of k such that the solution u of (1), (2) can be decomposed as $u = u_{H^2} + u_{\mathcal{A}}$ with*

$$\|u_{H^2}\|_{H^2(\Omega\setminus\Gamma_{\rm int})} \le C\left[\|f\|_{L^2(\Omega)} + \|g\|_{H^{1/2}(\Gamma)}\right], \qquad u_{\mathcal{A}} \in \mathcal{A}(Ck^\theta, \gamma, \Omega \setminus \Gamma_{\rm int}).$$

As a corollary, one obtains for the choice $V_N = S^{p,1}(\mathcal{T})$ of piecewise (mapped) polynomials of degree p on a mesh $\mathcal{T}$ of width h (under assumptions on the mesh spelled out in [6, 7, 1]) the following result:

Corollary 2 ([6, 7, 1])**.** *Given $c_2 > 0$ there are C, $c_1 > 0$ independent of k such that the scale resolution condition*

$$\frac{kh}{p} \le c_1 \quad \textit{and} \quad p \ge c_2 \log k \tag{6}$$

implies existence of the discrete approximation $u_N \in S^{p,1}(\mathcal{T})$ together with

$$\|u - u_N\|_{1,k} \le C \inf_{v \in S^{p,1}(\mathcal{T})} \|u - v\|_{1,k}. \tag{7}$$

Remark 3. Key to the proof of Cor. 2 is the decomposition of Thm. 1. The technique to prove Thm. 1 and Cor. 2 applies to several other time-harmonic wave propagation problems: the boundary condition (2) can be replaced by an exact Dirichlet-to-Neumann map, by second order absorbing boundary conditions, or by a fixed width PML, [1]. In the following section, we discuss in more detail a numerically realizable coupling procedure. Corresponding decomposition results for Maxwell's equation can be found in [5, 4].

2. k-explicit analysis of a FEM-BEM coupling

For $d \in \{2, 3\}$ we consider the heterogeneous Helmholtz equation

$$-\nabla \cdot (A(x)\nabla u) - k^2 n^2 u = f \quad \text{in } \mathbb{R}^d, \qquad u \text{ satisfies Sommerfeld rad. cond.} \tag{8}$$

with A of the form $A(x) = a(x)\,\mathrm{I}$ for a scalar function a, $\operatorname{supp}(A - \mathrm{I})$, $\operatorname{supp}(n-1)$, $\operatorname{supp} f \subset \overline{\Omega}$, and A, n are piecewise analytic as above. Again, we assume that (8) is polynomially well-posed, i.e., the solution u satisfies, for some $C > 0$ independent of $\theta \ge 0$

$$\|u\|_{1,k} \le Ck^\theta \|f\|_{L^2(\Omega)}. \tag{9}$$

[3, 2] proposes a three-field FEM-BEM coupling strategy to solve the full space problem (8). With single layer, double layer, adjoint double layer and hypersingular operators V_k, K_k, K_k', W_k for the Helmholtz equation and the three fields

$(u, u^m, u^{\text{ext}}) \in H^1(\Omega) \times H^{-1/2}(\Gamma) \times H^{1/2}(\Gamma)$ it reads as follows in strong form:

$$-\nabla \cdot (A(x)\nabla u) - k^2 n^2(x) u = f \quad \text{in } \Omega, \tag{10a}$$

$$\mathbf{n} \cdot (A\nabla u) + \mathbf{i}ku - u^m = 0 \quad \text{on } \Gamma, \tag{10b}$$

$$\mathcal{B}_k u^{\text{ext}} + \mathbf{i}k\mathcal{A}_k' u^{\text{ext}} - \mathcal{A}_k' u^m = 0 \quad \text{on } \Gamma, \tag{10c}$$

$$u - \left[(\frac{1}{2} + K_k) u_{\text{ext}} - V_k(u^m - \mathbf{i}k u_{\text{ext}}) \right] = 0 \quad \text{on } \Gamma, \tag{10d}$$

where $\mathcal{B}_k := -W_k - \mathbf{i}k(\frac{1}{2} - K_k)$ and $\mathcal{A}_k' := \frac{1}{2} + K_k' + \mathbf{i}kV_k$. The weak formulation on $H^1(\Omega) \times H^{-1/2}(\Gamma) \times H^{1/2}(\Gamma)$ satisfies a Gårding inequality so that a convergence analysis based on duality arguments is possible, [3, 2]. For a k-explicit analysis of conforming or discontinuous Galerkin discretizations, the key ingredient is the following "regularity by decomposition" result for an adjoint equation:

Theorem 4 ([8])**.** *There are constants C, γ, $\beta \geq 0$, and a neighborhood $\mathcal{O}$ of Γ (all independent of k) such that the following holds: Let (u, u^m, u^{ext}) solve for given $(R, R_m, R_{\text{ext}}) \in L^2(\Omega) \times H^{3/2}(\Gamma) \times H^{1/2}(\Gamma)$ the system*

$$\begin{aligned}
-\nabla \cdot (A(x)\nabla u) - k^2 n^2(x) u &= R \quad \text{in } \Omega, \\
\mathbf{n} \cdot (A(x)\nabla u) + \mathbf{i}ku + u^m &= 0 \quad \text{on } \Gamma, \\
W_k + \mathbf{i}k(\frac{1}{2} - K_k') - \mathbf{i}k(\frac{1}{2} + K_k + \mathbf{i}kV_k)u^{\text{ext}} - ((\frac{1}{2} + K_k') + \mathbf{i}kV_k)u^m &= R_{\text{ext}} \quad \text{on } \Gamma, \\
-u + (\frac{1}{2} + K_k + \mathbf{i}kV_k)u^{\text{ext}} + V_k u^m &= R_m \quad \text{on } \Gamma.
\end{aligned}$$

Then, $(u, u^m, u^{\text{ext}}) = (u_{H^2}, u^m_{H^2}, u^{\text{ext}}_{H^2}) + (u_{\mathcal{A}}, u^m_{\mathcal{A}}|_\Gamma, u^{\text{ext}}_{\mathcal{A}}|_\Gamma)$ with

$$\begin{aligned}
&\|u_{H_2}\|_{H^2(\Omega \setminus \Gamma_{\text{int}})} + \|u^m_{H_2}\|_{H^{1/2}(\Gamma)} + \|u^{\text{ext}}_{H_2}\|_{H^{3/2}(\Gamma)} \\
&\quad \leq C \left[\|R\|_{L^2(\Omega)} + \|R_m\|_{H^{3/2}(\Gamma)} + \|R_{\text{ext}}\|_{H^{1/2}(\Gamma)} \right]
\end{aligned}$$

and $u_{\mathcal{A}} \in \mathcal{A}(Ck^\beta D, \gamma, \Omega \setminus \Gamma_{\text{int}})$, $u^m_{\mathcal{A}}$, $u^{\text{ext}}_{\mathcal{A}} \in \mathcal{A}(Ck^\beta D, \gamma, \mathcal{O})$, where $D := \|R\|_{L^2(\Omega)} + \|R_m\|_{L^2(\Gamma)} + \|R^{\text{ext}}\|_{H^{-1/2}(\Gamma)}$.

Let $\mathcal{T}$ be a mesh of width h on Ω satisfying the conditions set out in [6, 7, 1] and let $\mathcal{T}_\Gamma$ be the trace mesh on Γ. As described in [3], let $S^{p,1}(\mathcal{T}) \subset H^1(\Omega)$ and $S^{p,1}(\mathcal{T}_\Gamma)$ be the spaces of piecewise (mapped) polynomials of degree p based on the meshes $\mathcal{T}$, $\mathcal{T}_\Gamma$, respectively, and let $S^{p-1,0}(\mathcal{T}_\Gamma) \subset L^2(\Gamma)$ be the space of piecewise (mapped) polynomials of degree $p-1$ based on $\mathcal{T}_\Gamma$. Set $\widetilde{V}_N := S^{p,1}(\mathcal{T}) \times S^{p-1,0}(\mathcal{T}_\Gamma) \times S^{p,1}(\mathcal{T}_\Gamma)$. With Thm. 4, one can show the following quasi-optimality result for the Galerkin approximation $(u_N, u_N^m, u_N^{\text{ext}}) \in \widetilde{V}_N$:

Theorem 5 ([8])**.** *Assume the hypotheses of Thm. 4. Then, given $c_2 > 0$ there is $c_1 > 0$ such that under the scale resolution condition (6) the conforming hp-FEM discretization of (10) is quasi-optimal, i.e., the discrete solution $(u_N, u_N^m, u_N^{\text{ext}}) \in$*

$\widetilde{V}_N$ exists and satisfies, for some $C > 0$ independent of k

$$\begin{aligned}&\|u - u_N\|_{1,k} + \|u^m - u_N^m\|_{H^{-1/2}(\Gamma)} + \|u^{\mathrm{ext}} - u_N^{\mathrm{ext}}\|_{H^{1/2}(\Gamma)}\\ &\quad\le C \inf_{v\in\widetilde{V}_N} \|u - v\|_{1,k} + \|u^m - v\|_{H^{-1/2}(\Gamma)} + \|u^{\mathrm{ext}} - v\|_{H^{1/2}(\Gamma)}.\end{aligned}$$

Remark 6. See [8, 2] for the extension to a *hp*-DGFEM discretization in Ω with corresponding best approximation result.

References

[1] M. Bernkopf, T. Chaumont-Frelet, J.M. Melenk, *Wavenumber-explicit stability and convergence analysis of hp-finite element discretizations of Helmholtz problems in piecewise smooth media*, `arXiv:2209.03601`

[2] C. Erath, L. Mascotto, J.M. Melenk, I. Perugia, A. Rieder, *mortar coupling of hp-discontinuous Galerkin and boundary element methods for the Helmholtz equation*, J. Sci. Comp., **92:1** (2022)

[3] L. Mascotto, J.M. Melenk, I. Perugia, A. Rieder, *FEM-BEM mortar coupling for the Helmholtz equation in three dimensions*, Comput. Math. Appl., **80** (2020), pp. 2351–2378

[4] J.M. Melenk, S. Sauter, *wavenumber-explicit hp-FEM analysis for Maxwell's equations with impedance boundary conditions*, `arXiv:2201.02602`

[5] J.M. Melenk, S. Sauter, *wavenumber-explicit hp-FEM analysis for Maxwell's equations with transparent boundary conditions*, J. Found. Comput. Math. **21** (2021), pp. 125–241

[6] J.M. Melenk, S. Sauter, *convergence analysis for finite element discretizations of the Helmholtz equation with Dirichlet-to-Neumann boundary conditions*, Math. Comput. **79** (2010), pp. 1871–1914

[7] J.M. Melenk, S. Sauter, *wavenumber-explicit convergence analysis for Galerkin discretizations of the Helmholtz equation*, SIAM J. Numer. Anal. **49** (2011), pp. 1210–1243

[8] J.M. Melenk, I. Perugia, A. Rieder, *FEM-BEM coupling for high-frequency Helmholtz problems*, (in prep.)

A Class of Parameter Configurations for Localization of Waves

Stefan Sauter

(joint work with Céline Torres)

1. Introduction

The numerical simulation of high frequency scattering problems is a topic of vivid research in numerical analysis. Besides the difficulties related to the "elliptic aspect" of the problem such as, e.g., singularities due to non-smooth boundary/coefficients, additional difficulties are related to the highly oscillatory behavior of the solution which strongly depends on the wavenumber and the coefficients in the underlying PDE. In this exposition, we consider the Helmholtz problem with variable wave speed as our model problem and present a class of parameter configurations where the wave is in near-resonance.

2. Setting

We consider the Helmholtz Equation on a bounded Lipschitz domain $\Omega \subset \mathbb{R}^d$ with boundary $\partial\Omega$. The underlying energy space is $\mathcal{H} := H^1(\Omega)$. The weak formulation of the problem reads: For given $\mathcal{F} \in \mathcal{H}'$, find $u \in \mathcal{H}$ such that

$$B(u,v) = \mathcal{F}(v) \quad \forall v \in \mathcal{H}, \tag{1}$$

where the sesquilinear form $B : \mathcal{H} \times \mathcal{H}$ is given by

$$B(u,v) := (\nabla u, \nabla v)_{L^2(\Omega)} - \left(\frac{\omega}{c}u, v\right)_{L^2(\Omega)} - (T_k u, v)_{L^2(\partial\Omega)}$$

and T_k denotes the DtN operator. The right-hand side is given via functions $f \in L^2(\Omega)$ and $g \in L^2(\partial\Omega)$ by $\mathcal{F}(v) = (f,v)_{L^2(\Omega)} + (g,v)_{L^2(\partial\Omega)}$. The frequency parameter ω is assumed to satisfy $\omega \geq \omega_0 > 0$. Further, we assume that $c \in L^\infty(\Omega)$ and that there exists $0 < c_{\min} \leq c_{\max} < \infty$ such that $c_{\min} \leq c \leq c_{\max}$.

In [4, Conj. 2] the following conjecture has been formulated.

Conjecture. *For any bounded Lipschitz domain $\Omega \subset \mathbb{R}^d$, $c \in L^\infty(\Omega)$, with $0 < c_{\min} \leq c \leq c_{\max} < \infty$, $\omega \geq \omega_0 > 0$ it holds*

$$\left(\int_\Omega |\nabla u|^2 + \left(\frac{\omega}{c}\right)^2 |u|^2\right)^{\frac{1}{2}} \leq C_{\text{stab}} \left(\|f\|^2_{L^2(\Omega)} + \|g\|^2_{L^2(\partial\Omega)}\right)^{\frac{1}{2}}, \tag{2}$$

with

$$C_{\text{stab}} \leq C_1 \exp(C_2 \omega), \tag{3}$$

$C_1, C_2 > 0$ depending on $c_{\min}$, $c_{\max}$ and Ω.

3. Parameter configurations for an exponentially growth of C_{stab}

Let Ω be the unit ball in $\mathbb{R}^3$. Next we define a wave speed c in $L^\infty(\Omega)$ with $0 < c_{\min} \leq c \leq c_{\max}$ such that the stability constant C_{stab} in (2) grows exponentially in ω. The coefficient c and the frequency ω will be correlated. Let $\Omega_j := \{\mathbf{x} \in \Omega \mid r_{j-1} < \|\mathbf{x}\| < r_j\}$, $1 \leq j \leq n+1$, denote circular layers in Ω for some partitioning $0 = r_0 < r_1 \ldots < r_{n+1} = 1$ of the radial direction and define, for some $c_0 > 0$ and relative jump height $q \in]-1,1[$, the coefficient

$$c|_{\Omega_j} := c_j := c_0\left(1 + (-1)^j q\right) \quad \text{in } \Omega_j, \quad 1 \leq j \leq n+1. \tag{4}$$

Theorem 1. *Let $f = 0$ and $g = g_0/(2\sqrt{\pi})$ for some $g_0 \in \mathbb{R}$. For any $c_0 > 0$, $q \in]-1,1[$, $n \in \mathbb{N}_0$ define c_ℓ as in (4) and set*

$$\omega := \frac{\pi}{2}\sum_{\ell=1}^{n+1} c_\ell, \quad r_j := \frac{\pi}{2\omega}\sum_{\ell=1}^{j} c_\ell \quad \text{for } 1 \leq j \leq n+1.$$

Then, the solution u has an exponentially growing stability constant:

$$\frac{\sqrt{\pi}}{2}\left(\frac{1+q}{1-q}\right)^{\lceil n/2 \rceil} |g_0| \leq \|u\|_{H^1(B_1),k} \leq C\alpha^\omega |g_0| \quad \text{for some } \alpha = \alpha(q) > 1. \tag{5}$$

For a proof we refer to [5, §4.2]. In the same geometrical setting for the wave speed c as described above, but with general jumping coefficients c_j, the same upper bound as in (5) is valid and can be found in [5, §3].

Other configurations of different nature with exponential growing stability constant are presented in [1], [2], [3].

References

[1] Y. Capdeboscq, G. Leadbetter, and A. Parker. On the scattered field generated by a ball inhomogeneity of constant index in dimension three. In *Multi-scale and high-contrast PDE: from modelling, to mathematical analysis, to inversion*, volume 577 of *Contemp. Math.*, pages 61–80. Amer. Math. Soc., Providence, RI, 2012.

[2] D. J. Hansen, C. Poignard, and M. S. Vogelius. Asymptotically precise norm estimates of scattering from a small circular inhomogeneity. *Appl. Anal.*, 86(4):433–458, 2007.

[3] A. Moiola and E. A. Spence. Acoustic transmission problems: wavenumber-explicit bounds and resonance-free regions. *Mathematical Models and Methods in Applied Sciences*, 29(2): 317–354, 2019.

[4] S. Sauter and C. Torres. Stability estimate for the Helmholtz equation with rapidly jumping coefficients. *Z. Angew. Math. Phys.*, 69(6):Art. 139, 30, 2018.

[5] S. Sauter and C. Torres. The heterogeneous Helmholtz problem with spherical symmetry: Green's operator and stability estimates. *Asymptotic Analysis*, 125(3-4):289–325, 2021.

Quantitative bounds on Impedance-to-Impedance operators

Thomas Beck

(joint work with Yaiza Canzani, Jeremy L. Marzuola)

Impedance-to-Impedance operators

The hierarchichal Poincaré-Steklov method is a non-overlapping domain decomposition method which can be used to approximate the Dirichlet-to-Neumann operator and scattering solutions of the Helmholtz equation in inhomogeneous media. This method involves first partitioning the domain into a hierarchical collection of boxes of varying scales, then obtaining an approximation of an appropriately chosen elliptic operator on the boundary of the leaf sub-domains at the finest level of the partition, and finally a merge process to recover the desired operator on the original domain.

One choice of boundary operator to approximate on the leaf sub-domains is the Dirichlet-to-Neumann operator [7], [6], [4]. Another option, which does not introduce artificial resonances into the problem is to use impedance-to-impedance operators [2], [5], [9]. The impedance-to-impedance (ItI) operator of a domain Ω, which we denote by R_Ω, is defined by

$$R_\Omega g = (\partial_\nu u - iku)\big|_{\partial\Omega}.$$

Here $g \in L^2(\partial\Omega)$ and $u \in H^1(\Omega)$ solves the boundary value problem

$$\begin{cases} \Delta u + k^2 V u = 0 & \text{in } \Omega, \\ \partial_\nu u + iku = g & \text{on } \partial\Omega. \end{cases}$$

In the above, V is the potential, ν is the outward pointing unit normal on $\partial\Omega$, and $k > 0$ is the frequency. The traces $(\partial_\nu u + iku)\big|_{\partial\Omega}$ and $(\partial_\nu u - iku)\big|_{\partial\Omega}$ are denoted as the *incoming* and *outgoing* impedance data on $\partial\Omega$.

A version of the hierarchical Poincaré-Steklov method has been implemented by Gillman, Barnett, and Martinsson [5], and their method requires the invertibility of the following merge operator: Consider the case where Ω is the rectangle $[0,2]\times[0,1]$, made up of the two unit squares $S_1 = [0,1]\times[0,1]$, $S_2 = [1,2]\times[0,1]$, with common edge $A = \{1\}\times[0,1]$. As shown in [5], the ItI operator, R_Ω, of the rectangle can be recovered from those of the two squares, provided that the *merge* operator $I - R_1R_2$ is invertible. Here R_j are ItI operators defined on the common edge A, given by $R_j f = (\partial_\nu v_j - ikv_j)\big|_A$, where

$$\begin{cases} \Delta v_j + k^2 V v_j = 0 & \text{in } S_j, \\ \partial_\nu v_j + ikv_j = 0 & \text{on } \partial S_j \backslash A, \\ \partial_\nu v_j + ikv_j = f & \text{on } A. \end{cases}$$

See Figure 1 for the set-up of the operators R_j. The invertibility of this merge operator holds for the numerical computations in [5].

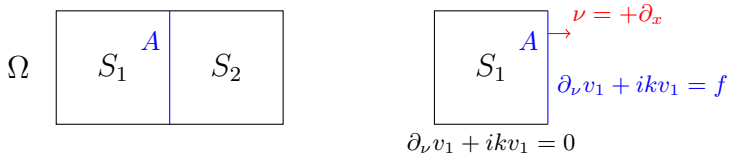

FIGURE 1. The impedance problem satisfied in the definition of R_1

Invertibility of the merge operator

We obtain invertibility properties of $I - R_1R_2$ under the following *non-trapping* assumption on the potential V.

Assumption. *The potential* $V \in C^1([0,2]\times[0,1])$ *satisfies*

$$2V(x,y) + (x-1,y)\cdot\nabla V(x,y) \geq c$$

for all $(x,y)\in\Omega$, *for some constant* $c > 0$.

Under this assumption, the merge operator

$$I - R_1R_2 = (I - R_1)(I + R_2) + (R_1 - R_2)$$

satisfies the following quantitative estimates in the frequency k, where we define the weighted H^1-Sobolev norm $\mathcal{H}^1_k(A)$ by,

$$\|h\|_{\mathcal{H}^1_k(A)} := \|kh\|_{L^2(A)} + \|\partial_\tau h\|_{L^2(A)}\,.$$

Theorem 1 ([1]). Provided that V satisfies the assumption above, the operator

$$I - R_1 R_2 : L^2(A) \to \mathcal{H}^1_k(A)$$

is a bijection, with a bounded inverse. Moreover, given $\delta > 0$, there exist constants $c^* > 0$, $c^*_\delta > 0$, such that for $f \in L^2(A)$ and all $k > 0$,

$$\|(I - R_j)f\|_{\mathcal{H}^1_k(A)} \geq c^* \|kf\|_{L^2(A)},$$
$$\|(I + R_j)f\|_{L^2(A)} \geq c^*_\delta (1+k)^{-3(1+\delta)} \|f\|_{L^2(A)}.$$

In the theorem above, it is not possible to replace the space $\mathcal{H}^1_k(A)$ by $L^2(A)$, and the operator $I + R_j$ is not uniformly bounded from below, as an operator from $L^2(A)$ to itself.

Remark 1. The estimates on $I \pm R_j$ also hold more generally for ItI operators defined on an edge A of a convex polygon.

Remark 2. A version of Theorem 1 also holds for the obstacle problem, where a convex obstacle with Dirichlet boundary conditions are placed in the squares S_j.

The operators $I \pm R_j$ appearing in Theorem 1 satisfy

$$(I - R_j)f = 2ikv_j\big|_A, \quad (I + R_j)f = 2\partial_\nu v_j\big|_A.$$

Therefore, the estimates in the theorem correspond to obtaining Dirichlet and Neumann trace estimates on one side of the square for solutions of boundary value problems with prescribed incoming impedance data. A key ingredient in the proof of the theorem is thus the following trace estimate, which uses techniques from [8], [3].

Proposition 1 ([1]). Let $V \in C^1(\Omega)$ satisfy the assumption above. Let w be $L^2(S_j)$-normalized and satisfy

$$(\Delta + k^2 V)w = h \text{ in } S_j, \quad \partial_\nu w = 0 \text{ on } \partial S_j,$$

for some function $h \in H^1(S_j)$, and $k > 1$. Then, there exists a constant $c > 0$, independent of k, such that, if $\|h\|_{\mathcal{H}^1_k(\Omega)} \leq ck^2$, then

$$\int_{\partial S \setminus A} |w|^2 \geq c.$$

References

[1] T. Beck, Y. Canzani, and J. Marzuola, *Quantitative bounds on Impedance-to-Impedance operators with applications to fast direct solvers for PDEs*, (2021), `https://arxiv.org/abs/2103.14700`.

[2] J.D. Benamou and B. Desprès, *A domain decomposition method for the Helmholtz equation and related optimal control problems*, Journal of Computational Physics, 136 (1) (1997), 68–82.

[3] H. Christianson, *Equidistribution of Neumann data mass on triangles*, Proc. Amer. Math. Soc., 145 (12) (2017), 5247–5255.

[4] D. Fortunato, N. Hale, and A. Townsend, *The ultraspherical spectral element method*, Journal of Computational Physics, 436 (2020), 110087.

[5] A. Gillman, A. Barnett, and P.G. Martinsson, *A spectrally accurate direct solution technique for frequency-domain scattering problems with variable media*, BIT Numerical Mathematics, 55 (1) (2015), 141–170.
[6] A. Gillman and P. G. Martinsson, *A direct solver with $O(N)$ complexity for variable coefficient elliptic pdes discretized via a high-order composite spectral collocation method*, SIAM Journal on Scientific Computing, 36 (4) (2014) 2023–2046.
[7] P.G. Martinsson, *A direct solver for variable coefficient elliptic PDEs discretized via a composite spectral collocation method*, J. Comput. Phys., 242 (2013), 460–479.
[8] J. Melenk, *On generalized finite element methods*, PhD thesis (1995).
[9] M. Pedneault, C. Turc, and Y. Boubendir, *Schur complement domain decomposition methods for the solution of multiple scattering problems*, IMA Journal of Applied Mathematics, 82 (5) (2017), 1104–1134.

Fast Boundary Element Methods to simulate underwater explosions and their interactions with submarines (a nice problem to illustrate a lot of modern numerical tools for waves)

Stéphanie Chaillat
(joint work with Marc Bonnet, Bruno Leblé, Damien Mavaleix-Marchessoux, Alice Nassor)

Assessing the impact of a remote underwater explosion on a submerged structure (submarine) is an important naval engineering problem. An underwater explosion mainly induces two distinct phenomena: a "shock wave" followed by an oscillating bubble of gas (see Fig. 1). The goal of this presentation was to show how to create an efficient numerical method that accounts for the effects of both phenomena on submerged structures.

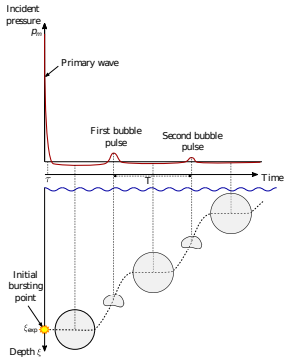

Figure 1. Schematic representation of the bubble motion and the pressure history after [6].

Due to the unbounded nature of the ocean and the complex mechanical behavior of the submarine we want to take into account, it is natural to consider a Boundary Element Method/Finite Element Method (BEM/FEM) coupling for both the modeling of the shock wave and the oscillating bubble of gas (Fig. 2).

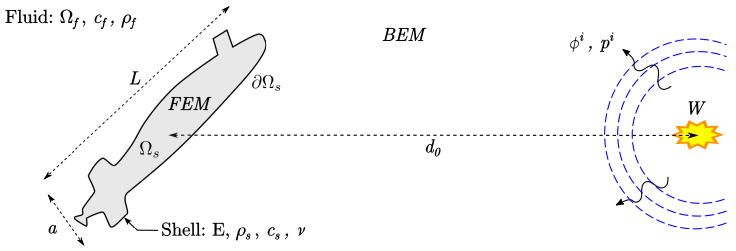

FIGURE 2. FEM/BEM coupling to simulate an underwater explosion.

Oscillating bubble of gas. In a first part, I have presented the modeling of the second stage of the underwater event: the oscillating bubble of gas. Hence, an incompressible potential flow is induced by the oscillations of the gas bubble created by the remote blast. The BEM is the best-suited approach for handling potential flow problems in large fluid domains (idealized as unbounded), whereas the FEM naturally applies to the transient structure analyses. To perform the FEM-BEM coupling we use a sub-cycling approach that alternates fluid and solid analyses with Neumann boundary conditions. The transient nature of the coupled analysis and the recourse to sub-cycling together make the overall procedure rely on a large number of BEM potential flow solutions, while the complexities of the wet surface and of the solid transient response imply a need for large BE models for the flow potential. This combination of reasons mandates accelerating the BE component. I have shown the feasibility and effectiveness of coupling the Hierarchical-matrix accelerated BEM (H-BEM) [3] and the FEM for the fluid-structure interaction (FSI) problems of interest. The same integral operators can be used at all time instants in spite of the expected global motion of the submarine, a feature that the H-BEM can exploit to full advantage. I have finally shown the validation of this numerical procedure on a complex configuration representative of target applications [5].

Shock wave. In a second part, I have considered the more challenging problem of the modeling of the shock wave stage and its interaction with the structure. Hence, 3D rapid transient acoustic problems are known to be difficult to solve numerically when dealing with large geometries, because numerical methods based on geometry discretisation, such as the BEM or the FEM, often require to solve a linear system (from the spacial discretisation) for each time step. We have proposed a numerical method to efficiently deal with 3D rapid transient acoustic problems set in large exterior domains. Using the Z-transform and the convolution quadrature method (CQM) [1], a straightforward way to reframe the problem to the solving of a large amount of frequency-domain BEMs is derived. Then, taking advantage of a well-designed high-frequency approximation (HFA), the number of frequency-domain BEMs to be solved is drastically reduced, with little loss of accuracy. The complexity of the resulting numerical procedure turns out to be O(1) in regards to

the time discretisation and O(N logN) for the spacial discretisation, the latter being prescribed by the complexity of the used fast BEM solver [4]. I have presented the validation of this procedure with the scattering of an abrupt wave by a realistic geometry (Fig. 3).

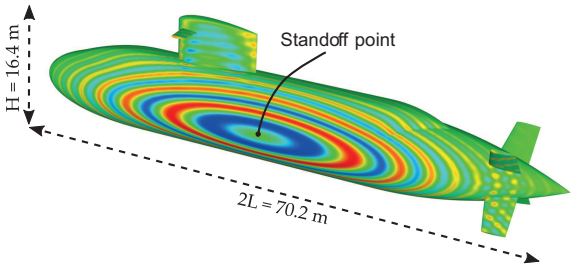

FIGURE 3. Illustration of the efficiency of the Z-BEM procedure for a scattering problem with a realistic geometry.

I have finally shown a naive approach to consider the FSI problem. It consists at iteratively solving the BEM-FEM coupling by alternating Neumann solutions in each domain. Unfortunately this simple approach fails (does not converge). We can show that the transient BEM-FEM coupling based on Neumann-Neumann iterations is problematic since energy estimates indicate that each iteration degrades the regularity of boundary traces (unlike in the elliptic case) [2]. To avoid this issue, an iterative algorithm based on Robin boundary conditions for the coupled elastodynamic/acoustic problem has been developed and proved to converge.

REFERENCES

[1] T. Betcke, N. Salles, W. Smigaj, *Overresolving in the Laplace domain for convolution quadrature methods*, SIAM J. Sci. Comput. **39** (2017), A188 - A213.
[2] M. Bonnet, S. Chaillat, A. Nassor, *Solvability results for the transient acoustic scattering by an elastic obstacle*, to be submitted soon.
[3] W. Hackbusch, *A sparse matrix arithmetic based on H-matrix. Part I: Introduction to H-matrices*, Computing, **62** (1999), 89–108.
[4] D. Mavaleix-Marchessoux, M. Bonnet, S. Chaillat, B. Leblé, *A fast BEM procedure using the $\mathcal{Z}$-transform and high-frequency approximations for large-scale 3D transient wave problems*, Int. J. Numer. Meth. Engng., **121** (2020), 4734-4767.
[5] D. Mavaleix-Marchessoux, M. Bonnet, S. Chaillat, B. Leblé, *$\mathcal{H}$-matrix accelerated BEM-FEM coupling for dynamic analysis of naval structures under pulsating potential flow motion*, under review.
[6] H.G. Snay, *Hydrodynamics of underwater explosions. Published in Symposium on Naval Hydrodynamics*, National Academy of Sciences, Washington D.C.,(1956), 325–346.

Static currents in type I superconductors: Numerical methods and the $\lambda_L \to 0$ limit

Charles Epstein

(joint work with Leslie Greengard, Manas Rachh)

In [3] we gave a Debye source representation (see [1]) for solving static problems connected to type-I superconductors. We assume that the superconducting material is homogeneous and isotropic, occupying a bounded region Ω. The boundary of Ω, $\partial\Omega$, is assumed to be a smooth, connected surface of genus g, embedded in $\mathbb{R}^3$. Within Ω there is a magnetic field, which we describe as a 2-form $\boldsymbol{\eta}^-$,

$$\boldsymbol{\eta}^- = \eta_1^- dx_2 \wedge dx_3 + \eta_2^- dx_3 \wedge dx_1 + \eta_3^- dx_1 \wedge dx_2, \tag{1}$$

and a current, which we describe as a 1-form $\boldsymbol{j}^-$,

$$\boldsymbol{j}^- = j_1^- dx_1 + j_2^- dx_2 + j_3^- dx_3. \tag{2}$$

According to the London equations, see [5] these satisfy the first order system:

$$d^*\boldsymbol{\eta}^- = \boldsymbol{j}^- \quad \text{and } d\boldsymbol{j}^- = -\frac{1}{\lambda_L^2}\boldsymbol{\eta}^- \text{ within } \Omega. \tag{3}$$

These equations preceded the BCS theory of superconductivity, see [6], by over 2 decades. Recall that, on p-forms in $\mathbb{R}^3$, the formal adjoint of d is $d^* = (-1)^p \star d\star$, where $\star$ is the Hodge-star operator defined by the Euclidean metric. These equations imply that

$$d\boldsymbol{\eta}^- = 0 \text{ and } d^*\boldsymbol{j}^- = 0. \tag{4}$$

The constant λ_L is called the London penetration depth. It measures the thickness of the current carrying portion of a superconducting material. In real materials this length is very small, typically ranging from 50 to 500nm. In the complementary region there is a static magnetic field $\boldsymbol{\eta}^{\text{tot}}$, which satisfies the usual equations of magnetostatics

$$d\boldsymbol{\eta}^{\text{tot}} = 0 \text{ and } d^*\boldsymbol{\eta}^{\text{tot}} = 0 \text{ in } \Omega^c. \tag{5}$$

The current $\boldsymbol{j}^-$ is supported in a (thin) neighborhood of $\partial\Omega$. As there is no current sheet on the boundary, the physically reasonable boundary conditions are

$$\boldsymbol{\eta}^-|_{\partial\Omega} = \boldsymbol{\eta}^{\text{tot}}|_{\partial\Omega} \text{ and } \star\boldsymbol{\eta}^-|_{\partial\Omega} = \star\boldsymbol{\eta}^{\text{tot}}|_{\partial\Omega}. \tag{6}$$

That is the normal *and* tangential components of the magnetic field are continuous across the boundary. This boundary condition and $d\star\boldsymbol{\eta}^{\text{tot}} = 0$ imply that

$$d_{\partial\Omega}[\star\boldsymbol{\eta}^-|_{\partial\Omega}] = 0, \tag{7}$$

that is $\star\boldsymbol{\eta}^-|_{\partial\Omega}$ is a closed 1-form on $\partial\Omega$. The London equation shows that $i_{\boldsymbol{n}}\boldsymbol{j}^- = 0$ is equivalent to $d_{\partial\Omega}[\star\boldsymbol{\eta}^-|_{\partial\Omega}] = 0$, hence the current is tangent to $\partial\Omega$. The magnitudes of both $\boldsymbol{\eta}^-(x)$, and $\boldsymbol{j}^-(x)$ decay like $e^{-\frac{\text{dist}(x,\partial\Omega)}{\lambda_L}}$.

In the standard "scattering" problem for this set-up the magnetic field in Ω^c is split into an incoming magneto-static field $\boldsymbol{\eta}^{\text{in}}$, and an outgoing scattered field,

$\boldsymbol{\eta}^+$. The field $\boldsymbol{\eta}^+$ is defined in all of Ω^c; the assumption that $\boldsymbol{\eta}^+$ is an outgoing field means that

$$\|\boldsymbol{\eta}^+(x)\| = o(\|x\|^{-1}). \tag{8}$$

The incoming field is a solution to Maxwell's equations generated by sources that are a positive distance from $\overline{\Omega}$. Hence in a neighborhood of $\partial\Omega$ we have that

$$\boldsymbol{\eta}^{\text{tot}} = \boldsymbol{\eta}^{\text{in}} + \boldsymbol{\eta}^+.$$

The boundary conditions can therefore be written as:

$$\boldsymbol{\eta}^-|_{\partial\Omega} - \boldsymbol{\eta}^+|_{\partial\Omega} = \boldsymbol{\eta}^{\text{in}}|_{\partial\Omega} \text{ and } \star\,\boldsymbol{\eta}^-|_{\partial\Omega} - \star\boldsymbol{\eta}^+|_{\partial\Omega} = \star\boldsymbol{\eta}^{\text{in}}|_{\partial\Omega}. \tag{9}$$

If $\partial\Omega$ is of genus $g > 0$, then these conditions need to be augmented with the flux conditions: Assume that $\partial\Omega$ is connected and has genus g, then there are g A-cycles $\{A_1, \ldots, A_g\}$, which bound surfaces $\{S_{A_1}, \ldots, S_{A_g}\}$ contained within Ω, and g B-cycles $\{B_1, \ldots, B_g\}$, which bound surfaces $\{S_{B_1}, \ldots, S_{B_g}\}$ contained in Ω^c. Since $[\star\boldsymbol{\eta}^{\text{tot}}]|_{\partial\Omega} = [\star\boldsymbol{\eta}^-]|_{\partial\Omega}$ are closed 1-forms, their integrals over a cycle in $\partial\Omega$ depend only on the homology class of the cycle. It follows from the boundary condition, and Stokes theorem that

$$\int_{B_j} \star\boldsymbol{\eta}^- = \int_{B_j} \star\boldsymbol{\eta}^{\text{tot}} = \int_{S_{B_j}} d\star[\boldsymbol{\eta}^{\text{in}} + \boldsymbol{\eta}^+] = 0, \tag{10}$$

provide that $\boldsymbol{\eta}^{\text{in}}$ is defined in a contractable neighborhood of Ω. If not, then

$$b_j = \int_{B_j} \star\boldsymbol{\eta}^- = \int_{B_j} \star\boldsymbol{\eta}^{\text{tot}} = \int_{B_j} \star\boldsymbol{\eta}^{\text{in}}, \tag{11}$$

which may not be zero, but is determined by $\boldsymbol{\eta}^{\text{in}}$.

On the other hand the fluxes

$$a_{=}j \int_{A_j} \star\boldsymbol{\eta}^{\text{tot}} = \int_{A_j} \star\boldsymbol{\eta}^- = \int_{S_{A_j}} d\star\boldsymbol{\eta}^- = \int_{S_{A_j}} \star\boldsymbol{j}^-, \text{ for } j = 1, \ldots, g, \tag{12}$$

are not determined a priori, and in fact, constitute additional data that must be specified to get a unique solution. As $\boldsymbol{\eta}^{\text{in}}$ is defined in a neighborhood of $\overline{\Omega}$, and $\partial S_{A_j} = A_j$, Stokes theorem shows that

$$\int_{A_j} \star\boldsymbol{\eta}^{\text{tot}} = \int_{A_j} \star\boldsymbol{\eta}^+. \tag{13}$$

In this talk we consider two aspects of the theory of type I superconductors, which are essential to use it in physically interesting situations:

(1) We give the a Debye source representation for the solution of the scattering problem, which is adequate for $\lambda_L > 10^{-2}$. This is explained in [3]. It requires the solution of the Laplace-Beltrami equation on $\partial\Omega$. A new approach to this difficult problem is given in [7].

(2) We analyze the behavior of solutions to the boundary value problem outlined above as $\lambda_L \to 0^+$. This is a singular limit, and we give a precise description of the solution for very small, but physically reasonable λ_L. This entails analysis of a boundary value problem for the PDE

$$dd^*\eta^-_{\lambda_L} + \frac{1}{\lambda_l^2}\eta^-_{\lambda_L} = 0 \text{ in } \Omega,$$

assuming that $d\eta^-_{\lambda_L} = 0$.

References

[1] C. L. Epstein and L. Greengard, *Debye sources and the numerical solution of the time harmonic Maxwell equations*, CPAM, **63** (2010), pp. 413–463.

[2] C. L. Epstein, L. Greengard, and M. O'Neil, *Debye sources and the numerical solution of the time harmonic Maxwell equations*, II, CPAM, **66**(2012), 753–789.

[3] C. L. Epstein, and M. Rachh, *Debye source representations for type-I superconductors, I The static type-I case*, J. Comp. Phys. **452**(2022), 110892, https://doi.org/10.1016/j.jcp.2021.110892.

[4] D. Colton and R. Kress, *Integral Equation Methods in Scattering Theory*, John Wiley & Sons, Inc., 1983.

[5] Fritz London and Heinz London, *The electromagnetic equations of the supraconductor*, Proc. R. Soc. Lond. Ser. A, Math. Phys. Sci. **149** (866) (1935) 71–88.

[6] John Bardeen, Leon N. Cooper and J. Robert Schrieffer, *Microscopic theory of superconductivity*, Phys. Rev. **106** (1) (1957) 162.

[7] D Fortunato, *A high-order fast direct solver for surface PDEs* - arXiv preprint arXiv:2210.00022, 2022 - arxiv.org

Space-time Boundary Integral Equations for the Wave Equation

Carolina Urzúa-Torres

(joint work with Daniël Hoonhout, Olaf Steinbach, Marco Zank)

In this talk, we discuss the work from [2], where we propose a new approach to boundary integral equations (BIEs) for the wave equation. Unlike previous attempts, our mathematical formulation allows us to show that the associated boundary integral operators are continuous and satisfy inf-sup conditions in trace spaces of the same regularity, which are closely related to standard energy spaces. This property is crucial from a numerical point of view, as it establishes the foundations to derive sharper error estimates and paves the way to develop efficient adaptive space-time boundary element methods.

We also present the stable discretization of the proposed boundary integral equations, so far only implemented in 1D. We report new preliminary results for the double layer operator and also explain what happens with the weakly singular operator. We conclude the presentation by noting that the use of a modified Hilbert transform gives us ellipticity [4] and hence unconditionally stability for the related Galerkin discretization [3].

1. New approach to time-domain BIEs for the wave equation

We begin by summarizing the main results of [2]. Let $\Omega \subset \mathbb{R}^n$, $n = 1, 2, 3$, with boundary $\Gamma := \partial\Omega$. We assume Ω to be a bounded Lipschitz domain. Let $0 < T < \infty$. We define the *space-time cylinder* $Q := \Omega \times (0, T) \subset \mathbb{R}^{n+1}$, and its lateral boundary $\Sigma := \Gamma \times [0, T]$. We denote the D'Alembert operator by $\Box := \partial_{tt} - \Delta_x$, and write the *interior Dirichlet initial boundary value problem for the wave equation* as

$$
\begin{aligned}
\Box u(x,t) &= f(x,t) && \text{for } (x,t) \in Q,\\
u(x,t) &= g(x,t) && \text{for } (x,t) \in \Sigma,\\
u(x,0) = \partial_t u(x,t)_{|t=0} &= 0 && \text{for } x \in \Omega.
\end{aligned} \tag{1}
$$

Let $\mathcal{O} \subseteq \mathbb{R}^m$, $m \in \mathbb{N}$. We stick to the usual notation for the space $L^2(\mathcal{O})$ of Lebesgue square integrable functions; and the Sobolev spaces $H^s(\mathcal{O})$. For a Hilbert space X we denote its dual space by X'.

We consider the spaces

$$
\begin{aligned}
H^1_{0,}(0,T;L^2(\Omega)) &:= \Big\{ v \in L^2(Q) : \partial_t v \in L^2(Q), \quad v(x,0) = 0 \quad \text{for } x \in \Omega \Big\},\\
H^1_{,0}(0,T;L^2(\Omega)) &:= \Big\{ v \in L^2(Q) : \partial_t v \in L^2(Q), \quad v(x,T) = 0 \quad \text{for } x \in \Omega \Big\}.
\end{aligned}
$$

With these, we introduce

$$
\begin{aligned}
H^{1,1}_{;0,}(Q) &:= L^2(0,T;H^1(\Omega)) \cap H^1_{0,}(0,T;L^2(\Omega)),\\
H^{1,1}_{;,0}(Q) &:= L^2(0,T;H^1(\Omega)) \cap H^1_{,0}(0,T;L^2(\Omega)),
\end{aligned}
$$

with their corresponding graph norms. Next, we consider the Banach space

$$
\mathcal{H}(Q) := \Big\{ u = \widetilde{u}_{|Q} : \widetilde{u} \in L^2(Q_-),\ \widetilde{u}_{|\Omega\times(-T,0)} = 0, \quad \Box\widetilde{u} \in [H^1_0(Q_-)]' \Big\},
$$

with the norm $\|u\|^2_{\mathcal{H}(Q)} := \|u\|^2_{L^2(Q)} + \|\Box\widetilde{u}\|^2_{[H^1_0(Q_-)]'}$ (we refer to [2, Page 4] for further details). By completion, we define the Hilbert space

$$
\mathcal{H}_{;0,}(Q) := \overline{H^{1,1}_{;0,}(Q)}^{\|\cdot\|_{\mathcal{H}(Q)}} \subset \mathcal{H}(Q).
$$

Now we turn our attention to the required trace spaces and operators. We begin by introducing the lateral interior trace operator $\gamma^i_\Sigma : u \mapsto u_{|\Sigma}$ as continuous extension of the trace map defined in the pointwise sense for smooth functions.

Let us consider the spaces

$$
\begin{aligned}
H^{1/2}_{0,}(\Sigma) &:= L^2(0,T;H^{1/2}(\Gamma)) \cap H^{1/2}_{0,}(0,T;L^2(\Gamma)),\\
H^{1/2}_{,0}(\Sigma) &:= L^2(0,T;H^{1/2}(\Gamma)) \cap H^{1/2}_{,0}(0,T;L^2(\Gamma)),
\end{aligned}
$$

with $H^{1/2}_{0,}(0,T;L^2(\Gamma))$ and $H^{1/2}_{,0}(0,T;L^2(\Gamma))$ defined by interpolation. Then we have the following result [2, Lemmas 3.1 and 3.2]:

Lemma 1. The mappings

$$
\gamma^i_\Sigma : H^{1,1}_{;0,}(Q) \to H^{1/2}_{0,}(\Sigma), \qquad \gamma^i_\Sigma : H^{1,1}_{;,0}(Q) \to H^{1/2}_{,0}(\Sigma),
$$

are continuous and surjective.

Additionally, we define the lateral trace space

$$\mathcal{H}_{0,}(\Sigma) := \left\{ v = \gamma_\Sigma^i V \quad \text{for all } V \in \mathcal{H}_{;0,}(Q) \right\}$$

with the norm $\|v\|_{\mathcal{H}_{0,}(\Sigma)} := \inf_{V \in \mathcal{H}_{;0,}(Q): \gamma_\Sigma^i V = v} \|V\|_{\mathcal{H}(Q)}$.

Finally, we are in the position to present the main result of [2, Sec. 5].

Theorem 1. *The boundary integral operators*

$$\mathsf{V} : [H^{1/2}_{,0}(\Sigma)]' \to \mathcal{H}_{0,}(\Sigma), \qquad \mathsf{W} : \mathcal{H}_{0,}(\Sigma) \to [H^{1/2}_{,0}(\Sigma)]',$$
$$\frac{1}{2}\,\mathsf{Id} \pm \mathsf{K} : \mathcal{H}_{0,}(\Sigma) \to \mathcal{H}_{0,}(\Sigma), \qquad \frac{1}{2}\,\mathsf{Id} \pm \mathsf{K}' : [H^{1/2}_{,0}(\Sigma)]' \to [H^{1/2}_{,0}(\Sigma)]',$$

are continuous and satisfy their corresponding inf-sup stability conditions.

2. Stable discretization of the double layer operator

We consider the following variational problem for the double layer operator K: Find $w \in \mathcal{H}_{0,}(\Sigma)$ st

$$\langle \left(-\frac{1}{2}\,\mathsf{Id} + \mathsf{K} \right) w, v \rangle_\Sigma = \langle g, v \rangle_\Sigma, \qquad \forall v \in [\mathcal{H}_{0,}(\Sigma)]', \tag{2}$$

where $\langle \cdot\,, \cdot \rangle_\Sigma$ denotes the duality pairing induced by the extension of the $L^2(\Sigma)$-inner product.

We pursue a Galerkin discretization with the following discrete trial and test boundary element spaces:

$$S^1_{0,}(\Sigma_h) \subset \mathcal{H}_{0,}(\Sigma), \qquad S^1_{0,}(\Sigma_h) \subset [\mathcal{H}_{0,}(\Sigma)]',$$

where $S^1_{0,}(\Sigma_h)$ is spanned by space-time piecewise linear basis functions with zero-initial conditions.

We test this discretization numerically in 1D with $\Omega := (0, 3)$, and $T = 6$. For this, we compare with the following exact solution for (1)

$$u(x,t) = \begin{cases} \frac{1}{2}|\sin(\pi(x-t))|, & x \le t, \\ 0 & \text{else.} \end{cases} \tag{3}$$

The obtained results are displayed in Table 1, where N denotes the number of elements used to discretize the lateral boundary. We reconstruct the solution u on the interior domain plugging w in the double layer potential. We point out that the expected convergence rate is achieved for the measured error.

3. Stable discretization of the weakly singular operator

We confirmed the observation done in [1] that the weakly singular operator V discretized with piecewise constant basis functions is in general not stable. However, as predicted in [4] and later shown in [3], one achieves unconditionally stability in 1D when composing V with a *modified Hilbert transform*.

N	$\|u-u_h\|_{H^1(Q)}$	eoc
64	9.22E+00	-
128	4.36E+00	1.08
256	2.11E+00	1.05
512	1.04E+00	1.02
1024	5.16E-01	1.01
2048	2.57E-01	1.01
4096	1.28E-01	1.00

TABLE 1. Numerical results for (2) using $S^1_{0,}(\Sigma_h)$ for test and trial discrete spaces.

REFERENCES

[1] C. Guardasoni, *Wave Propagation Analysis with Boundary Element Method*, Ledizioni LediPublishing (2010).

[2] O. Steinbach, and C. Urzúa-Torres, *A New Approach to Space-Time Boundary Integral Equations for the Wave Equation*, SIAM J. on Math. Analysis **54** (2), 1370–1392 (2022).

[3] O. Steinbach, C. Urzúa-Torres, and M. Zank, *Towards coercive boundary element methods for the wave equation*, arXiv:2106.01646, accepted at J. of Integral Eq. and App. (2021).

[4] C. Urzúa–Torres (joint work with O. Steinbach), *A new approach to time-domain boundary integral equations for the wave equation*. Oberwolfach Reports **17** (2021) 371–373.

Imaginary part of resonances in the scattering by transparent or negative obstacles, part I

MONIQUE DAUGE

(joint work with Zoïs Moitier)

1. FRAMEWORK

Motivated by various devices in optoelectronics [1], we investigate transmission operators

$$P\colon \quad u \mapsto Pu := -\operatorname{div}\left(\frac{1}{\varepsilon}\,\nabla u\right) \quad \text{in} \quad \mathbb{R}^2 \tag{1}$$

where ε accounts for relative electric permittivity.

a) Outside a smooth bounded domain $\Omega \subset \mathbb{R}^2$, $\varepsilon \equiv 1$ (for air or vacuum).
b) Inside the "cavity" Ω, ε is a function ε_{c} smooth up to the boundary.
c) At the interface $\partial\Omega$, ε has a jump.

Ω represents either

(i) A dielectric micro cavity and $\varepsilon_{\mathsf{c}} > 1$ in $\overline{\Omega}$
(ii) A negative metallic nano-cavity Ω and $\varepsilon_{\mathsf{c}} < 0$ in $\overline{\Omega}$.

We study scattering resonances k of P.

In the book [4] DYATLOV and ZWORSKI state a generalization of the notion of scattering resonances to the framework of the black box formalism. This formalism is described in [4, §4.1] and can be summarized as follows:

A family of self-adjoint operators $\{P(h)\}_{0<h\leq 1}$ on a Hilbert space $\mathcal{H}$ and with domain $\mathcal{D}$ is called a *semiclassical black box Hamiltonian* if

a) Outside a bounded region $\mathcal{B}$ of $\mathbb{R}^d$, $P(h)$ coincides with $-h^2\Delta$ and $\mathcal{D}$ coincides with the Sobolev space H^2
b) The resolvent $\mathbb{1}_{\mathcal{B}}(P(h)+i)^{-1}$ cut-off inside this region $\mathcal{B}$, is compact.

This definition also makes sense when the parameter h is fixed. According to [4, Theorem 4.5], the spectrum of a black box Hamiltonian P satisfies

a) Its continuous spectrum coincides with $[0,+\infty)$
b) Its point spectrum is a discrete real sequence $\{z_n\}_{N_-\leq n\leq N_+}$ with possible accumulation points at $\pm\infty$ (if $N_\pm=\pm\infty$)

Resonances are classically defined via a meromorphic continuation of the resolvent $(P-z)^{-1}$. As parametrization of the spectral parameter z we choose (like [4]) the frequency $k=\sqrt[+]{z}$ (where $\sqrt[+]{\ }$ stands for the square root with positive imaginary part). With $\mathbb{C}^\pm=\{k\in\mathbb{C}|\ \pm\operatorname{Im}k>0\}$, the resolvent $k\mapsto(P-k^2)^{-1}$ of a black box Hamiltonian P as an operator $\mathcal{H}\to\mathcal{D}$ is meromorphic in $\mathbb{C}^+$.

[4, Theorem 4.4] states that the resolvent $k\mapsto(P-k^2)^{-1}$ as an operator $\mathcal{H}_{\text{comp}}\to\mathcal{D}_{\text{loc}}$ has a emphmeromorphic continuation from $\mathbb{C}^+$ to

(i) $\mathbb{C}\setminus\mathbb{R}_-=\mathbb{C}^+\cup(0,+\infty)\cup\mathbb{C}^-$ in any dimension d,
(ii) $\mathbb{C}$ if the dimension d is odd,
(iii) the logarithmic plane $\Lambda=\exp^{-1}(\mathbb{C}\setminus\{0\})$ if d is even.

The poles of $k\mapsto(P-k^2)^{-1}$ in $\mathbb{C}^-$ are called *(scattering) resonances*.

A scattering resonance k is associated with a resonance mode $u\in\mathcal{D}_{\text{loc}}$ that is solution to the equation $(P-k^2)u=0$, completed with the *outgoing radiation condition* that is a condition on the asymptotic of u as $|x|\to\infty$. When $P=-\Delta$ outside $\mathcal{B}$ (i.e. $h=1$) and the dimension d is 2, u expands in polar coordinates (r,θ) using Hankel functions of first and second kind

$$u=\sum\nolimits_{m\in\mathbb{Z}}\big(a_m\mathrm{H}_m^{(1)}(kr)+b_m\mathrm{H}_m^{(2)}(kr)\big)e^{im\theta}. \tag{2}$$

Since $\mathrm{H}_m^{(1)}$ and $\mathrm{H}_m^{(2)}$ are exponentially decreasing and increasing, respectively, in $\mathbb{C}^+$, the outgoing radiation condition consists in stating that $b_m=0$ for any $m\in\mathbb{Z}$.

2. Results

For P a transmission operator (1) in the plane we have two disjoint situations in which P is a black box Hamiltonian:

(i) if $\varepsilon_{\mathsf{c}}>1$ on $\overline{\Omega}$, and then P has no point spectrum,
(ii) if $\varepsilon_{\mathsf{c}}<0$ on $\overline{\Omega}$ and $\varepsilon_{\mathsf{c}}(\gamma)\neq-1\ \forall\gamma\in\partial\Omega$, and then the point spectrum of P is an unbounded sequence of negative eigenvalues $z_n=k_n^2$, with $k_n\in i\,\mathbb{R}_+$.

The underlying spaces are $\mathcal{H} = L^2(\Omega)$ and $\mathcal{D} = \{u \in H^1(\mathbb{R}^2),\ Pu \in L^2(\mathbb{R}^2)\}$.

We highlight some results of [2, 3] on asymptotics of resonances with small imaginary parts by considering the case when Ω is a disc (with R its radius), and ε_c a constant, which allows a classification of resonances and eigenvalues according to the polar mode index m present in (2), the inverse of which plays the role of a semiclassical parameter ($h = \frac{1}{m}$).

We have a construction of quasi-resonances $\underline{k}(m)$ modulo $\mathcal{O}(m^{-\infty})$ with explicit expansions, whose first terms are:

(i) If $\varepsilon_c = n_c^2 > 1$, for each $j = 1, 2, \ldots$ exists a distinct family $m \mapsto \underline{k}_j(m)$

$$\underline{k}_j(m) = \frac{m}{Rn_c}\Big[1 + \frac{a_j}{2}\Big(\frac{2}{m}\Big)^{\frac{2}{3}} - \frac{1}{2n_c\sqrt{\varepsilon_c - 1}}\Big(\frac{2}{m}\Big) + \mathcal{O}(m^{-\frac{4}{3}})\Big] \tag{3}$$

in which $-a_1 > -a_2 > \ldots$ are the zeros of the Airy function.

(ii) If $\varepsilon_c = -\eta_c^2 < -1$, exists one family $m \mapsto \underline{k}(m)$

$$\underline{k}(m) = \frac{m}{R\eta_c}\sqrt{-\varepsilon_c - 1}\Big[1 + \frac{\varepsilon_c + 1}{2\eta_c}\frac{1}{m} + \mathcal{O}(m^{-2})\Big] \tag{4}$$

The quasi-resonances are real positive. In case (i) the corresponding (quasi)modes are so-called *Whispering Gallery Modes* (WGM) and concentrate to the boundary at scale $m^{-2/3}$ while in case (ii) they concentrate at scale m^{-1}, *cf* plasmons.

For any $m \geq 1$, exists a true resonance $k_*(m)$ such that

$$k_*(m) = \underline{k}_*(m) + \mathcal{O}(m^{-\infty}), \tag{5}$$

where $*$ stands for any j in case (i) and is void in case (ii).

With quasi-resonances at hand, the proof relies on an application of [6] once a supplementary spectral assumption on corresponding black box operators is proved, obvious for positive ε_c, and proved in [5] for negative ε_c.

Resembling asymptotics to (3) and (4) hold for square roots (pure imaginary numbers) of negative eigenvalues when ε_c is negative. We illustrate all these results by graphs of computed resonances in three representative cases.

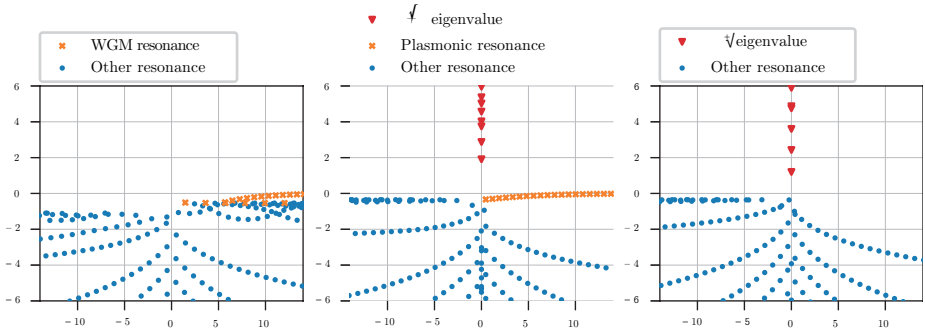

$\varepsilon_c = 2.25$ $\varepsilon_c = -2.25$ $\varepsilon_c = -2/3$

References

[1] S. Balac, M. Dauge, Y. Dumeige, P. Féron, and Z. Moitier, *Mathematical analysis of whispering gallery modes in graded index optical micro-disk resonators*, Eur. Phys. J. D, **74**, 221 (2020).

[2] S. Balac, M. Dauge, and Z. Moitier, *Asymptotics for 2D whispering gallery modes in optical micro-disks with radially varying index*, IMA Journal of Applied Mathematics, **86**, 6 (2021), pp 1212–1265

[3] C. Carvalho and Z. Moitier, *Scattering resonances in unbounded transmission problems with sign-changing coefficient*, arXiv:2010.07583.

[4] S. Dyatlov, M. Zworski, *Mathematical theory of scattering resonances*, Graduate Studies in Mathematics, **200** (2019).

[5] R. Mandel, Z. Moitier, and B. Verfürth, *Nonlinear Helmholtz equations with sign-changing diffusion coefficient*, Comptes Rendus. Mathématique 360 (2022)

[6] S.-H. Tang and M. Zworski, *From quasimodes to resonances*, Mathematical Research Letters, 5 (1998), 261–272.

Imaginary part of resonances in the scattering by transparent or negative obstacles, part II

Zoïs Moitier

(joint work with Monique Dauge)

Scattering resonances have negative imaginary part. However, the quasi-resonances $\underline{k}_*(m)$ in Part I are real positive. Therefore, a corollary of the quasi-resonances to resonances theorem is that $\operatorname{Im} k_*(m) = \mathcal{O}(m^{-\infty})$. In few cases, we have more precise decay rate. For 1d Schrödinger equations of the form $-u'' + m^2 V u = k^2 u$ if the potential V is analytic (*puits dans l'isle*) [2] proves that $\operatorname{Im} k(m) \sim -c\, m^{-3/2}\, \mathrm{e}^{-2S_0 m}$ with c, $S_0 > 0$ as $m \to +\infty$. In [1], for the discontinuous potential $V(x) = (1+x^2)\mathbf{1}_{[-1,1]}(x)$ the authors prove that $\operatorname{Im} k(m) \sim -4\pi^{-1}\, m^{-3/2}\, \mathrm{e}^{-m}$ with $S_0 > 0$ as $m \to +\infty$.

1. Numerical experiments

The difficulty to see this exponential decay is that the real part of the resonances are proportional to m, so we can only compute $k_*(m)$ when $\operatorname{Im} k_*(m)/\operatorname{Re} k_*(m)$ is greater than machine precision. To go beyond the usual precision, we use quadruple precision with a method that also works with variable coefficients, namely finite difference method with a six stage extrapolation to get the desired precision. With a `Julia` program, we get the results Fig. 1. In our setting, using a Schrödinger analogy, we can formally find an expression for the values of S_0:

$$S_0 = \int_R^{\lambda_0^{-1/2}} \sqrt{r^{-2} - \lambda_0}\, \mathrm{d}r \qquad \text{where } \lambda_0 = \lim_{m\to+\infty} \frac{\operatorname{Re} k_*(m)^2}{m^2}.$$

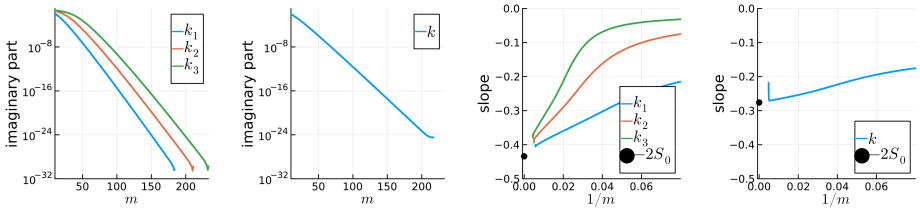

(A) $\varepsilon_{\mathsf{c}} = 2.25$ (B) $\varepsilon_{\mathsf{c}} = -2.25$ (C) $\varepsilon_{\mathsf{c}} = 2.25$ (D) $\varepsilon_{\mathsf{c}} = -2.25$

FIGURE 1. On Fig. 1a and 1b, we have the imaginary part $\operatorname{Im} k_*(m)$ with respect to m. On Fig. 1c and 1d, we have the slope $\log|\operatorname{Im} k_*(m+1)| - \log|\operatorname{Im} k_*(m)|$ with respect to $1/m$ that should converge to $-2S_0$.

2. Conjectures

We present two conjectures supported by numerical experiment. The first one on the distribution of scattering resonances in the negative case.

- If $-1 < \varepsilon_{\mathsf{c}} < 0$, for any $\beta > 0$, there are at most finitely many resonances lying in the strip $-\beta \leq \operatorname{Im} k < 0$.
- If $\varepsilon_{\mathsf{c}} < -1$, for any $\beta > 0$, resonances lying in the strip $-\beta \leq \operatorname{Im} k < 0$ are the plasmonic resonances $k(m)$ (except possibly a finite number).

The second conjecture applies to the imaginary part of the scattering resonances close to the real axis: There holds, for some computable S_0 accounting for tunneling effect, that $\operatorname{Im} k_*(m) \sim \mathrm{e}^{-2S_0 m}$. This conjecture can also be formulated for smooth variable coefficient ε_{c}.

References

[1] S. Dyatlov and M. Zworski, *Mathematical theory of scattering resonances*, Graduate Studies in Mathematics, 200, American Mathematical Society (2019).
[2] B. Helffer and J. Sjöstrand, *Résonances en limite semi-classique*, Mémoires de la Société Mathématique de France, 24-25 (1986).

Dispersive estimates for the wave equation outside a general strictly convex obstacle in $\mathbb{R}^3$

Oana Ivanovici

1. Introduction

We are concerned with localization properties of solutions to hyperbolic PDEs, especially problems with a geometric component: how do boundaries influence spreading and concentration of solutions.

Studying the same hyperbolic or dispersive equations on manifolds (curved geometry, e.g., variable metric) started in part with Bourgain's work on KdV and Schrödinger on the torus, and then expanded in several different directions, all of

them with low regularity requirements (e.g. Staffilani & Tataru, Burq, Gérard & Tzvetkov for Schrödinger, Smith, Bahouri & Chemin, Klainerman & Rodnianski and Smith & Tataru for wave equations). Even though the boundary-less case has been well understood for some time, obtaining results for the case of manifolds *with* boundary has been surprisingly elusive and the problem of whether such estimates can be extended to the case of manifolds with boundary has preoccupied many outstanding mathematicians (such as C. Sogge, H. Smith, N. Burq, G. Lebeau, D. Tataru) in recent years. Besides harmonic analysis tools, the starting point for these estimates is the knowledge of a parametrix for the linear flow, which turns out to be closely connected to propagation of singularities. It should be noted that parametrices have been available for the boundary value problem for a long time (see Eskin, Melrose & Sjöstrand, Melrose & Taylor) as a crucial tool to establish propagation of singularities for the wave equation on domains. However, while efficient at proving that singularities travel along the (generalized) bicharacteristic flow, they do not seem strong enough to obtain dispersion, as they are not precise enough to capture separation of wave packets traveling with different initial directions.

Despite considerable progress in recent years, we still have limited knowledge of dispersive effects occuring near the boundary. Going beyond this recent activity requires new tools. In fact, to be able to deal with important applications to nonlinear problems and control theory it is crucial to obtain **quantitative refinements** concerning the propagation of singularities near the boundary.

1.1. **What is dispersion ?** This property of a wave to spread out as time goes by, while keeping its energy conserved, is called dispersion: it measures the amplitude of a wave.

There are two useful ways to measure dispersive decay: the dispersive estimates and the Strichartz estimates.

- The dispersive estimates measure the uniform decay properties as a function of time for a localized data. For instance, if the data is a Dirac at a point $Q_0 \in \mathbb{R}^d$, and if the frequency $1/h$ is large, then the dispersive estimates in $\mathbb{R}^d$ read as follows :

$$\sup \left| \chi(hD_t) e^{\pm it\sqrt{|\Delta_{\mathbb{R}^d}|}}(\delta_{Q_0}) \right| \leq Ch^{-d} \min\left(1, \left(\frac{h}{t}\right)^{\frac{d-1}{2}}\right), \tag{1}$$

  where $h \in (0,1)$ is a small parameter and $\chi \in C^\infty([1/2,2])$ a smooth function supported near 1. For the wave equation, this property holds in $\mathbb{R}^d$ or on manifolds without boundary as long as time is less than the injectivity radius. When there is a boundary, these estimates may not hold anymore as above (they hold with a *loss* in the right hand side of (1)), because optical rays, issued from the same source point, may refocus and give rise to caustics, which are points where the light is singularly intense.
- On the other hand, when the data is not localised but just in L^2, we cannot have uniform decay, so the goal is to measure average decay (in time and space). This is what Strichartz estimates are for.

We call admissible indices the pairs (q, r) such that $q, r \geq 2$, $(q, r, \alpha) \neq (2, \infty, 1)$, $\frac{1}{q} \leq \alpha(\frac{1}{2} - \frac{1}{r})$.

Consider the wave equation: $(\partial_t^2 - \Delta)u = 0$, $u|_{t=0} = u_0$, $\partial_t u|_{t=0} = u_1$, then the Strichartz estimate reads as

$$h^{(d-\alpha)(\frac{1}{2}-\frac{1}{r})}\|\chi(hD_t)u\|_{L^q([0,T],L^r_x)} \lesssim \|u_0\|_{L^2} + \|hu_1\|_{L^2}.$$

Known results: in $\mathbb{R}^d$ with flat metric (wave and Schrödinger): Strichartz, Pecher, Ginibre-Velo, Lindblad & Sogge, Keel &Tao...; if $\partial\Omega = \emptyset$ (wave): Kapitanski, Mockenhaupt, Seeger & Sogge, Smith, Bahouri & Chemin, Tataru...; if $\partial\Omega = \emptyset$ (Schrödinger): Staffilani & Tataru, Burq, Gérard & Tzvetkov...

On manifolds without boundary, the Strichartz estimates can be obtained by interpolation between the dispersive estimates and the energy conservation. When there is a boundary, the results obtained in this way may not be sharp: in fact, the loss in the dispersive estimates may be intermittent in time, so some of it may dissapear when averaging in time.

The decay properties of waves are closely related to the structure of the geodesic flow, therefore we can distinguish two main situations: of geodesically convex and geodesically concave domain. As mentioned before, a loss in dispersion is informally related to the presence of caustics, which occur when optical rays are non longer diverging from each other: as such, in order to study dispersion, the first thing we need to understand is the structure of the wave front.

1.2. **Geometry of the wavefront and light cones.** One of the most striking features of solutions to the wave equation is the geometrical character of propagation. The statement on propagation of singularities for the wave flow has two main ingredients: locating singularities of a distribution, as captured by the wave front set (which measures *where* the wave is singular and *in which direction*), and describing the curves along which they propagate, namely the generalized geodesics. The simplest example is the propagation of a spherical wave, whose singularities are located on the sphere of radius $|t|$ (t is the elapsed time), centered at the source point, like in the figure below. For a variable coefficients metric, one can make good of this heuristic as long as two different light rays emanating from the source do not cross: in other words, as long as t is smaller than the injectivity radius. One may then construct short time parametrices for the wave, using oscillatory integrals, where the (non degenerate) phase encodes the geometry of the wave front.

Wavefront (**WF**) $\sim$ the "sphere" of radius t centered at the source point; if *non-empty* boundary, the WF can become a very degenerate object developing large number of singularities of different types in arbitrarily small times.

In the case of a non-empty boundary, the main difficulties arise from the behavior of the singularities near it: it becomes essential to understand the geometry

of wave front: the underlying light cones (where the space-time singularities lie) might undergo dramatic changes compared to the usual flat ones, because of multiple reflections that generate caustics and cluster points (where light is singularly intense).

We distinguish several situations:

- transverse: rays reflect according to "angle of incidence equals angle of reflection", like a billiard ball;
- tangency to a strictly convex obstacle: rays carrying WF tangent to a convex obstacle can stick to it and re-release energy near the "shadow region", producing diffractive effects (e.g. the Poisson spot);
- glancing inside a strictly convex: The "sphere" of radius t, i.e. the locus of end points of generalized geodesics (broken or gliding rays) of length t, soon degenerates and develops singularities in arbitrarily small times, depending on the frequency and the distance to the boundary of the source.
- tangency, no convexity: if the ray has infinite order tangency with the boundary, even *deciding* what should be the continuation of a ray striking the boundary is difficult...

A **caustic/cluster point/ singularity** in the wavefront should yield **losses in dispersion**. In fact, at large frequency, our goal is to obtain an approximate solution to the wave equation as a sum of oscillatory integrals, located near the wave front, and whose phase functions encode the geometry of the WF. When the WF is smooth, these phase functions have no degenerate critical points and therefore the corresponding L^∞ bounds are the same as in $\mathbb{R}^d$. On the other hand, if the WF has singularities (of cusp, swallowtail, butterfly type etc), then these phase functions have degenerate critical points of different orders (2, 3, 4, etc) which involve losses the L^∞ estimates. It turns out that the possible dispersive or Strichartz estimates that can be obtained should reflect the geometry of the domain and especially its boundary.

Understanding dispersion requires a deep knowledge of the geometry of the wave front which become a very degenerate object. If the boundary is strictly convex, between every two consecutive reflections, the wave packets refocus, the wave shrinks in size and its maximum increases. With G. Lebeau and F. Planchon, we showed that the wave front develops a large number of swallowtail and cusp singularities in arbitrarily small times.

However, understanding the wave front it is not sufficient! rays can stick to the boundary and re-release energy near the "shadow region", producing diffractive effects (e.g. the Poisson-Arago spot). We have recently shown that in the exterior of a sphere in dimensions 4 or higher light intensity at the Poisson spot is stronger than in the illuminated region, quite an unexpected result.

For general domains, there have been important contributions by many experts in the field (see for example [Blair, Smith & Sogge] and [Smith & Sogge] and references therein). Essentially all the positive results are based on a clever reduction from a boundary problem to a boundary less one, by extending the metric across it **and use techniques developed for low regularity metrics** (see [Smith 98],

[Tataru 02], etc). This tric allows to deal with any kind of boundary but is blind by design to the full effect of dispersion (so very far from sharp, essentially because it reduces to wave packets which cross the boundary once, while the bad things appear just after the first reflection!).

1.3. **Concave boundaries.** From now on we will focus on the case of a smooth, strictly concave boundary. Our goal in this work is to obtain dispersive estimates for the wave equation with the Dirichlet boundary condition outside a general strictly convex obstacle in $\mathbb{R}^3$.

1.3.1. *The geometry of the wave front outside a convex obstacle with smooth boundary.* The geometry of the wavefront outside a convex obstacle :

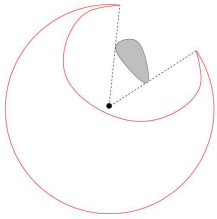

- (part of) a **circular front** of directly propagated singularities
- a **curved front of singularities reflected off the obstacle** in accordance with Snell's law.

Most crucially, if C^∞ boundary there are **NO** singularities behind the obstacle in the *"shadow region"*, as a consequence of the parametrix construction of [Melrose & Taylor]. In particular, there are no geometric singularities (in the sense of a peak of light), but we may have diffractive effects.

However, the rules of the geometric optics are no longer so simple when we are not on a domain with smooth boundary: in this case singularities may indeed go into the shadow region.

1.3.2. *What about the diffractive effects ?*

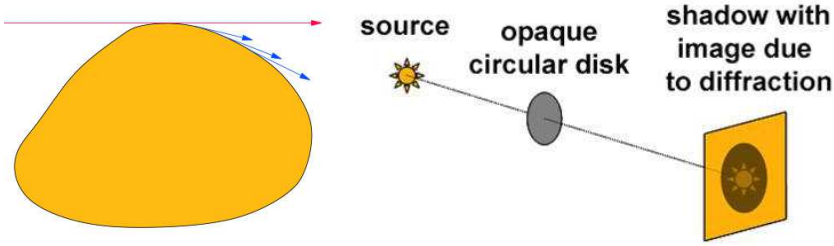

An incoming (incident) ray that is tangent to the boundary splits into two branches: one branch goes along the shadow boundary (without being deviated) while the other travels along the boundary and radiates surface diffracted rays into the shadow region, so the boundary acts as a secondary source. Because of this radiation, the intensity on the surface decays exponentially with distance along the ray. The transition and the shadow regions are reached by rays that are creeping on the boundary surface (following boundary geodesics).

A result stated by Keller (and proved by [Hargé & Lebeau, 1994] in case of C^∞ boundaries) states that rays can carry a non-negligeble amount of energy when

travelling on the surface of the boundary only for a time/distance at most $\tau^{-1/3}$, where τ is the frequency. After that, the amount of energy becomes exponentially small.

If the boundary is perfectly circular (a ball), light waves bend around its sides: the perfect symmetry of the obstacle means that all light waves should interact constructively in the exact center of the shadow behind it, where one should see a bright spot (the Poisson spot).

The Poisson spot is due to diffraction, contradicting the prediction of geometrical optics and also that of the particle theory of light. It played an important role in the discovery of the wave nature of light and is a common way to demonstrate that light behaves as a wave.

Study of diffraction: first by Grimaldi (1665) (who named it), Huygens, Newton, Delisle and Maraldi (1715), Fresnel, Poisson ; experiment by Arago, (1818) which led to the **wave theory of light**.

2. Dispersive estimates for waves outside a ball in $\mathbb{R}^d$

The main difficulty comes from rays which hit the boundary without being deviated: for this diffractive regime we already have a strong and very useful tool at our disposal (the Melrose & Taylor parametrix); on the other hand this situation seemed to have been quite well understood and many (sharp) positive results in that direction had been established lately ([Zworski 1990], [Smith & Sogge 1995], [Ivanovici 2008] or, in the radial case, [Li, Smith & Zhang 2012]). However, whether dispersion did hold remained an open question, even for the exterior of a sphere (for which explicit formulas exist, involving special functions). In [Ivanovici & Lebeau 2020] we obtained the validity of sharp dispersive estimates for the wave equation (and also for the classical Schrödinger equations, for which we had to overcome an additional difficulty related to its infinite speed of propagation) outside any strictly convex obstacle in $\mathbb{R}^3$. Moreover, we showed that in higher dimensions $d \geq 4$, counterexamples to dispersion do exist, even (and especially) in the simplest case of the exterior of a sphere.

Theorem 1. [I. & Lebeau, 2020]) Let $\Omega_d = \mathbb{R}^d \setminus B_d(0,1)$.

- The dispersive estimates for the wave equation with Dirichlet condition inside Ω_3 **hold true**.
- If $d \geq 4$, these estimates fail at the **Poisson spot**. If $Q_\pm(r)$ denote the source and the observation points at (same) distance r from the ball, symmetric w.r.t. the center of the unit ball $B_d(0,1)$ of $\mathbb{R}^d$ with $d \geq 3$, taking $r \sim h^{-1/3}$, $t \sim 2h^{-1/3}$ yields

$$\Big|(\chi(hD_t)e^{i2h^{-1/3}\sqrt{|\Delta|}}(\delta_{Q_+})\Big|(Q_-) \sim \frac{1}{h^d}\Big(\frac{h}{2h^{-1/3}}\Big)^{-\frac{d-1}{2}} h^{-\frac{d-3}{3}}.$$

  This shows that for $d \geq 4$, light intensity at the Poisson spot is stronger than in the illuminated region.

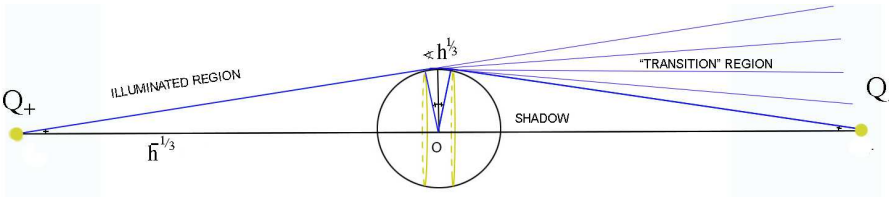

Theorem 2. (2022) Let $\Omega = \mathbb{R}^3 \setminus \Theta$, Θ strictly convex obstacle. The dispersive estimates for the wave equation with Dirichlet condition inside Ω hold true.

Stability analysis of the DDA for Dielectric Scattering

Martin Costabel
(joint work with Monique Dauge, Khedijeh Nedaiasl)

1. Background

In computational physics concerned with the dielectric scattering of time-harmonic electromagnetic waves (absorption of light by dust particles in interstellar clouds, scattering of light by gold nanoparticles or red blood cells, simulation of optical tweezers etc.), DDA (Discrete Dipole Approximation) has been a very popular method for almost 50 years [1, 2]. This is a discretization method for strongly singular volume integral equations that is very simple to implement, fast and apparently reliable. It is, however, virtually unknown in the mathematical community. Thus there is still no published proof of the stability (and hence, convergence) of this method. On the way to such a stability proof, recently some partial results have been obtained that show that the question is non-trivial. The DDA can be described as a Delta-Delta Approximation (Dirac deltas as both test and trial functions), but it does not fit in the known framework of projection methods. Some tools that are not standard in numerical analysis have to be used for its analysis.

2. Volume integral equation and discretization

Applying a Lippmann-Schwinger style perturbation idea to the time-harmonic Maxwell scattering by a penetrable object described by a permittivity (or refractive index) differing from a constant value only in a compact subset Ω of $\mathbb{R}^3$, one arrives at the volume integral equation $\frac{1}{\eta}u - A_\kappa u = E^{\mathrm{inc}}$ with

$$A_\kappa u(x) = -\nabla \operatorname{div} \int_\Omega g_\kappa(x-y)u(y)\,dy - \kappa^2 \int_\Omega g_\kappa(x-y)u(y)\,dy\,.$$

Here $g_\kappa(x) = e^{i\kappa|x|}/(4\pi|x|)$ is the Helmholtz fundamental solution, $u = \eta E$ is the polarization vector function, and $\eta = \varepsilon_r - 1$ with the relative permittivity ε_r. For

the DDA one chooses a regular cubic grid $(x_m)_{m\in\mathbb{Z}^3}$ of meshwidth h and replaces the strongly singular volume integral equation by the system

$$\lambda u_m - h^3 \sum_{x_n\in\Omega, n\neq m} K(x_m - x_n)u_n = f_m \tag{1}$$

with suitably chosen λ. Here $K = -(\nabla\otimes\nabla + \kappa^2\mathbb{I})g_\kappa(x)$ is the kernel of the integral operator A_κ. One expects that the system matrix in (1) approximates the operator $A_\kappa - \frac{1}{3}\mathbb{I}$.

3. Some stability results

Writing the system (1) in the form $(\lambda\mathbb{I} - T_\kappa^h)U = F$, stability means here a uniform resolvent estimate $\|(\lambda\mathbb{I} - T_\kappa^h)^{-1}\| \le C$ with C independent of h. Such stability results (publications in preparation) have been presented in the talk in three cases using different techniques: The quasi-static case ($\kappa = 0$), non-real frequencies ($\kappa \in \mathbb{C}\setminus\mathbb{R}$), and real frequencies ($\kappa > 0$).

3.1. **The quasi-static case $\kappa = 0$.** In this case, the kernel K is positively homogeneous of degree -3. Therefore the matrix elements $h^3K(x_m - x_n) = K(m-n)$ are independent of h, and the matrix T_0^h is a finite section of an infinite block Toeplitz matrix T, which has the symbol

$$F(t) = \sum_{m\in\mathbb{Z}^3, m\neq 0} K(m)e^{im\cdot t} \quad (t\in\mathbb{R}^3)\,.$$

This Fourier series is not absolutely convergent, and to find precise bounds or even to prove that F is bounded requires some work. We found that the Ewald summation method can be applied. It writes F as the sum of a rapidly convergent Fourier series and a slowly convergent one that can be transformed into a rapidly convergent series via the Poisson summation formula. One obtains the boundedness of F and a fast method to evaluate it numerically.

For $\kappa = 0$, the integral operator and the matrix T are selfadjoint, their numerical range is therefore a real interval, the convex hull of the spectrum. For A_0 this is known [3] to be $[0,1]$ (corresponding to negative permittivities ε_r), for T one finds numerically (by computing maximal and minimal eigenvalues of $F(t)$) an interval $[\Lambda_-, \Lambda_+]$ strictly larger by about 20% than the expected interval $[-1/3, 2/3]$.

Theorem 1. *For $\kappa = 0$, the method (1) is stable in the ℓ^2 norm for $\lambda \in \mathbb{C}\setminus[\Lambda_-,\Lambda_+]$. The method does not provide a spectral approximation of the volume integral operator, and for $\lambda\in[\Lambda_-,\Lambda_+]\setminus[-1/3,2/3]$ (corresponding to very small or very large positive ε_r), the method is unstable, whereas the corresponding volume integral equation is well posed.*

In the corresponding two-dimensional case, the expected interval is $[-1/2, 1/2]$, and one can prove that the spectrum of T is $[-\Lambda_+, \Lambda_+]$ with $\Lambda_+ \ge \frac{\Gamma(\frac{1}{4})^4}{32\pi^2} = 0.5471...$

3.2. **Non-zero frequencies.** For $\kappa \neq 0$, the infinite Toeplitz matrix is no longer independent of h, depending rather on κh.

If κ is non-real, one can still use Ewald's method and obtain explicit bounds for the numerical range of T_κ^h, implying stability of the DDA for λ outside of the subset of $\mathbb{C}$ described by these bounds. Compared with the numerically obtained spectrum of T_κ^h, these bounds become less and less sharp as $\arg \kappa^2$ approaches zero.

Finally, for real positive κ, the infinite Toeplitz matrix T no longer defines a bounded operator in $\ell^2(\mathbb{Z}^3)$, and so far only estimates for the imaginary part of the DDA system matrices were obtained, by using a representation of the Green function by plane waves that is related to the so-called Optical Theorem. This implies stability for certain ranges of non-real ε_r.

4. Open question

From numerical computations of the eigenvalues of the matrices T_κ^h, one sees that apart from accumulation of eigenvalues around the real interval $[\Lambda_-, \Lambda_+]$, there is a discrete set of non-real eigenvalues of the volume integral equation that seem to be well approximated as $h \to 0$, so that whereas DDA does not strictly speaking provide a spectrally correct approximation, it does so outside of a rather small set in the complex plane. To describe this behavior correctly and to find a way how to prove it is currently an open problem.

References

[1] E. Purcell, C. R. Pennypacker, *Scattering and absorption of light by nonspherical dielectric grains*, The Astrophysical Journal **186** (1973), 705–714.

[2] M. A. Yurkin, A. G. Hoekstra, *The discrete dipole approximation: an overview and recent developments*, Journal of Quantitative Spectroscopy and Radiative Transfer, **106**(1-3) (2007), 558–589.

[3] M. Costabel, E. Darrigrand, H. Sakly, *The essential spectrum of the volume integral operator in electromagnetic scattering by a homogeneous body*, Comptes Rendus Mathematique, **350**(3-4) (2012), 193–197.

Reporter: Martin Averseng

Participants

Dr. Martin Averseng
Seminar für Angewandte Mathematik
ETH - Zentrum
Rämistrasse 101
8092 Zürich
SWITZERLAND

Dr. Dean Baskin
Mailstop 3368
Department of Mathematics
Texas A & M University
College Station, TX 77843-3368
UNITED STATES

Dr. Thomas Beck
Department of Mathematics
Fordham University
441 East Fordham Road
Bronx NY 10458
UNITED STATES

Dr. Anne-Sophie Bonnet-Ben Dhia
ENSTA Paris
UMA-POEMS
828, Boulevard des Maréchaux
91762 Palaiseau Cedex
FRANCE

Prof. Dr. Nicolas Burq
Laboratoire de Mathématiques d'Orsay
Université Paris Saclay
Batiment 307
91405 Orsay Cedex
FRANCE

Dr. Stéphanie Chaillat-Loseille
ENSTA - UMA ParisTech
Laboratoire POEMS
Bureau 2226
828, Boulevard des Maréchaux
91120 Palaiseau Cedex
FRANCE

Prof. Dr. Simon N. Chandler-Wilde
Department of Mathematics and Statistics
University of Reading
Whiteknights
P.O. Box 220
Reading RG6 6AX
UNITED KINGDOM

Dr. Theophile Chaumont-Frelet
INRIA Sophia Antipolis
B.P. 93
2004 Route des Lucioles
06902 Sophia-Antipolis Cedex
FRANCE

Dr. Xavier Claeys
Laboratoire Jacques-Louis Lions
Université Pierre et Marie Curie
Bureau 15-25-310
4 place Jussieu
75005 Paris Cedex
FRANCE

Prof. Dr. Martin Costabel
Département de Mathématiques
Université de Rennes I
Campus de Beaulieu
35042 Rennes Cedex
FRANCE

Prof. Dr. Marion Darbas
Université Sorbonne Paris Nord
LAGA UMR CNRS 7539
99 avenue Jean-Baptiste Clément
93430 Villetaneuse Cedex 1
FRANCE

Prof. Dr. Monique Dauge
IRMAR
Université de Rennes I
Campus de Beaulieu
35042 Rennes Cedex
FRANCE

Prof. Dr. Victorita Dolean Maini
Department of Mathematics & Statistics
University of Strathclyde
Livingstone Tower
26, Richmond Street
Glasgow G1 1XH
UNITED KINGDOM

Prof. Dr. Semyon Dyatlov
Room 2-377
Department of Mathematics
MIT
Cambridge 02139
UNITED STATES

Dr. Fatih Ecevit
Bogazici University
Department of Mathematics
34342 Bebek, Istanbul
TURKEY

Prof. Dr. Björn Engquist
Department of Mathematics
The University of Texas at Austin
2515 Speedway
Austin TX 78712-0257
UNITED STATES

Prof. Dr. Charles L. Epstein
Center for Computational Mathematics
Flatirion Institute of the Simons
Foundation
162 5th Avenue
New York 10010
UNITED STATES

Prof. Dr. Clotilde Fermanian-Kammerer
UFR des Sciences et Technologie
Université Paris Est - Créteil
Val-de-Marne
61, ave. du Général de Gaulle
94010 Créteil Cedex
FRANCE

Dr. Sonia Fliss
POEMS, ENSTA Paris, IPP
828, Boulevard des Maréchaux
91762 Palaiseau Cedex
FRANCE

Prof. Dr. Jeffrey Galkowski
Department of Mathematics
University College London
Gower Street
London WC1E 6BT
UNITED KINGDOM

Prof. Dr. Martin Gander
Département de Mathématiques
Université de Geneve
Case Postale 64
Rue du Conseil-Général 7-9
P.O. Box Case Postale 64
1205 Genève
SWITZERLAND

Prof. Dr. Ivan G. Graham
Dept. of Mathematical Sciences
University of Bath
Claverton Down
Bath BA2 7AY
UNITED KINGDOM

Prof. Dr. Laurence Halpern
Laboratoire Analyse, Géométrie &
Applications
UMR 7539 CNRS
Université Sorbonne Paris Nord
93430 Villetaneuse Cedex
FRANCE

Prof. Dr. Andrew Hassell
Mathematical Sciences Institute
Australian National University
Canberra ACT 0200
AUSTRALIA

Prof. Dr. Luc Hillairet
Institut Denis Poisson
Université d'Orleans
rue de Chartres, B. P. 6759
45067 Orléans Cedex 2
FRANCE

Prof. Dr. Ralf Hiptmair
Seminar für Angewandte Mathematik
ETH - Zentrum
Rämistrasse 101
8092 Zürich
SWITZERLAND

Prof. Dr. Lise-Marie Imbert-Gérard
Department of Mathematics
University of Arizona
P.O.Box 210089
Tucson AZ 85721-0089
UNITED STATES

Dr. Maxime Ingremeau
Département de Mathématiques
Université Côte d'Azur
Parc Valrose
06108 Nice Cedex 2
FRANCE

Dr. Oana Ivanovici
Sorbonne Université
Laboratoire d'Informatique de Paris 6
4 Place Jussieu
P.O. Box 169
75252 Paris
FRANCE

Prof. Dr. Katya Krupchyk
Department of Mathematics
University of California, Irvine
Irvine CA 92697-3875
UNITED STATES

Dr. David Lafontaine
Institut de Mathématiques de Toulouse
Université Paul Sabatier
118, route de Narbonne
31062 Toulouse Cedex 9
FRANCE

Dr. Pierre Marchand
INRIA
828 Boulevard des Maréchaux
91762 Palaiseau Cedex
FRANCE

Prof. Dr. Jeremy L. Marzuola
Department of Mathematics
University of North Carolina at Chapel Hill
Phillips Hall
Chapel Hill, NC 27599-3250
UNITED STATES

Prof. Dr. Anna Mazzucato
Department of Mathematics
Pennsylvania State University
305 McAllister Building
University Park, PA 16802
UNITED STATES

Prof. Dr. Jens M. Melenk
Institut für Analysis und Scientific Computing
Technische Universität Wien
Wiedner Hauptstrasse 8 - 10
1040 Wien
AUSTRIA

Prof. Dr. Richard B. Melrose
Department of Mathematics
Massachusetts Institute of Technology
77 Massachusetts Avenue
Cambridge MA 02139-4307
UNITED STATES

Dr. Andrea Moiola
Dipartimento di Matematica
Università degli studi di Pavia
Via Ferrata, 5
27100 Pavia
ITALY

Dr. Zois Moitier
Fakultät für Mathematik
Institut für Analysis
Karlsruher Institut für Technologie (KIT)
Englerstraße 2
76131 Karlsruhe
GERMANY

Prof. Dr. Serge Nicaise
LAMAV
Université Polytechnique Hauts-de-France
Le Mont Houy
59313 Valenciennes Cedex 9
FRANCE

Prof. Dr. Stephane Nonnenmacher
Institut de Mathématiques d'Orsay
Université Paris-Saclay
Batiment 307
Rue Michel Magat
91405 Orsay Cedex
FRANCE

Donnell Obovu
Department of Mathematics
University College London
Gower Street
London WC1E 6BT
UNITED KINGDOM

Prof. Dr. Jeffrey Rauch
Department of Mathematics
University of Michigan
East Hall, 525 E. University
Ann Arbor, MI 48109-1109
UNITED STATES

Prof. Dr. Nicolas Raymond
Dept. de Mathématiques
Faculté des Sciences
Université d'Angers
2, Boulevard Lavoisier
49045 Angers Cedex
FRANCE

Prof. Dr. Simona Rota Nodari
Laboratoire J.-A. Dieudonne
UMR CNRS-UNS 7351
Université de Nice
Sophia Antipolis
Parc Valrose
06108 Nice Cedex 2
FRANCE

Prof. Dr. Stefan A. Sauter
Institut für Mathematik
Universität Zürich
Winterthurerstrasse 190
8057 Zürich
SWITZERLAND

Prof. Dr. Christoph Schwab
Seminar für Angewandte Mathematik
ETH Zurich
ETH Zentrum, HG G 57.1
Rämistrasse 101
8092 Zürich
SWITZERLAND

Prof. Dr. Valery P. Smyshlyaev
Department of Mathematics
University College London
Gower Street
London WC1E 6BT
UNITED KINGDOM

Prof. Dr. Euan Spence
Department of Mathematical Sciences
University of Bath
Claverton Down
Bath BA2 7AY
UNITED KINGDOM

Prof. Dr. Alexander Strohmaier
School of Mathematics
University of Leeds
Leeds LS2 9JT
UNITED KINGDOM

Dr. Melissa Tacy
Department of Mathematics
The University of Auckland
Auckland 1052
NEW ZEALAND

Dr. Carolina Urzúa-Torres
Dept. of Applied Math.
Delft University of Technology
2628 CD Delft
NETHERLANDS

Prof. Dr. Alden Waters
Bernoulli Institute
University of Groningen
PO Box 407
9700 AK Groningen
NETHERLANDS

Dr. Jared Wunsch
Department of Mathematics
Northwestern University
2033 Sheridan Road
Evanston, IL 60208-2730
UNITED STATES

Dr. Leonardo Zepeda-Núñez
Department of Mathematics
University of Wisconsin-Madison
480 Lincoln Drive
Madison WI 53706-1388
UNITED STATES

Dr. Ruming Zhang
Mathematisches Institut II
Universität Karlsruhe
Englerstr. 2
76131 Karlsruhe
GERMANY

Prof. Dr. Hongkai Zhao
Department of Mathematics
Duke University
P.O.Box 90320
Durham NC 27708-0320
UNITED STATES

Dr. Joey Zou
Department of Mathematics
Northwestern University
2033 Sheridan Road
Evanston, IL 60208-2730
UNITED STATES